Jochen Pramhas, Dipl.-Ing.

Evaluation of Valve Train Variability in Passenger Car Diesel Engines

DOCTORAL THESIS

to achieve the university degree of
Doktor der technischen Wissenschaften
submitted to

Graz University of Technology

Institute for Internal Combustion Engines and Thermodynamics
Head: Univ.-Prof. Dipl.-Ing. Dr.techn. Helmut Eichlseder

Supervisor
Univ.-Prof. Dipl.-Ing. Dr.techn. Helmut Eichlseder
Em.Univ.-Prof. Dr.-Ing. Günter Merker

Graz, January 2015

JP

JP

Give every day the chance to become the most beautiful day of your life

(Mark Twain)

Abstract

The continuously decreasing emission limits lead to a growing importance of exhaust aftertreatment in passenger car diesel engines. Hence methods for achieving a rapid catalyst light off after engine cold start and for maintaining the catalyst temperature during low load operation will become more and more necessary. The present work evaluates several valve timing strategies concerning their ability for doing so. For this purpose simulations as well as experimental investigations were conducted.

A special focus of simulation was on pointing out relevance of exhaust temperature and mass flow for these thermomanagement tasks. An increase of exhaust temperature is beneficial for both heat up catalyst and maintaining catalyst temperature. In case of the exhaust mass flow, high values are advantageous only in case of a catalyst heat up process, while maintaining catalyst temperature is supported by a low mass flow. Another focus of simulation was on analysing the exhaust temperature gaining effects relevant for the considered alternative valve timings. This leads to the finding that the exhaust temperature increase of the most efficient strategies is based on a reduction of the overall aspirated cylinder mass (air and EGR), what means a reduction of exhaust mass flow. A late intake valve closing (LIVC), cylinder deactivation but also internal EGR are examples of this group of methods. In contrast to these methods the exhaust temperature gain resulting from an early exhaust valve opening (EEVO) is not based on a reduction of mass flow but on a cut of effective expansion. However, EEVO leads not only to an increase of exhaust temperature at a constant mass flow and hence to an increase of enthalpy flow, but also to a significant penalty in fuel consumption.

EEVO, LIVC and cylinder deactivation were considered also by means of engine test bed measurements, which were conducted on a state of the art passenger car diesel engine. Besides the validation of simulation results the main focus was on analysing effects which are not covered by simulation (transient operation, cold engine conditions, emissions). Hence not only steady state operation points but also transient test cycles (NEDC, FTP 75), even with respect to cold engine conditions (20 °C) were considered. The correlation between measurement and simulation concerning fuel consumption and exhaust temperature in steady state operation points is well. Using an EEVO in a cold started transient test leads similar to the stationary operation to a considerable gain in exhaust enthalpy flow, however also to a clear disadvantage in efficiency, which is even higher for cold engine conditions. In case of LIVC, measurement results point out the ability for maintaining catalyst temperature, however not for an application during engine cold start, what is due to a drawback in ignitability (low cylinder pressure and temperature). Measurement results achieved by operating the considered 4-cylinder engine by only 2-cylinders verifiy that cylinder deactivation allows an exhaust temperature increase nearly without a drawback in efficiency. However, the available engine output is not sufficient to cope with the most relevant driving cycles (NEDC or FTP 75). Even not if only the first, for exhaust thermomanagement particularly relevant sections are considered.

Affidavit

I declare that I have authored this thesis independently, that I have not used other than the declared sources/resources, and that I have explicitly indicated all material which has been quoted either literally or by content from the sources used. The text document uploaded to TUGRAZonline is identical to the present doctoral dissertation.

Graz, 22.01.2015

Jochen Pramhas

Preface

The present thesis arose from my activities as a scientific assistant at Graz University of Technology – Institute for Internal Combustion Engines and Thermodynamics. All investigations presented in this work were carried out inside the COMET K2 project "Combustion Concepts for Passenger Cars – Combustion Engine and Drivetrain Optimization".

The support, patience and guidance of the following people was essential for the development of this thesis. It is to them that I owe my deepest gratitude.

Univ.-Prof. Dipl.-Ing. Dr.techn. Helmut Eichlseder for supervising this thesis and for giving me the opportunity to research within a very professional framework.

Em.Univ.-Prof. Dr.-Ing. Günter Merker for being co-supervisor of this thesis.

Dipl.-Ing. Dr.techn. Eberhard Schutting for supporting me from the beginning. I would like to thank him in particular for organizing the project. Due to this I was able to focus on my research activities.

Dipl.-Ing. Ortwin Dumböck for a number of exciting discussions in the field of thermodynamics as well as for his support in terms of LaTeX.

All other colleagues at the institute for creating a very pleasant and friendly working atmosphere.

Dipl.-Ing. Ludwig Bürgler for his non-bureaucratic manner which made a great contribution to an effective cooperation.

Graz, January 2015

Jochen Pramhas

Contents

Nomenclature

Abbreviations

1-D	One-dimensional	ICE	Internal Combustion Engine
BDC	Bottom Dead Centre	IT	Intake Throttling
CFD	Computerized Fluid Dynamics	IVC	Intake Valve Closing
CO	Carbon Monoxide	IVL	Intake Valve Lift
CO_2	Carbon Dioxide	IVO	Intake Valve Opening
CAC	Charge Air Cooler	LIVC	Late Intake Valve Closing
DOC	Diesel Oxidation Catalyst	LIVO	Late Intake Valve Opening
DOHC	Double Overhead Camshaft	LNT	Lean NO_x Trap
DPF	Diesel Particulate Filter	LPEGR	Low Pressure Exhaust Gas Recirculation
EAS	Exhaust Aftertreatment System		
ECU	Engine Control Unit	NEDC	New European Driving Cycle
EGR	Exhaust Gas Recirculation	NO_x	Nitrogen Emissions
EE	Early Exhaust Cam Shaft Timing	NVH	Noise Vibration and Harshness
EELI	Early Exhaust Late Intake Cam Shaft Timing	ROHR	Rate of Heat Release
		TDC	Top Dead Centre
EEVO	Early Exhaust Valve Opening	SHP	Start of High Pressure Cycle
EVC	Exhaust Valve Closing	SCR	Selective Catalytic Reduction
EVL	Exhaust Valve Lift	SDPF	SCR on Diesel Particulate Filter
EVO	Exhaust Valve Opening	SOC	Start of Combustion
FTP 75	Federal Test Procedure (established in 1975)	UDC	Urban Driving Cycle
		VNT	Variable Nozzle Turbine
HC	Hydro Carbon	VVT	Variable Valve Train
HCCI	Homogenious Charge Compression Ignition	WLTP	Worldwide harmonized Light Vehicles Test Procedure
HPEGR	High Pressure Exhaust Gas Recirculation		
ds	Downstream	us	Upstream

Subscripts

0	Reference state (20 °C)
001	Position upstream Compressor
002	Position downstream Compressor
21	Position upstream Charge Air Cooler
2_1	Position downstream Charge Air Cooler
31	Position upstream Turbine
41	Position downstream Turbine
51	Position downstream Catalyst
BB	Blow By
CAC	Charge Air Cooler
Cat	Catalyst
Comp	Compressor
Cyl	Cylinder
EGR	Exhaust Gas Recirculation
EH	Electrical Heater
EV	Exhaust Valve
EVC	Exhaust Valve Closing
EVO	Exhaust Valve Opening
EP	Exhaust Port
Exh	Exhaust System
EX	Position between Exhaust Ports and Manifold
Fuel	Fuel
HP	High Pressure Cycle
IM	Intake Manifold
In	Intake System
IP	Intake Port
IV	Intake Valve
IVC	Intake Valve Closing
IVO	Intake Valve Opening
Loss	Losses
oEV	Crank Angle Interval characterized by opened Exhaust Valves
MI	Main Injection
PoI	Post Injection
SHP	Start of High Pressure Cycle
SOC	Start of Combustion
TC	Turbo Charger
Tb	Turbine
TP	Tail Pipe
V	Valve
W	Wall
ad	Adiabatic
ds	Downstream
eff	Effective
exh	Exhaust
ext	External
f	Friction
i	Indicated, Inner
in	Intake
int	Internal
m	Mechanical
s	Isentropic
us	Upstream

Formula Symbols

A	m^2	Area
AFR	-	Air Fuel Ratio
BMEP	bar	Break Mean Effective Pressure
BSFC	g/kWh	Break Specific Fuel Consumption
C	-	Constant
CFR	-	Charge Fuel Ratio
CO	ppm	Carbon Monoxide Concentration
DC	-	Discharge Coefficient
E	J/m^3	Specific Total Energy
EGR	%	Rate of Exhaust Gas Recirculation
F	N	Force
HC	ppm	Hydro Carbon Concentration
FMEP	bar	Friction Mean Effective Pressure
IMEP	bar	Indicated Mean Effective Pressure
I	$kg\,m^2$	Inertia
$MFB_{50\%}$	°CA	Mass Fraction Burned 50%
$MFB_{90\%}$	°CA	Mass Fraction Burned 90%
NO_X	ppm	Nitrogen Concentration
O_2	%	Oxygen Concentration
P	W	Power
PMEP	bar	Pumping Mean Effective Pressure
Q	J	Heat
R	J/(kg K)	Specific Gas Constant
T	°C	Temperature
V	m^3	Volume
W	J	Work
d	m	Diameter
f	-	Factor
h	J/kg	Specific Enthalpy
m	kg	Mass
n	min^{-1}	Engine Speed
p	bar	Pressure
t	s	Time
u	J/kg	Specific Internal Energy
w	m/s	Velocity
x	m	Length
ε	-	Geometric Compression Ratio
η	-	Efficiency
η_v	-	Volumetric Efficiency
κ	-	Isentropic Coefficient
λ	-	Air Excess Ratio
π	-	Pressure Ratio
ρ	-	Density
φ	-	Crank Angle
ω	-	Angular Velocity

1 Introduction

From analysing the market situation of passenger car propulsion systems in Europe, a share of diesel engines higher than 50 % is known. This high value has of course several reasons. However, the most relevant one is the high efficiency and hence the low fuel consumption. Taking into account both the high market share and the efficiency benefit of diesel engines, compared to spark ignition engines, it seems to be clear, that a further increase of the diesel share is one of the most effective ways for a reduction of fleet-average CO_2 emissions. Hence – keeping in mind the more and more challenging targets concerning fleet-average CO_2 emissions – it can be assumed, that the diesel engine will play a key role also for future passenger car propulsion systems.

However, not only CO_2 but also pollutant targets become more and more challenging. As a result of this trend, keeping engine out emissions below these limits, is even today not possible any more in case of HC, CO and soot emissions. Considering the world wide strictest emission targets, this applies also for NO_x emissions. Despite the progress of diesel combustion system development, a significant reduction of engine out emission is not assumed for the near future. Hence the relevance of exhaust aftertreatment will further grow.

One of the most relevant reasons for the efficiency benefit of diesel engines compared to spark ignition engines – namely the high air fuel ratio (AFR) – means also a drawback when it comes to exhaust aftertreatment, which has several reasons. One of them is a more complex aftertreatment system. In other words the high AFR avoids using a three-way catalyst. From the present point of view, besides the already established diesel oxidation catalyst (DOC) and diesel particulate filter (DPF), also a NO_x aftertreatment will become standard. Another reason for the drawback of a high AFR concerning aftertreatment is the lower exhaust temperature, which is critical when keeping in mind that most aftertreatment components require relatively high temperatures for achieving high conversion rates. Thus it seems to be clear, that the continuously decreasing pollutant limits are challenging for the diesel engine in particular.

Considering the pointed out potentials and challenges, the objectives of today's diesel engine development seems to be clear: Further enhancement of engine working cycle and aftertreatment concerning pollutant emissions while improving or at least maintaining efficiency. However, this should be not understood in the way, that a separated development of engine working cycle – gas exchange and high pressure cycle – and aftertreatment is recommended. Keeping in mind the challenges resulting from too low temperatures of exhaust aftertreatment system (EAS) components, quite the contrary – an adaption of gas exchange and combustion with respect to the needs of the aftertreatment system – seems to be promising. Doing so may be supported by new technologies. One of these technologies is a variable valve train (VVT). As it will be pointed out in more detail in section 1.1, a variable valve train is not a new technology for combustion engines in general. However, in case of passenger car diesel engines it is not yet established.

1.1 Application of Valve Train Variability in Passenger Car Engines

A VVT, as it is understood in this work, characterizes a system providing any additional degrees of freedom compared to a conventional valve train, comprising the whole range from a simple cam phaser to devices for variation of valve lift and timing. Also switching off valve actuation for one or more cylinders, as it is used for cylinder deactivation, is contained by the term VVT in this work.

Analysing state of the art passenger car engines concerning VVT technologies delivers a clear result: Cam phasers and systems for switching between two or more cam profiles are a wide spread technology in case of spark ignition engines [1, 3, 11, 24]. Also more complex systems for a continuously variation of valve lift [2, 10, 44] could be found as well as valve trains providing a deactivation of valve actuation for half of the total cylinders, as part of a variable downsizing concept (cylinder deactivation) [12, 23]. However, in terms of diesel engines only a few series-production engines featured with a VVT are known at this point of time [25, 29, 42], what has several causes. To sum up, as a consequence of fundamental differences between diesel and spark ignition engines – quality and quantity control – efficiency potentials concerning gas exchange are smaller in case of diesel engines as a matter of principle.

However, when it comes to research and development activities, valve train variability has been treated also in case of the diesel engine for a considerable time [34]. As proved by publications, the objectives of these investigations are various:

- Reduction of engine out NO_x emissions [18, 37, 40]
- Generating in-cylinder charge motion [36, 48]
- Optimization of volumetric efficiency at full load [36, 40, 43]
- Controlling of homogenious charge compression ignition (HCCI) [6, 45]
- Improve cold run stability [25, 36]
- Increasing exhaust temperature [9, 8, 15, 22, 31, 32]

The last mentioned item – increasing exhaust temperature – is also a main objective of VVT strategies considered in this work. However, in contrast to most of the quoted publications, the focus of the present work is not only on evaluation of the exhaust temperature gain. Instead, identifying the potential of a VVT for supporting exhaust aftertreatment in a broader sense will be achieved. The motivation for doing so should be cleared in section 1.2.

1.2 Exhaust Thermomanagement

As mentioned above, exhaust aftertreatment is a key factor for compliance with emission legislation, in future even more than today. Of course, this requires using adequate components like DOC, DPF, lean NO_x trap (LNT) or selective catalytic reduction (SCR) systems.

However, defining an aftertreatment system, comprising suitable catalysts and filters is not sufficient for achieving high conversion rates. Additionally, it must be ensured that these components will be operated under convenient conditions. Dependent from engine type, exhaust aftertreatment systems and emission targets this requires using adequate methods, hereinafter referred to as exhaust thermomanagement methods. Following tasks are of particular interest in this context:

- Catalyst heat up after engine cold start
- Maintaining catalyst temperature during low load operation
- Increase of the exhaust temperature for regeneration of a DPF
- Providing cylinder charge conditions appropriate for rich combustion mode (regeneration of LNT)

One of the greatest challenges concerning emission targets is achieving high conversion rates of catalysts already a short period of time after engine cold start. Since the conversion of catalysts is mainly dependent from the monolith temperature, a rapid heat up of the catalyst after engine cold start is necessary. Of course, high exhaust temperatures are beneficial for this purpose. However, when it comes to the exhaust mass flow, the effect on catalyst heat up is not that clear. Hence this effect should be considered in detail in the present work. In this context it has to be taken into account also that the heat up process is not the same for all catalysts. Besides the location and hence the upstream heat sink also the coating of the catalyst is relevant. This is due to the fact that a catalyst which provides exothermic reactions is able to support the heat up process. Hence the optimum heat up strategy may be not the same for a DOC and a SCR catalyst. Since nearly all aftertreatment concepts of modern diesel engines are featured with an oxidation catalyst – DOC or LNT – at the most upstream position of the EAS, this type of catalyst is considered in the present work when it comes to the thermal behaviour of aftertreatment components.

The second item of the listed above tasks – maintaining catalyst temperature – takes into account that exhaust thermomanagement is not finished after the catalyst light off. When the light off is achieved, it has to be ensured that the catalyst temperature subsequently does not drop below a critical level, what is challenging in particular during low load operation.

The additional listed methods, relevant for DPF regeneration and rich combustion could be understood also as part of exhaust thermomanagement. However, these issues are not considered in detail in the present work.

As mentioned above, the focus of this work is on evaluation of valve train variability in terms of exhaust thermomanagement methods. Nevertheless, it is worth mentioning that there are also alternative ways for exhaust thermomanagement. Widely spread is an increase of exhaust temperature by an adaption of the combustion process. For this purpose a retarded combustion – realized mainly due to a late main injection timing and/or the application of a post injection – is necessary [41]. Also the reduction of aspirated cylinder charge by means of a throttle located between compressor and intake manifold is an often used method for increasing the exhaust temperature [39]. Another way is the application of an electrical heater in the exhaust duct located ideally directly upstream the EAS [16, 20, 19]. These methods will be used in the present work as reference for the considered VVT methods.

1.3 Methodology

The evaluation of valve train variability – with special focus on exhaust thermomanagement – will be conducted in the present work by means of both simulation and measurement. The simulation allows considering a wide range of virtual hardware variations by means of a more or less negligible effort, compared to experimental investigations. This is relevant in particular for valve train variability. Moreover simulation enables analysing parameters (e.g. residual gas concentration in cylinders, wall heat flow in exhaust ports, ...) which could be not measured, or only by means of a very high effort. Also the benefit of simulation in terms of reproducibility should be mentioned in this context. However, needless to say, engine test bed measurement is inevitable when it comes to combustion engine development. On the one hand measurement results are necessary for the validation of the simulation model. On the other hand, there are – dependent from the simulation model – more or less parameters which could be not, or not in a sufficiently accurate way, evaluated by means of simulation. This applies e.g. for most pollutants (HC, CO, soot). Taking into account these matters, the combination of simulation and measurement seems to be reasonable. Not only for the present work, but for combustion engine development in general.

A detailed explanation of the used simulation models is given in chapter 2. The results calculated by these models should be discussed in chapter 3. The experimental investigations, which will be analysed in chapter 4, refer to engine test bed measurements on a state of the art passenger car diesel engine.

This engine – hereinafter referred to as engine A – which was considered also for the creation of the simulation model, is a modern 4-cylinder passenger car diesel engine, characterized by one stage turbo charging with a variable nozzle turbine, cooled low pressure exhaust gas recirculation (EGR) and uncooled high pressure EGR. The fuel injection equipment consists of a 1600 bar common rail system and solenoid injectors. The exhaust aftertreatment system comprises a DOC and a DPF in a close coupled canning. Due to this features the engine achieves – in series configuration – the EU 5 emission legislation. The valve train – in particular interesting for this work – is a chain driven DOHC valve train layout with 2 exhaust and 2 intake valves per cylinder. The valve actuation is done via roller finger followers.

2 Simulation Model

This chapter contains the most important fundamentals of the simulation models used in this work. Validation of simulation models by means of measurement data is another part of this chapter. In section 2.1 the 1-D engine model is considered while in section 2.2 the catalyst simulation is treated.

2.1 1-D Engine Cycle and Gas Exchange Simulation

Using numerical tools based on one-dimensional computerized fluid dynamics (CFD) for simulation of the engine working cycle is a wide spread method in the engine development process. Due to this, besides programs developed by research institutions (PROMO, THEMOS, ...), also several commercial software packages have been established. Most widely known commercial solutions are GT-POWER from Gamma Technologies and BOOST from AVL. Last mentioned software package was used for the creation of the engine model considered in this work.

Characteristic for engine models created with BOOST is a one-dimensional treatment of gas flow in pipes and ports of the intake and exhaust system. That means variables of state – as pressure or temperature – are calculated as function of time and one local dimension – in longitudinal direction of the pipe. For this reason, it seems to be clear that variables are considered homogeneous in the cross section of a pipe. All other engine components like cylinders or plenums are modelled zero-dimensional, hence without any local dependence.

For model creation, BOOST provides a graphical user interface. Thereby various elements, representing engine components (cylinder, pipes, turbocharger, ...), could be selected and parameterized.

2.1.1 Elements [26, 27]

The following section provides a mathematical description of the most important elements for the creation of an engine model in BOOST. The fundamental thermodynamic equations behind these elements as well as the main input parameters should be discussed subsequently. Further elements like coolers, filters, catalysts and so forth are assemblies of these basic elements. Further information concerning zero- and one-dimensional modelling of the engine process can be found in [21, 30].

Cylinder

As already mentioned the cylinder is treated zero-dimensional. The crank angle based calculation of cylinder state is done by the first law of thermodynamics, see equation 2.1. Due to this a conservation of energy is ensured. For the high pressure cycle this means a balance between change of internal energy in cylinder and the sum of piston work, fuel heat input,

wall heat losses and blow by enthalpy flow. During gas exchange also enthalpy flow through intake and exhaust ports has to be taken into account.

$$\frac{d(m_{\mathrm{Cyl}} \cdot u_{\mathrm{Cyl}})}{d\varphi} = -p_{\mathrm{Cyl}} \cdot \frac{dV_{\mathrm{Cyl}}}{d\varphi} + \frac{dQ_{\mathrm{Fuel}}}{d\varphi} - \frac{dQ_{\mathrm{W}}}{d\varphi} - h_{\mathrm{BB}} \cdot \frac{dm_{\mathrm{BB}}}{d\varphi} + \sum \frac{dm_{\mathrm{in}}}{d\varphi} \cdot h_{\mathrm{in}} - \sum \frac{dm_{\mathrm{exh}}}{d\varphi} \cdot h \tag{2.1}$$

The combustion is modelled by defining the rate of heat release through input of crank angle based functions derived from measurement data. The cylinder wall heat flow is calculated by means of Newton's approach for convective heat flow. However, this requires determining a model for the calculation of heat transfer coefficient. For the engine model considered in this work the AVL 2000 model [46] was selected. This approach is based on the well known model of Woschni/Huber. However, the calculation of the wall heat transfer coefficient during gas exchange was adapted.

Besides energy also the conservation of mass (equation 2.2) is taken into account by the cylinder element. The port mass flow rates are calculated based on the equation for steady state orifice flow. In this context the effective flow area dependent from valve lift is an important input parameter.

$$\frac{dm_{\mathrm{Cyl}}}{d\varphi} = \sum \frac{dm_{\mathrm{in}}}{d\varphi} - \sum \frac{dm_{\mathrm{exh}}}{d\varphi} - \frac{dm_{\mathrm{BB}}}{d\varphi} + \frac{dm_{\mathrm{Fuel}}}{d\varphi} \tag{2.2}$$

The relation between cylinder temperature and pressure is given by the equation of state for ideal gases, see equation 2.3.

$$p_{\mathrm{Cyl}} \cdot V_{\mathrm{Cyl}} = m_{\mathrm{Cyl}} \cdot R_{\mathrm{Cyl}} \cdot T_{\mathrm{Cyl}} \tag{2.3}$$

Formula 2.1, 2.2 and 2.3 build a set of non-linear differential equations which could be solved numerical.

Plenum

Plenums are zero-dimensional elements used e.g. for modelling exhaust or intake manifold. A plenum is based on the same equations as a cylinder. Of course terms for piston work, heat release and blow by losses disappear.

Pipe

As mentioned above, pipes are modelled one-dimensional. Hence, besides the time dependence, also variations and effects dependent from a local dimension x will be considered. Thus, conservation of mass can be defined as

$$\frac{\partial \rho}{\partial t} + \frac{\partial(\rho \cdot w)}{\partial x} + \rho \cdot w \cdot \frac{1}{A} \cdot \frac{\partial A}{\partial x} = 0 \tag{2.4}$$

Contrary to zero-dimensional elements also the conservation of momentum is taken into account, see equation 2.5.

$$\frac{\partial w}{\partial t} + w \cdot \frac{\partial w}{\partial x} + \frac{1}{\rho} \cdot \frac{\partial p}{\partial x} + \frac{1}{\rho} \cdot \frac{F_{\mathrm{f}}}{V} = 0 \tag{2.5}$$

The pipe wall friction (F_f) is calculated as a function of friction coefficient and Reynolds number. Laminar and turbulent friction coefficients are input parameters.

Formulating the energy balance for pipe flow delivers

$$\frac{\partial E}{\partial t} + \frac{\partial (w \cdot (E+p))}{\partial x} - \frac{\dot{Q}_\mathrm{W}}{V} = 0 \tag{2.6}$$

Therein E stands for specific total Energy, the summation of internal and kinetic energy.

$$E = \rho \cdot u + \frac{1}{2} \cdot \rho w^2 \tag{2.7}$$

The pipe wall heat flow (Q_W) in general is modelled by a Nusselt approach. Thereby the calculation of Nusselt number is done by means of Reynolds analogy.

In case of pipes modelling the intake and exhaust ports, the wall heat flow is calculated by means of an approach which is a modified version of this introduced originally from Zapf [47]. In contrast to the other pipes this means a crank angle dependent calculation of the heat transfer coefficient instead of a cycle averaged consideration. Hence, using this approach takes into account the extremely instationary characteristics of temperature, pressure and flow velocity versus crank angle in the ports. As shown in equation 2.8, this means a calculation of the exhaust port heat transfer coeffcient (α_EP) dependent from the temperature upstream exhaust valves (T_us), the instantaneous mass flow ($\dot{m}$), the inner valve seat diameter (d_V) and the valve lift (h_V). C_4, C_5 and C_6 are constants. The heat transfer coefficient in the intake ports will be calculated in a similar way.

$$\alpha_\mathrm{EP} = \left[\mathrm{C}_4 + \mathrm{C}_5 \cdot T_\mathrm{u} + \mathrm{C}_6 \cdot T_\mathrm{u}^2\right] \cdot T_\mathrm{us}^{0,44} \cdot \dot{m}^{0,5} \cdot d_\mathrm{V}^{-1,5} \cdot \left[1 - 0.797 \cdot \frac{x_\mathrm{V}}{d_\mathrm{V}}\right] \tag{2.8}$$

Turbocharger

The turbocharger calculation for steady state engine operation is based on a balance of mean power consumption of the compressor and mean power provided by the turbine. The averaging is done over a whole engine working cycle. The mechanical efficiency ($\eta_{\mathrm{m,\,TC}}$) considering bearing friction losses is an input parameter.

$$P_\mathrm{Comp} = \overline{\dot{m}_\mathrm{Comp} \cdot (h_{002} - h_{001})} = \eta_{\mathrm{m,\,TC}} \cdot P_\mathrm{Tb} = \eta_{\mathrm{m,\,TC}} \cdot \overline{\dot{m}_\mathrm{Tb} \cdot (h_{31} - h_{41})} \tag{2.9}$$

Enthalpy differences across compressor and turbine can be written as

$$h_{002} - h_{001} = \frac{1}{\eta_{\mathrm{s,\,Comp}}} \cdot c_{p,\,\mathrm{Comp}} \cdot T_{001} \cdot \left[\left(\frac{p_{002}}{p_{001}}\right)^{\frac{\kappa-1}{\kappa}} - 1\right] \tag{2.10}$$

$$h_{31} - h_{41} = \eta_{\mathrm{s,\,Tb}} \cdot c_{p,\,\mathrm{Tb}} \cdot T_{31} \cdot \left[1 - \left(\frac{p_{41}}{p_{31}}\right)^{\frac{\kappa-1}{\kappa}}\right] \tag{2.11}$$

The isentropic efficiency of compressor ($\eta_\mathrm{s,Comp}$) and turbine ($\eta_\mathrm{s,Turbine}$) are input parameters. However, the input of isentropic efficiencies depends on whether the turbocharger is defined

as simplified model or as full model. In the first case the input of mean isentropic efficiencies is done by constants. BOOST uses these constant parameters over the whole engine cycle. In contrast to the simplified model, the full model considers not only mean values but calculates an instantaneous wheel speed by considering the momentum balance of the turbocharger wheel every time step (equation 2.12). Simultaneously isentropic efficiencies defined as functions of mass flow, pressure ratio and wheel speed are updated. Hence, considering the turbocharger as full model requires the input of characteristic maps for the compressor as well as for the turbine. In case of a VNT there are even more maps required, representing the turbine behaviour of different vane positions. Since the simplified model does not calculate the wheel speed it is not qualified for modelling dynamic engine operation.

$$\frac{d\omega_{\mathrm{TC}}}{dt} = \frac{1}{I_{\mathrm{TC}}} \cdot \frac{P_{\mathrm{Tb}} - P_{\mathrm{Comp}}}{\omega_{\mathrm{TC}}} \tag{2.12}$$

Formula Interpreter

A Formula Interpreter allows conducting calculations of a self-developed code during simulation. These opportunity was used for the present model in an extensive way. For instance this option offers the definition of wall temperatures dependent from parameters which vary versus simulation time (fuel mass, gas temperatures, ...). Another application of the formula interpreter in this work concerns the calculation of virtual thermo couple temperatures. The motivation for doing so will be explained in section 4.5.1.

2.1.2 Evaluation of Base Engine Model

As base for development and validation of the engine model, engine A (see also section 1.3), a state of the art 4-cylinder diesel engine with one stage turbo charging and low pressure EGR was considered. Since at the beginning of this work an engine model has not existed, the model creation started from scratch. Of course, a considerable part of time spent in the present work was consumed by model development. However, the focus of this work is on engine development and not on simulation methodology. Hence only the evaluation of the final model version is considered subsequently. The model creation process with all its intermediate steps is not discussed in detail.

For evaluation purpose following boundary conditions were used:

- The combustion is defined by relative rate of heat releases, calculated by analysing measurement results of cylinder pressure indication. The injected fuel mass was controlled in order to achieve the measured engine load.
- The turbo charger was modelled by using swallowing capacity and efficiency maps for compressor and turbine (full model). The VNT position of the turbine was controlled in order to achieve the measured compressor mass flow.
- The low pressure EGR valve was controlled in order to reach the measured rate of recirculated exhaust gas.
- The charge air cooler (CAC) was modelled by using the measured gas temperature in intake manifold as target value.

For evaluation of the gas exchange, full load operation will be considered. Although full load is not the main focus of the present work it is adequate for modell verification due to covering a wide range of engine speeds. This is important in particular when it comes to validation of parameters relevant for volumetric efficiency, which is a well known parameter for characterization of gas exchange quality in internal combustion engines. Dependent from the reference position it covers valve lift timings, turbo charging, several flow restrictions and gasdynamic effects. The left chart in figure 2.1 shows a comparison of measured and calculated volumetric efficiency related to the position downstream charge air cooler ($\eta_{v,2\_1}$). Hence, the good correlation of plotted curves means a good model accuracy concerning valve lift timings, flow behaviour of intake manifold and ports as well as internal EGR.

To include also turbo charging in evaluation by means of volumetric efficiency, the reference conditions are switched to those upstream compressor ($\eta_{v,001}$, figure 2.1 – right). Also this characteristic shows a good correlation between simulation and measurement. Compared to the more downstream reference condition, this defintion delivers higher values since it contains the pressure increase across the compressor and the temperature decrease in the charge air cooler. Although correlation of measured and calculated volumetric effiecienies is good, slight differences across the whole operation area can not be avoided entirely. Nevertheless, when it comes to validation of other engine characteristics (discharge coefficients, exhaust gas temperatures, ...) having exactly equal mass flows of measurement and simulation is an advantage. Hence, the compressor pressure ratio used in the simulation model is defined in order to achieve exactly the same mass flows as in measurement. However, it should be mentioned that this leads only to very small differences between measured and calculated compressor pressure ratio.

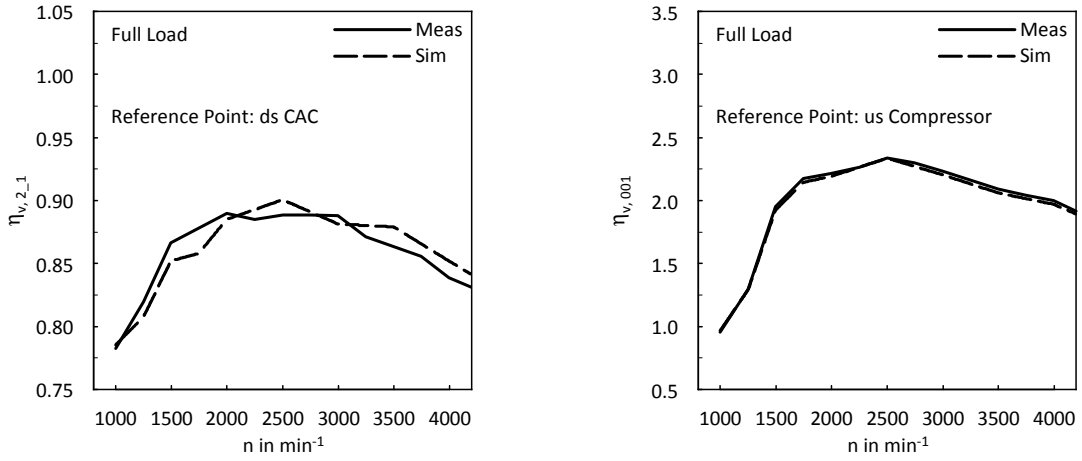

Figure 2.1: Comparison of measurement and simulation concerning volumetric efficiency under full load operation

Another relevant parameter concerning gas exchange is the PMEP (Pumping Mean Effective Pressure). It is of particular interest when it comes to evaluation of gas exchange effects

on overall engine efficiency and hence on fuel consumption. A good correlation between measurement and simulation can be identified also in this context, see figure 2.2.

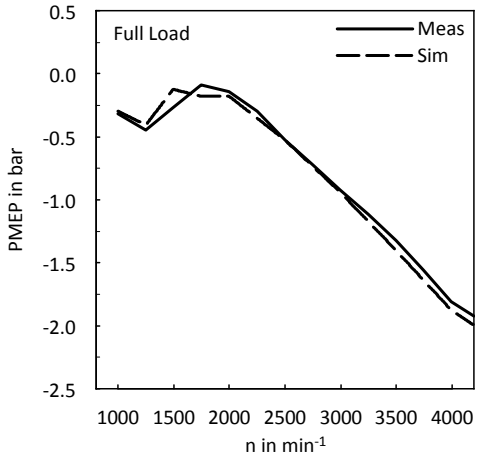

Figure 2.2: Comparison of measurement and simulation concerning pumping mean effective pressure unter full load operation

Moreover full load operation was used to identify flow coefficients of air filter, charge air cooler and other parts of the intake and exhaust system. The characteristic of discharge coefficients versus mass flow identified in this way are used for subsequently conducted calculations. As an example, figure 2.3 shows the pressure drop (ΔP_{CAC}) and the discharge coefficient ($\mathrm{DC}_{\mathrm{CAC}}$) of the charge air cooler (CAC). The discharge coefficient was adapted in order to achieve the measured pressure drop. Besides the CAC flow characteristics calculated based on analysing full load operation (dashed curves) also curves based on part load operation (dash-dotted curves) are illustrated. As obvious the pressure drop is more or less only dependent from mass flow. Moreover this chart points out the wide operation range of the full load curve, which is a main reason why it was used for model validation.

Since the focus of this work is on exhaust thermomanagement, special interest is spent to exhaust temperatures and fuel consumption. The charts in figure 2.4 show a good correlation of measurement and calculation concerning both break specific fuel consumption (BSFC) and exhaust gas temperature upstream turbine (T_{31}). Of course, this good correlation is not only due to the correct modelling of gas exchange but also considerably affected by the high pressure cycle. However, in contrast to the gas exchange, there exist only a few parameters relevant for the high pressure cycle, what is typical for this sort of models. This is true especially for defining the combustion process in a predictive way, as it is done in this work. Besides combustion, the high pressure cycle is mainly dominated by cylinder wall heat flow. As explained in section 2.1.1 this effect is modelled by means of the AVL 2000 approach. An adaption by defining a cylinder wall heat calibration factor higher or lower than one was not done. Another relevant effect for the exhaust temperature is modelling the wall heat transfer in exhaust ports. As mentioned also in section 2.1.1, a model similar to these published originally by Zapf [47] was used for this purpose.

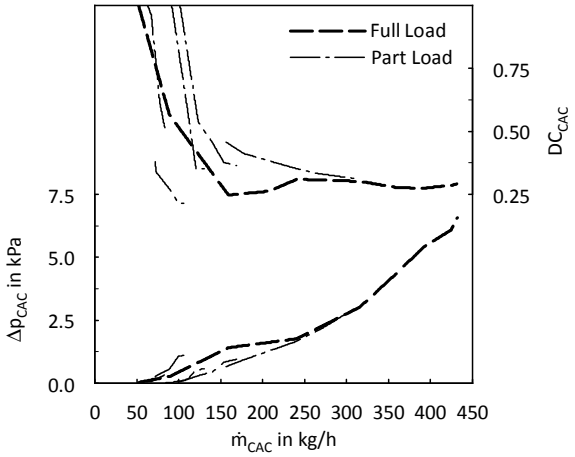

Figure 2.3: Comparison of part load and full load operation concerning calculated pressure drop and discharge coefficient of the charge air cooler. The discharge coefficients used in the simulation model were defined in order to achieve a correlation between measured and calculated pressure drops.

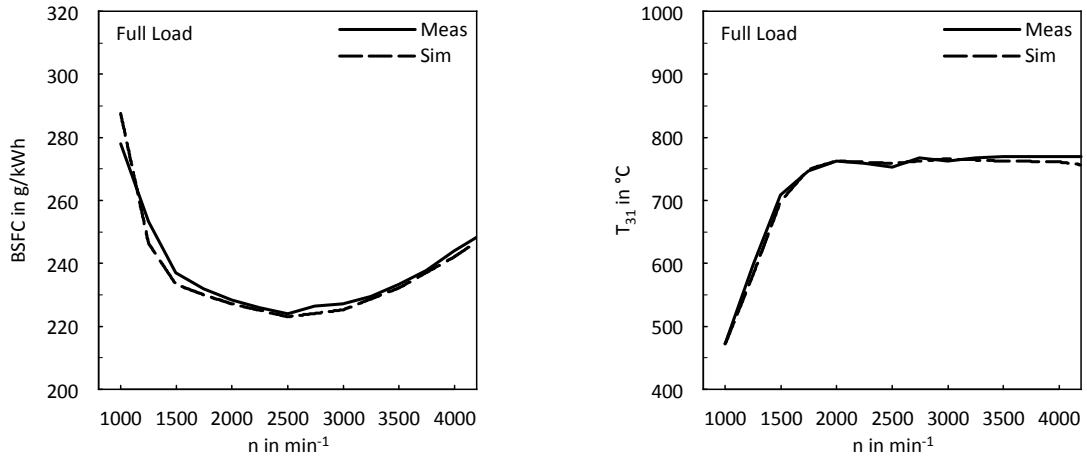

Figure 2.4: Comparison of measurement and simulation concerning specific fuel consumption and exhaust temperature upstream turbine under full load operation

Assuming a conventional layout of the exhaust aftertreatment system characterized by an arrangement of catalysts and filters downstream turbine, the relevant exhaust temperature is not the considered above T_{31} (upstream turbine) but T_{41} (downstream turbine). Hence also a correct modelling of the temperature drop across turbine is essential. This temperature drop has two reasons: Expansion of exhaust gas by delivering energy ($\dot{H}_{\mathrm{Tb}}$) to the turbine wheel and wall heat flow through turbine housing ($\dot{Q}_{\mathrm{W,\,Tb}}$). The first effect will be calculated by equation 2.13. Given that the turbine efficiency (η_{Tb}) is known, the calculation could be performed very accurate.

$$\dot{H}_{\mathrm{Tb}} = \dot{m}_{\mathrm{Tb}} \cdot c_{p,\,\mathrm{Tb}} \cdot T_{31} \cdot \eta_{\mathrm{Tb}} \cdot \left[1 - \left(\frac{1}{\pi_{\mathrm{Tb}}} \right)^{\frac{\kappa-1}{\kappa}} \right] \tag{2.13}$$

The second effect – turbine wall heat flow ($\dot{Q}_{\mathrm{W,\,Tb}}$) – is taken into account by equation 2.14. As obvious this equation contains a heat transfer factor (f_{α}), which has to be defined based on analysing measurement data. Hence it seems to be clear that this phenomenological approach is subject to uncertainties.

$$\dot{Q}_{\mathrm{W,\,Tb}} = \dot{m}_{\mathrm{Tb}} \cdot c_{p,\,\mathrm{Tb}} \cdot \left(\frac{T_{31}}{T_{\mathrm{W,\,Tb}}} - 1 \right) \cdot \left(1 - e^{-\frac{\mathrm{f}_{\alpha} \cdot \alpha \cdot A_{\mathrm{W,\,Tb}}}{c_{p,\,\mathrm{Tb}} \cdot \dot{m}_{\mathrm{Tb}}}} \right) \tag{2.14}$$

However, turbine wall heat losses are extremely relevant, especially in part load operation. This fact is pointed out in figure 2.5 by considering measurement data of low load operation at 1000 min^{-1}. A low turbine pressure ratio (π_{Tb}) and a low turbine efficiency – both typical for one stage turbo charged diesel engines in part load – lead to a low expansion work delivered by turbine. Due to this, the temperature drop ($T_{31} - T_{41,\,\mathrm{ad}}$) resulting from expansion in turbine is low or nearly disappears. However, considering the measured temperature downstream turbine (T_{41}), makes obvious a considerable overall temperature drop ($T_{31} - T_{41}$), which is an evidence for high wall heat losses. In other words, nearly the entire temperature drop across turbine – observed in this operation area – is caused by wall heat flow and not by delivering energy to the turbo charger wheel.

As explained above, considering the full load operation curve is essential for validation and adaption of the simulation model. However, since exhaust thermomanagement is a part load issue, also this operation area has to be covered by the validation process. Figure 2.6 gives an survey of the considered part load operation area. To point out the relevance of this operation area, also 14 mode operation points are plotted. These 14 steady state operation points and their weighting factors are representative for a WLTP (Worldwide harmonized Light Vehicles Test Procedure). The operation points were calculated for the considered engine in combination with a medium-sized passenger car.

As example for validation of part load operation, figure 2.7 shows low load operation points at 1000 min^{-1} (see figure 2.6). These operation area is particularly interting for exhaust thermomanagement since it is part of the first time section of nearly all relevant driving cycles. As obvious there is a good correlation of measurement and simulation concerning most critical parameters in this matter – fuel consumption (BSFC) and exhaust temperatures (T_{31}, T_{41}).

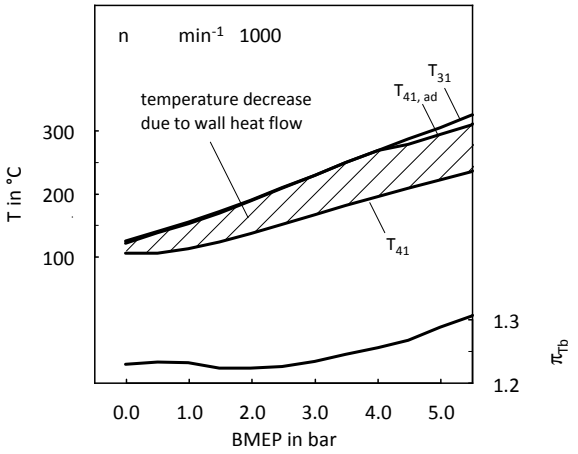

Figure 2.5: Share of expansion and wall heat flow in temperature drop across turbine for low engine load and low turbine pressure ratios

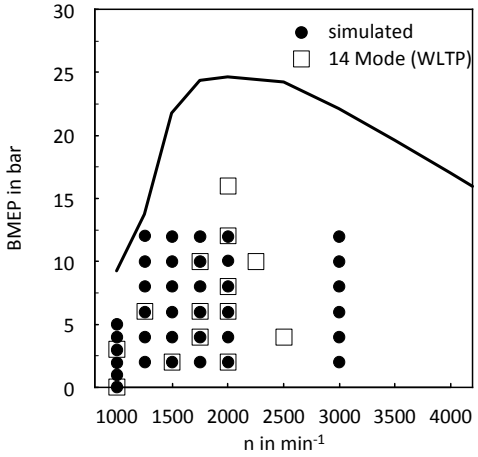

Figure 2.6: Overview of part load operation points considered for evaluation of base engine simulation model

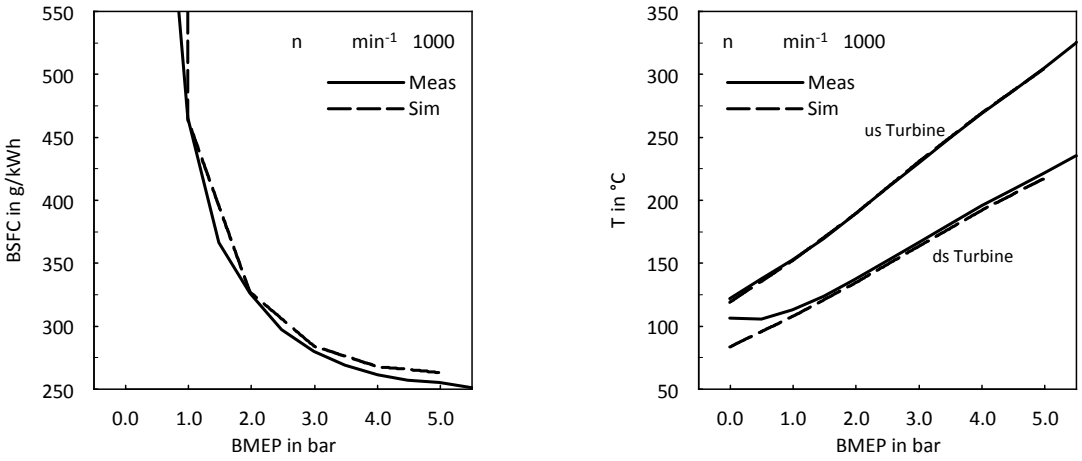

Figure 2.7: Comparison between measurement and simulation concerning specific fuel consumption and exhaust temperatures at 1000 min^{-1} and low engine load

2.2 Catalyst Simulation

As mentioned in chapter 1, exhaust aftertreatment and hence exhaust thermomanagement becomes more and more important for passenger car diesel engines. Thus, the simulation should be able to evaluate relevant effects on the exhaust aftertreatment system caused by various operation strategies (e.g. variation of valve timings). Due to this, additional to the engine model, which considers the aftertreatment system only in terms of flow resistance, a separate model of a catalyst was created using the aftertreatment environment of the simulation software BOOST (BOOST Aftertreatment). The motivation for doing so is having a more detailed look on the thermal behaviour of the catalyst. However, chemical reactions were not considered. The catalyst model comprises besides the monolith only a pipe for inflow and another for outflow of exhaust gas, see figure 2.8. Similar to the pipe element explained in section 2.1.1, also the catalyst in BOOST Aftertreatment is modelled one-dimensional. Hence it is based on the same framework of conservation equations. However, there are differences concerning the thermal behaviour. Contrary to a simple pipe in the engine model, the catalyst model comprises several layers which are characteristic for the components of a catalyst (wash coat, substrate, canning). In other words the properties (thermal behaviour, flow resistance) of a real monolith which has thousands of channels is concentrated in one single channel which interacts with the exhaust gas flow in the same way as the real monolith does. The temperature of the layers will be calculated in every time step, dependent from the surrounding layers, the ambient conditions and the instantaneous gas properties. Thus, a transient heat up or cool down process of the catalyst could be considered.

As mentioned in chapter 1, a special focus of exhaust thermomanagement methods is on the catalyst which is relevant for oxidation of HC and CO emissions. For the known aftertreatment concepts of state of the art passenger car diesel engines this is either a DOC or a LNT, located at the most upstream position of the EAS. Hence, the specification – geometry and material

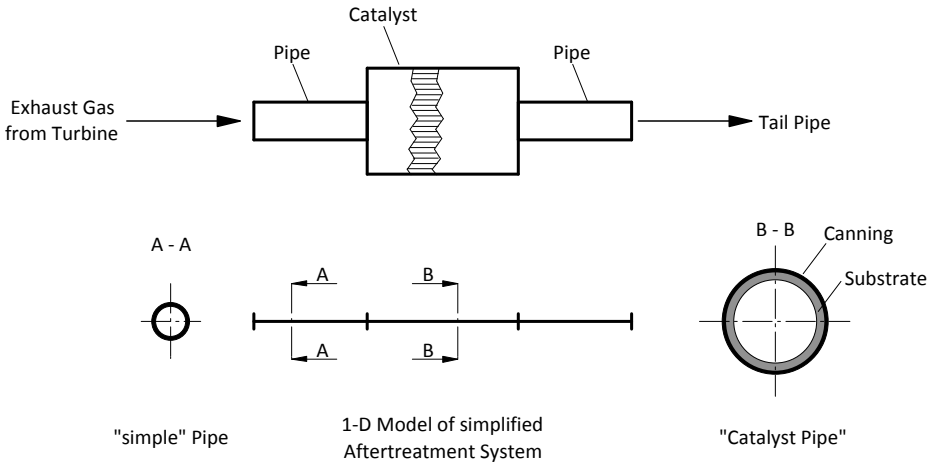

Figure 2.8: Modelling of a simplified exhaust aftertreatment system by means of 1-D CFD

properties – of the catalyst model was defined in a way that it is suitable for a DOC of the considered engine (diesel engine with a displacement of about 2 l).

The boundary conditions of the catalyst model are defined by mass flow, temperature and composition (air excess ratio) of the exhaust gas upstream catalyst and the pressure downstream catalyst. With respect to the flow regime upstream the catalyst observed in the engine model, the boundary conditions are defined stationary. This allows a larger time step size compared to the crank angle based engine cycle simulation, what is of course beneficial when it comes to calculation time. In addition to the boundary conditions also the initial temperature of the catalyst – relevant for all layers – has to be defined.

The most relevant result of the catalyst simulation is the monolith temperature versus its length, available at every time step during the heat up or cool down process of the catalyst. For the present work, the model was applied usually for a full factorial set of exhaust mass flows and temperatures (boundary conditions). This enables considering the effect of exhaust temperature and mass flow on catalyst temperature by means of 2 dimensional maps (see e.g. figure 3.3). These maps refer to a defined time after start of heat up or cool down process as well as to a defined position between the entry and the exit cross section of the catalyst. Of course, instead of the temperature in a single cross section, also the mean value of the whole catalyst could be considered. Moreover these maps refer in general to a given air excess ratio. However, simulations have shown that the effect of air excess ratio is negligible compared to the effect of exhaust temperature and mass flow. This applies at least for the air excess ratio range which is relevant for diesel engines.

3 Simulation Results

This chapter contains results calculated by means of the simulation models – engine model and catalyst model – introduced in chapter 2. The main focus of simulation was on pointing out fundamental effects of VVT strategies, which are relevant for increasing exhaust temperature and enthalpy flow. As explained later, this requires considering not only exhaust temperature but also mass flow.

Section 3.1 deals with evaluation methods used in this work for assessment of different VVT strategies. Special attention was paid to fuel consumption in this context. The aim of section 3.2 is finding out conditions of exhaust gas (temperature, mass flow) adequate for typical exhaust thermomanagement tasks like rapid heat up of a catalyst or maintaining catalyst temperature. Section 3.3 offers a discrimination of valve lift strategies concerning fundamental heat up effects. Section 3.4 provides a detailed discussion of most promising VVT strategies in context of exhaust thermomanagement. In section 3.5 these strategies are compared to each other concerning typical objectives of exhaust thermomanagement like rapid heat up or maintaining temperature of a catalyst.

3.1 Evaluation Methodology

The comparison of different VVT strategies for exhaust thermomanagement requires an adequate evaluation methodology. Thus, in a first step objective parameters must be defined. It seems to be clear that all exhaust thermomanagement methods shall achieve a low fuel consumption and hence a high efficiency. However, it is not so easy when it comes to characterize parameters available from engine cylce simulation results which are relevant for catalyst temperature. At least not without modelling the thermal behaviour of the catalyst. As examined in section 3.2 in detail, neither exhaust gas temperature nor enthalpy flow is an adequate objective parameter for exhaust thermomanagement methods in general. Due to this, it is challenging to find an approach which is convenient for the assessment of all considered exhaust thermomanagement methods. Subsequently two possible ways are introduced.

3.1.1 Energy Balance based Approach

Considering energy balance is an established way for evaluation of engine operation strategies. Hence, applying this approach for evaluation of VVT methods in context of exhaust thermomanagement seems to be reasonable. However, characteristic of this evaluation strategy is considering the exhaust enthalpy flow and hence the product of exhaust temperature and mass flow. Thus, the energy balance based approach seems to be not convenient for evaluation of methods applied for thermomanagement tasks requiring a high exhaust temperature regardless of consequences to mass flow. Of course, it is even less reasonable for evaluation of

strategies which benefit from a reduction of mass flow – e.g. methods for maintaining catalyst temperature during low load operation, refer to section 3.2. Nevertheless, there are also known applications which profit not only from a high exhaust temperature but also from a high mass flow and hence a high enthalpy flow. Apart from that, the evaluation by means of the energy balance should be discussed in any case, since it provides an valuable contribution for understanding of effects relevant for exhaust thermomanagement.

Formula 3.1 shows the energy balance of an engine using the system boundaries shown in figure 3.1. Characteristic for this definiton of boundaries is crossing the exhaust flow between turbine and exhaust aftertreatment system. This position is labelled in the present work with the number 41. Hence $\dot{H}_{\text{exh }41}$ in equation 3.1 is defined as the exhaust enthalpy flow upstream the catalyst. Special attention must be paid to the supplied intake enthalpy flow $\dot{H}_{\text{in}}$. In case of a low pressure exhaust gas recirculation, $\dot{H}_{\text{in}}$ comprises not only intake air, but also recirculated exhaust gas. $\dot{Q}_{\text{Fuel}}$ considers the heat release resulting from combustion of supplied fuel while P_{eff} stands for the mechanical power output and $\dot{Q}_{\text{Loss}}$ for the entire heat losses over system boundaries, comprising heat flow in cylinders, ports, pipes, CAC and so forth.

$$\dot{H}_{\text{exh }41} = \dot{H}_{\text{in}} + \dot{Q}_{\text{Fuel}} - P_{\text{eff}} - \dot{Q}_{\text{Loss}} \tag{3.1}$$

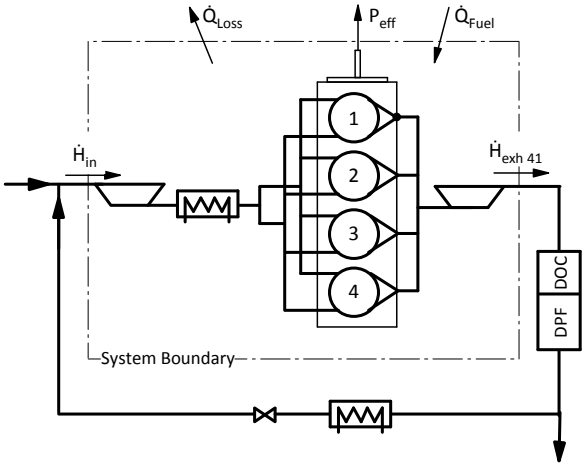

Figure 3.1: System boundary and energy flows considered for the energy balance of the overall engine

Studying the energy balance makes clear that a reduction of heat losses ($\dot{Q}_{\text{Loss}}$) – while keeping constant power output (P_{eff}), supplied fuel energy ($\dot{Q}_{\text{Fuel}}$) and intake enthalpy flow ($\dot{H}_{\text{in}}$) – is the most obvious way when it comes to efficient strategies for increasing exhaust enthalpy flow ($\dot{H}_{\text{exh }41}$). A well known method for illustration of these energy flows is by means of bar charts, see figure 3.2 (right). To reduce the number of considered parameters, the intake enthalpy flow is – appropriately signed – added to the heat losses. That means, whenever speaking subsequently from heat losses in context of this evaluation method, the heat losses reduced by the enthalpy of intake flow is meant. Besides the base (0) and the

strategy of exhaust enthalpy increase only by means of declining heat losses (1), two more bars are illustrated. Applying strategy (2) does not affect heat losses, hence an increase of fuel energy leads to an increase of exhaust enthalpy in the same degree. Since the increase of exhaust enthalpy is as high as in case of (1) while the supplied fuel energy is higher, it seems to be clear that this strategy is less efficient. However, it is more efficient than a strategy characterized by an identical increase of exhaust enthalpy and wall heat losses (3).

The left chart in figure 3.2 shows another way for illustration of the discussed idealised exhaust thermomanagement methods. As obvious the exhaust enthalpy flow ($\dot{H}_{\mathrm{exh\,41}}$) is plotted versus heat losses ($\dot{Q}_{\mathrm{Loss}}$). Hence the bars of the right chart appear as dots in this diagram. The curves connecting the results of the mentioned above idealised strategies – (1), (2) and (3) – with the base dot (0), illustrate the interaction of variation in heat losses and exhaust enthalpy flow for these methods. Consequently, these curves are characteristic for exhaust thermomanagement efficiency. To evaluate the effect of exhaust thermomanagement methods – e.g. realized by alternative valve timings – on exhaust enthalpy flow and heat losses, the $\dot{H}_{\mathrm{exh\,41}}$ versus $\dot{Q}_{\mathrm{Loss}}$ characteristics of these methods can be plotted in the same chart and hence compared with the idealised strategies.

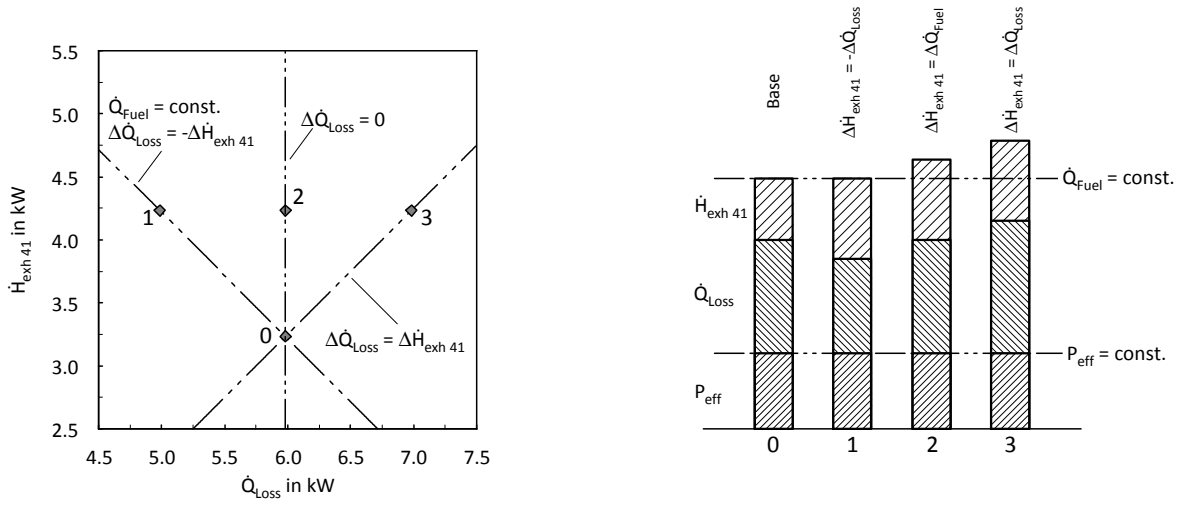

Figure 3.2: Considering idealised exhaust thermomanagement methods by means of an enthalpy flow versus heat losses illustration and by means of a bar chart

3.1.2 Evaluation based on Catalyst Maps

As it will be pointed out in detail in section 3.2, exhaust mass flow and temperature do not affect all exhaust thermomanagement objectives – heating up a catalyst, maintaining catalyst temperature – in the same way. For instance in case of heating up a large underfloor SCR catalyst, the exhaust mass flow is clearly more relevant than for heating up a small close coupled DOC. Since enthalpy flow depends from mass flow and temperature in the same way, the energy balance based evaluations are not adequate for all exhaust thermomanagement tasks.

The evaluation of the catalyst temperature (solid temperature) instead of the exhaust temperature and mass flow is one way to overcome this problem. However, doing so requires modelling the thermal behaviour of the catalyst. Due to the fact that reactions from the catalyst heat up process to the engine working cycle could be neglected, a dynamic interaction between engine and catalyst model is not necessary. Hence the catalyst is considered – as explained in section 2.2 – in a separate model. The connection does only exist by means of mass flow, temperature and composition of exhaust gas. Thus, the catalyst model was applied for a full factorial pattern of different exhaust mass flows and temperatures. The results of these calculations could be illustrated by means of two dimensional maps, see figure 3.3. Strictly speaking, these maps are relevant only for one composition of exhaust gas. However, results have shown that the effect resulting from variations in air excess ratio – while keeping constant temperature and mass flow of exhaust gas – on catalyst heat up or cool down process is negligible.

Dependent from the objective of the considered exhaust thermomanagement task, the temperature in a certain cross section – e.g. entry or exit – as well as the mean temperature of the whole catalyst may be considered. Of course, these charts refer to a certain time after start of heat up or cool down process. When it comes to initial conditions, assuming a thermal equilibrium between catalyst and ambient seems to be reasonable. In terms of methods developed for application in test procedures the ambient conditions are defined by legislation. In the present work the initial catalyst temperature of a heat up process is 25 °C, if not expressly differently declared. The maps illustrated exemplarily in figure 3.3 show the catalyst temperature at two different positions and periods of time after the start of the heat up process. The left chart shows catalyst temperature in the entry cross section ($T_{\mathrm{Cat,\,0mm}}$) after 10 seconds. As obvious the catalyst temperature is nearly independent from mass flow, what is reasonable for the considered position. The right chart provides the same information for a cross section 75 mm downstream entry after 120 seconds ($T_{\mathrm{Cat,\,75mm}}$). It can be seen clearly that the catalyst temperature at this position is affected not only by the exhaust temperature but also by the mass flow. In the next section (3.2) illustrations like these are used to find out most beneficial relations of mass flow and temperature for different exhaust thermomanagement tasks, e.g. heating up the catalyst. Since gas exchange simulation delivers the effect of adjusting arbitrary engine parameters on exhaust temperature and mass flow upstream catalyst, by means of the introduced catalyst temperature maps it is easy to find out the corresponding effect on catalyst temperature. This is used in section 3.5 for analysing the effect of VVT methods on the catalyst temperature.

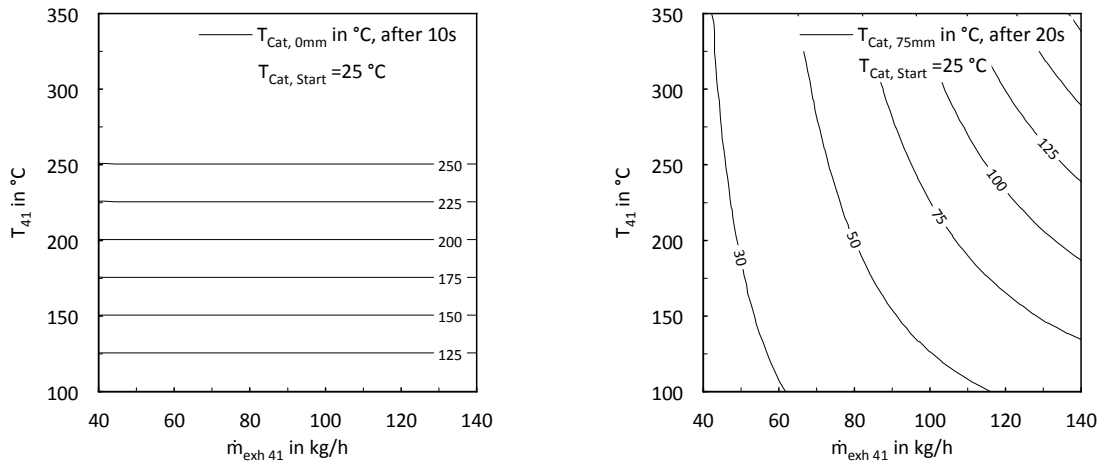

Figure 3.3: Catalyst monolith temperatures dependent from exhaust temperature and mass flow considered during a heat up process, in the entry cross section after 10 seconds (left) and in a cross section 75 mm downstream entry after 20 seconds (right)

3.2 Preliminary Investigations concerning Catalysts

The aim of the following preliminary investigations is to find out the influence of exhaust temperature and mass flow on catalyst heat up and cool down processes. It seems to be clear that an increase in exhaust temperature in combination with a constant mass flow accelerates the heat up process. Since the reduction of overall aspirated cylinder mass and hence exhaust mass flow is a relevant strategy for gaining exhaust temperature, see section 3.3, also the consequences of an increase in temperature in combination with a decrease in mass flow should be considered.

As pointed out in chapter 1, various exhaust aftertreatment system (EAS) layouts are used for today's passenger car diesel engines. Nearly all concepts use at the most upstream position a catalyst which is able to convert HC and CO emissions. A rapid heat up of this catalyst – which is dependent from the EAS concept an oxidation catalyst (DOC) or a lean NO_x trap (LNT) – is a key factor for achieving low HC and CO emissions. Hence also the focus of exhaust thermomanagement methods is on this catalyst. Thus, for calculation of the subsequently discussed results a catalyst with the properties of a DOC was considered. Since chemical reactions are not taken into account, this concerns only the thermal behaviour (heat capacity, heat conductivity, ...). The dimensions of the modelled catalyst were defined with respect to the considered engine. For more information to the catalyst model refer to section 2.2.

The left chart in figure 3.4 shows the catalyst temperature in the entry cross section ($T_{\mathrm{Cat,\,0mm}}$) after 10 seconds of a heat up process, which is characterized by a steady-state exhaust mass flow ($\dot{m}_{\mathrm{exh\,41}}$) and temperature ($T_{41}$). The short period of time was chosen with regard to the fact that exceeding the light off temperature would require modelling exothermic reactions in the catalyst model. By means of markers for engine operating points

and curves of constant enthalpy flow the effect of different exhaust temperature increasing methods on catalyst temperature is shown. Both keeping constant mass flow (1) and keeping constant enthalpy flow (2) was considered. Also the consequences of increasing mass flow while remaining constant temperature (3) is illustrated. The base conditions are typical for a low load operation point. It is obvious that the catalyst temperature in the entry cross section is independent from mass flow. Hence it makes no difference whether the mass flow or the enthalpy flow is kept constant while increasing the exhaust temperature. Of course, raising exhaust mass flow while remaining constant temperature has no effect on catalyst temperature at this position. However, at a more downstream catalyst position the situation is quite different. This could be figured out by analysing the right chart, which provides the same information after 20 seconds for a cross section half of the total catalyst length (75 mm) downstream the entry. Comparing both charts, a higher significance of mass flow at the more downstream positon can be seen. A higher gradient of constant catalyst temperature curves ($T_{\mathrm{Cat},75\mathrm{mm}}$) compared to this of the constant enthalpy flow curves ($\dot{H}_{\mathrm{exh}\,41}$) means even a higher significance of mass flow compared to this of temperature.

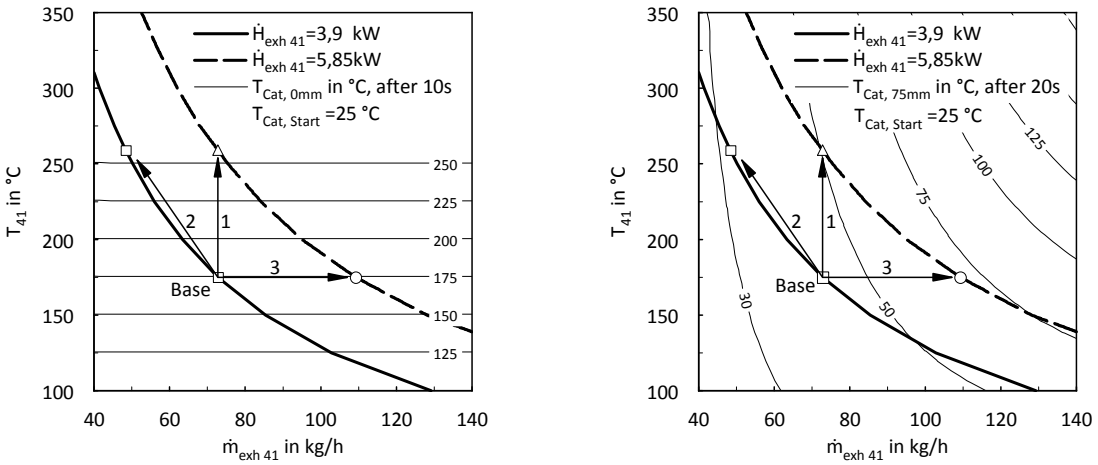

Figure 3.4: Effect of exhaust temperature and mass flow on the catalyst temperature in the entry (left) and in a more downstream cross section (right) during a heat up process

In figure 3.5 the characteristic of catalyst temperature versus catalyst length can be seen for the boundary conditions – exhaust temperature (T_{41}) and mass flow ($\dot{m}_{\mathrm{exh}\,41}$) – marked in figure 3.4. Based on the fact that the released heat resulting from the light off in the first section of a DOC will support the heat up of the more downstream part, only the first 40mm are considered. The left chart shows a comparison of exhaust temperature increase at constant mass flow (dash-dotted curve) and constant enthalpy flow (dotted curve). In addition also the characteristic of the catalyst temperature resulting from the base conditions is plotted. Independent from mass flow and hence from enthalpy flow, the increase of catalyst temperature in the very first section of the catalyst is equal to the exhaust temperature increase – from 175 to 258 °C. In case of the lower enthalpy flow ($\dot{H}_{\mathrm{exh}\,41} = 3,9\,\mathrm{kW}$) the drop of the catalyst temperature versus catalyst length is clearly more significant. About 30 mm

downstream the entry, the catalyst temperature is even lower than this achieved with base conditions. This comparison supports the assumption that exhaust gas enthalpy flow is a more convenient parameter for evaluation of heat up strategies than exhaust temperature. However, it has to be considered that also an increase in mass flow at a constant temperature will lead to a higher enthalpy flow. The right chart in figure 3.5 points out that this strategy (dashed curve) leads to a clear drawback concerning catalyst temperature in the upstream part compared to achieving the same enthalpy increase at a constant mass flow and hence an increasing temperature (dash-dotted curve).

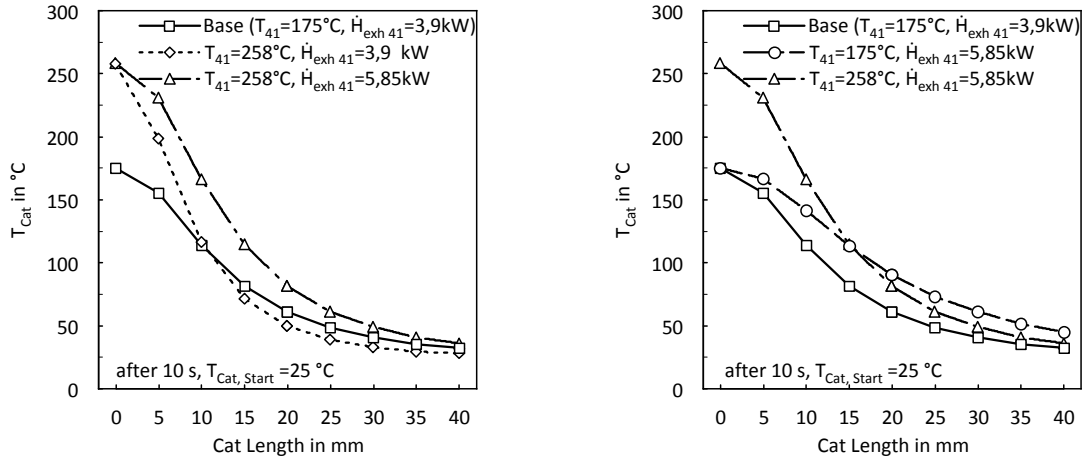

Figure 3.5: Catalyst temperature versus catalyst length for various exhaust temperatures and mass flows

Keeping in mind that fuel consumption is a critical parameter also in case of exhaust thermomanagement methods, not only the catalyst temperature but also the efficiency of the heat up process has to be considered. Figure 3.6 shows the distribution of enthalpy available at catalyst entry ($H_{\mathrm{exh}\,41}$) to internal energy (U_{Cat}), heat transferred via wall to ambient (Q_{W}) and enthalpy downstream catalyst ($H_{\mathrm{exh}\,\mathrm{TP}}$, Tail Pipe).

This breakdown is considered versus mass flow ($\dot{m}_{\mathrm{exh}\,41}$). Since exhaust enthalpy flow is kept constant ($\dot{H}_{\mathrm{exh}\,41} = 3,9\,\mathrm{kW}$), an increase of mass flow means a decrease of exhaust temperature. The higher the internal energy flow which is directly proportional to the increase of mean catalyst temperature, the higher the efficiency. The distribution after 10 seconds (left chart) as well as this after 30 seconds (right chart) shows a benefit of low mass flows and hence high temperatures. However, the wall heat losses are slightly higher in case of high temperatures and low mass flows. Comparing both charts a slightly decreasing efficiency over heat up time could be derived. This effect could be explained by the decrease of difference between exhaust temperature and monolith temperature, which is relevant for heat flow from the gas to the monolith. The decreasing difference comes from the increase of monolith temperature and the stationary exhaust temperature.

A short gas path with a small heat capacity between exhaust valves and catalyst is a key factor for a rapid heat up of the catalyst. For considering the effect of this upstream heat

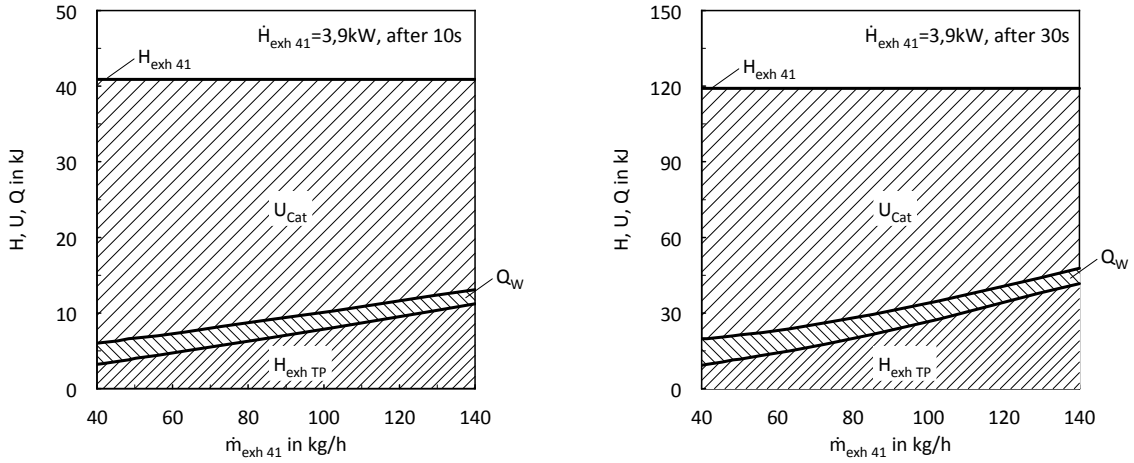

Figure 3.6: Distribution of enthalpy available upstream catalyst to internal energy of the catalyst, wall heat losses and enthalpy downstream catalyst after 10 (left) and 30 (right) seconds

capacity on a catalyst heat up process, a pipe upstream the catalyst was implemented in the model. Of course, the considered gas path including the exhaust ports, the exhaust manifold and the turbine housing of a real engine is not as simple as a straight pipe. Nevertheless, in case of this preliminary investigation it seems to be an adequate model. The pipe parameters (length, diameter, wall thickness) were chosen with respect to this simplification.

Figure 3.7 shows – similar to the illustrations in figure 3.6 – the break down of exhaust enthalpy upstream the additional heat sink and the catalyst (H_{exh}). As obvious, H_{exh} is spent not only to the internal energy of catalyst (U_{Cat}), the heat transferred via wall to the ambient (Q_{W}) and the enthalpy downstream catalyst ($H_{\mathrm{exh\,TP}}$) but also tho the internal energy of the additional pipe (U_{Pipe}). It can be seen that a low mass flow and hence a high temperature will lead to a higher $\dot{U}_{\mathrm{Pipe}}$ than a high mass flow and a low temperature. It can be seen also that this effect nearly compensates the difference in enthalpy flow downstream catalyst. Both U_{Pipe} and $H_{\mathrm{exh\,TP}}$ mean a decrease of catalyst heat up efficiency. Hence, depending on heat capcacity of the exhaust system which is modelled by the additional pipe, the efficiency advantage of high exhaust gas temperatures becomes smaller or even inverts in a disadvantage.

Nevertheless, as figure 3.7 (right) shows, the catalyst temperature in the first section is still higher in case of high temperatures and low mass flows. However, it can be seen that the difference is smaller when taking into account the additional upstream heat sink. Moreover the intersection point between the high temperature ($T_{\mathrm{exh}} = 258\,°C$) and the low temperature ($T_{\mathrm{exh}} = 175\,°C$) strategy is shifted to a more downstream position when the additional heat sink is considered.

After achieving the catalyst light off, the drop of catalyst temperature below a critical temperature must be avoided. This is a challenge particularly during low load operation. Hence exhaust thermomanagement methods are relevant not only for heating up but also for maintaining catalyst temperature. In the latter case, the catalyst temperature is higher than

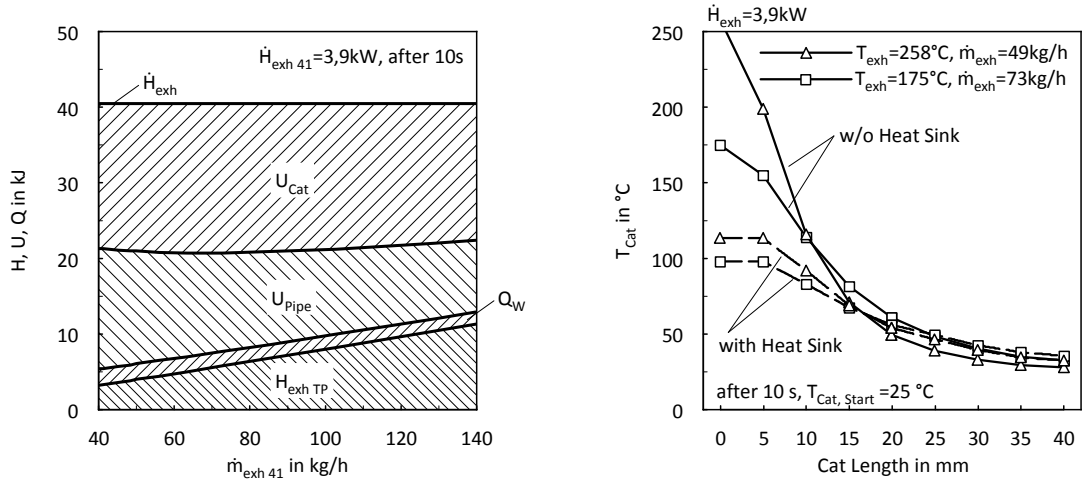

Figure 3.7: Effect of an additional heat sink upstream catalyst on heat up efficiency and characteristic of catalyst temperature versus catalyst length

the exhaust temperature. Hence a reduction of the heat transfer between catalyst and exhaust gas must be achieved, contrary to the heat up process with a opposed direction of the heat flow. Due to this, the requirements for methods used for maintaining catalyst temperature and these used for active heating up are not identical. Thus, also a cool down process of a catalyst should be analysed. The left chart in figure 3.8 illustrates the mean catalyst temperature after 30 seconds ($T_{\mathrm{Cat,\,mean}}$) in a cool down process, as function of exhaust temperature (T_{41}) and mass flow ($\dot{m}_{\mathrm{exh\,41}}$). At the beginning of the cool down process the entire catalyst had a temperature of 300 °C. Similar to the considered above heat up process, both temperature and mass flow are steady-state. It is obvious that not only an increase of temperature but also a decrease of mass flow is a convenient way for a deceleration of the cool down process. As shown in figure 3.8 (left) the same gain of mean monolith temperature could be achieved by raising the exhaust temperature at constant mass flow as well as by a reduction of mass flow at a constant temperature. Taking into account this, is important since, in general, a mass flow reduction could be achieved in a more efficient way than an increase of exhaust temperature. While a higher exhaust temperature will lead to a higher exhaust enthalpy flow ($\dot{H}_{\mathrm{exh\,41}}$), a reduction of mass flow will lead to a decrease, see figure 3.8 (right). Hence the enthalpy flow is not an adequate evaluation parameter in terms of exhaust thermomanagement methods used for maintaining catalyst temperature.

To sum up, the preliminary investigations have shown that the evaluation of catalyst heat up methods only based on exhaust gas temperature is not reasonable. The exhaust enthalpy flow which implicates temperature as well as mass flow seems to be more adequate for a considerable number of exhaust thermomanagement tasks. However, not for all. In this context, it must be taken into account that also an increasing mass flow and a constant temperature will lead to a higher enthalpy flow. Depending on the initial parameters, this will lead to a less accelerated heat up process than an increase of enthalpy flow achieved by both rise of mass flow and temperature. By means of these parameters – exhaust temperature and

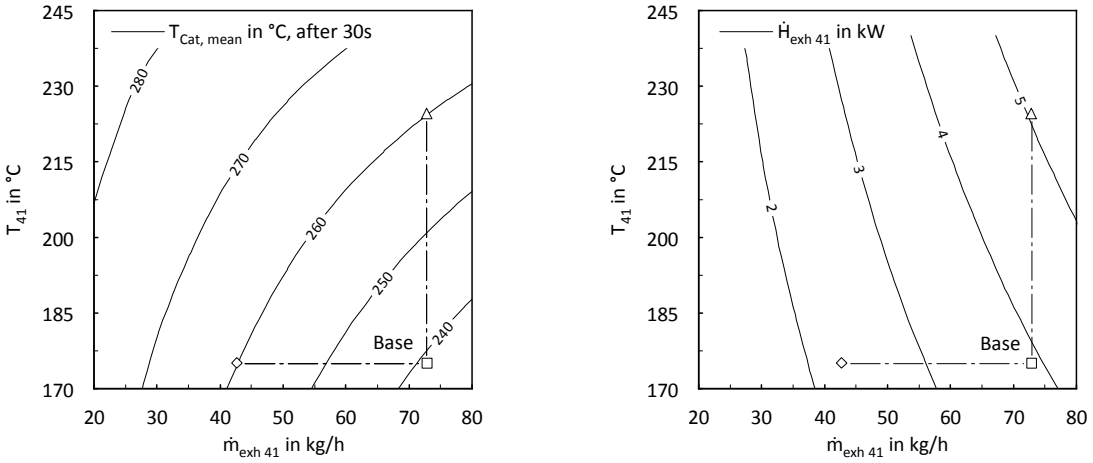

Figure 3.8: Effect of exhaust temperature and mass flow on exhaust enthalpy flow (right) and on the mean catalyst temperature during a cool down process (left)

mass flow – the characteristic of catalyst temperature versus its length could be controlled. Thus, it is reasonable to define the exhaust thermomanagement method – and hence the variation of exhaust mass flow versus the increase of exhaust temperature – with respect to the focussed aftertreatment component. As mentioned at the beginning of the section, the modelled catalyst is characterized by properties of a DOC. Nevertheless, the main findings concerning effect of exhaust temperature and mass flow on heat up and cool down behaviour could be transferred also to other catalyst types (LNT, SCR). Doing so, it has to be considered that a SCR in general does not lead to relevant exothermic reactions. Hence, the effect known from a DOC – heat release from exothermic reactions after the light off in the very first section of the monolith will heat up the rest of the catalyst – is not relevant for a SCR catalyst. Thus, it is not sufficient heating up only the first section, what means an increasing significance of the mass flow. Of course, besides the type of the catalyst, also the position and hence the upstream heat sink is relevant. This means for instance, in case of a relatively small close-coupled DOC the mass flow has less relevance than for a large underfloor SCR.

Another relevant finding of the preliminary investigations concerning catalysts is that using the same evaluation parameters for active catalyst heat up and maintaining catalyst temperature is not reasonable. Of course, an increase of exhaust temperature is beneficial for both. However, while a high mass flow – at a given temperature – is an advantage for heat up methods it is not in terms of deceleration of the cool down. This is reasonable, because of the different direction of heat flow. During the heat up process, heat is transferred from the hot exhaust gas to the cold catalyst. Maintaining catalyst temperature becomes relevant when the catalyst temperature is higher than the exhaust gas temperature and hence heat is transferred from the catalyst to the exhaust gas. Nevertheless, when it comes to avoid a drop down of the catalyst temperature below a critical threshold neither exhaust temperature nor enthalpy flow is a reasonable evaluation parameter. Hence at least for these applications the evaluation method introduced in section 3.1.2 is recommended.

3.3 Exhaust Temperature Gaining Effects

Since there exist numerous VVT strategies achieving an increase of exhaust temperature, a discrimination concerning basic effects responsible for this increase seems to be reasonable. Thus, the aim of this section is the identification of these effects by studying the main equations of thermodynamics. Understanding the difference between relevant exhaust temperature gaining effects should also clear, why several VVT strategies for exhaust thermomanagement provide an exhaust temperature increase, but do not lead to an increase of exhaust enthalpy flow, or only in a minor way compared to the temperature gain.

Before focussing on methods which could be realized by means of a VVT, fundamental ways for increasing exhaust temperature should be discussed in general. Doing so leads to the subsequently listed approaches.

- Increase of injected fuel mass
- Adaption of net rate of heat release
- Increasing exhaust temperature by a heating device
- Increasing temperature of aspirated cylinder charge
- Declining heat capacity of aspirated cylinder charge
- Reduction of effective expansion

Maybe the easiest way for gaining exhaust temperature is an increase of fuel mass. Keeping in mind that engine load should be maintained and not increased, this means also a drawback concerning efficiency. In other words, the exhaust temperature gaining effect of a higher fuel mass is relevant for all methods which result in an efficiency penalty.

An adaption of the net rate of heat release – released heat of fuel energy less wall heat losses – can be achieved by a modification of the combustion process. A retarded injection timing and hence a retarded heat release is an established way in this context.

Another way for increasing exhaust temperature is heating up the exhaust gas by means of an electrical heater or a burner. Doing so enables heating up exhaust gas directly upstream the catalyst. This is beneficial concerning heat losses – compared to methods achieving the temperature increase in a more upstream position e.g. in the cylinder.

Generally speaking, an increase of cylinder charge temperature means an increase of exhaust temperature. Assuming a constant net rate of heat release, this is also true if mass of cylinder charge remains constant, what requires an increase of boost pressure. Assuming a constant boost pressure, what is more realistic in operation points relevant for exhaust thermomanagement, an increase of temperature means a decrease of mass and hence a decrease of heat capacity.

Decreasing cylinder charge heat capacity is already the next point. Of course, cylinder mass and hence heat capacity could be reduced not only by a temperature increase but also due to a reduction of pressure. Referring not to one single cylinder but to the whole engine, the overall aspirated mass and hence heat capacity could be reduced also by a deactivation of one ore more cylinders.

The last quoted item takes into account that also a reduction of expansion could be used for an increase in exhaust temperature. An adaption of the geometrical compression ratio (ε) is one way for declining expansion. Another way is the modification of exhaust valve timings, which is in particular relevant for the present work.

Besides the increase of fuel mass, which is relevant for all methods resulting in an efficiency penalty, cutting expansion is of particular interest when it comes to VVT methods. Hence this method will be discussed in detail in section 3.3.1. Also increasing temperature and declining heat capacity of aspirated cylinder charge is relevant for exhaust thermomanagement methods based on a VVT. Thus, the effect on exhaust temperature and enthalpy flow caused by these variations will be analysed more detailed in section 3.3.2. Of course, the variation of pressure, temperature and composition of aspirated cylinder charge in general has consequences for the combustion process. Moreover the combustion could be affected by a VVT e.g. due to a variation of in-cylinder charge motion. However, as explained in section 2.1, the combustion process in the simulation model is not calculated dependent from these parameters, but by defintion of a relative rate of heat release. Thus, the effect of VVT methods on combustion heat release is not considered by the simulation results of the present work.

3.3.1 Reduction of Effective Expansion Ratio

In general, a reduction of expansion could be achieved either by declining the geometric compression ratio (ε) or by a reduction of exhaust stroke. Since not geometric expansion ratio defined by the cylinder volumes in dead centres but the effective expansion ratio depending from exhaust valve opening is relevant for exhaust temperature, a reduction of effective expansion could be achieved also by a modification of valve timings. If the injected fuel mass is kept constant, an advanced opening of exhaust valves – while keeping constant closing of exhaust valves as well as intake valve timings – will lead to a decrease in power output. Based on the assumption that heat losses do not increase in the same way as the power output decreases, a gain in exhaust enthalpy flow could be achieved, refer to equation 3.1. Since the egnine is operated more or less naturally aspirated in considered operation areas, taking into account effects on turbocharging is not necessary for this general consideration. Also effects on intake enthalpy flow due to the higher temperature of recirculated exhaust gas (upstream EGR cooler) are neglected, what seems to be reasonable with respect to the high cooling efficiencies and – especially after engine cold start – low coolant temperatures of the EGR cooler. Hence the aspirated mass flow (air and EGR) will remain nearly constant. Due to this the increase in exhaust temperature causes an increase in exhaust enthalpy flow in the same way, what is unique among considered VVT strategies as section 3.3.2 will show.

If a constant power output and not a constant injected fuel mass is defined as boundary condition, the decline in power output due to the earlier exhaust valve opening has to be compensated by an increase of supplied fuel energy. Of course, the required additional energy of fuel does not only avoid a decrease of power output, but means also higher wall heat losses and a higher exhaust enthalpy flow. Hence there are two effects causing a higher exhaust enthalpy flow when applying a reduction of effective expansion ratio: First, the higher exhaust temperature at EVO due to the shorter expansion, what is relevant also if the supplied fuel energy remains constant. Second, the reduction of efficiency, which requires an increase of fuel energy for keeping constant engine output (hereinafter referred to as secondary effect).

3.3.2 Adjustment of aspirated Cylinder Charge

As already mentioned, a variation of valve timings enables not only a modificiation of effective expansion, but also a manipulation of aspirated cylinder charge in terms of pressure and temperature. Thus, the way how exhaust temperature and/or enthalpy flow could be affected by pressure and temperature of cylinder charge, should be discussed subsequently. Before going into detail, a defintion of what is meant exactly by aspirated cylinder charge – or briefly called cylinder charge – should be given. In this work, cylinder charge means the whole cylinder mass of the high pressure cycle containing aspirated intake air as well as internal and external EGR but not injected fuel mass. In this context it is also worth mentioning that in general not the whole aspirated cylinder charge is relevant, but only the trapped part of it. However, scavenging losses are negligible for passenger car diesel engines – at least for the considered operation area. Hence, referring to aspirated instead of trapped cylinder charge dose not make a relevant difference. The most relevant parameters for characterisation of cylinder charge as well as their interaction could be shown by the gas state equation. One way for doing so is considering the start of the high pressure cycle (SHP), see equation 3.2. The crank angle position of SHP is determined not in dead centre but by closing of valves.

$$p_{\mathrm{SHP}} \cdot V_{\mathrm{SHP}} = m_{\mathrm{SHP}} \cdot R \cdot T_{\mathrm{SHP}} \tag{3.2}$$

As mentioned above the influence of aspirated cylinder charge on both exhaust temperature and enthalpy flow should be discussed. At first the enthalpy flow is considered.

Keeping in mind the overall energy balance of the engine (equation 3.1), it becomes clear that increasing exhaust enthalpy flow ($H_{\mathrm{exh\,41}}$) by an adjustment of aspirated cylinder charge – while keeping constant fuel mass – is possible only if an increase of aspirated enthalpy flow (H_{in}) could be achieved. The intake enthalpy flow is defined as

$$H_{\mathrm{in}} = m_{\mathrm{SHP}} \cdot \int_{T_0}^{T_{\mathrm{SHP}}} c_p \cdot (T_{\mathrm{SHP}} - T_0) \tag{3.3}$$

The substitution of mass by means of the gas state equation leads to

$$H_{\mathrm{in}} = p_{\mathrm{SHP}} \cdot \frac{T_{\mathrm{SHP}} - T_0}{T_{\mathrm{SHP}}} \cdot \frac{\int_{T_0}^{T_{\mathrm{SHP}}} c_p \cdot V_{\mathrm{SHP}}}{R} \tag{3.4}$$

This definition allows deriving several findings. First of all, a pressure increase while keeping constant temperature will raise exhaust enthalpy flow. As mentioned above, exhaust thermomanagement methods are relevant in particular for engine operation areas where the turbocharger is not able to provide a compressor pressure ratio much greater than one. Hence increasing pressure of cylinder charge is no option for raising exhaust enthalpy flow. Apart from that, from experience is known that an increase of boost pressure at a constant injected fuel mass is not promising concerning exhaust thermomanagement. The reason for this is the effect on exhaust temperature, which will be pointed out later. Nevertheless, increasing boost pressure, means an increase of exhaust enthalpy flow, what confirms the assumption that both enthalpy flow and temperature must be taken into account.

Considering the adjustment of cylinder charge temperature (T_{SHP}) in terms of increasing intake enthalpy flow (H_{in}) makes obvious two conflictive effects (equation 3.4). A higher temperature on the one hand leads to a higher enthalpy flow (T_{SHP} in numerator), on the other hand it decreases the mass flow and hence the enthalpy flow (T_{SHP} in denominator). How far the first effect is compensated by the second depends on the defintion of the reference temperature (T_0). As obvious in case of a reference temperature equal to the absolute zero point, raising cylinder charge temperature does not lead to an increase of intake enthalpy flow. Due to the fact that an exhaust enthalpy flow characterized by a temperature equal or even below the temperature of the EAS is not reasonable, T_0 is set to the value defining cold start conditions (20 °C). According to this, increasing cylinder charge temperature – while keeping constant pressure – means raising intake and hence also exhaust enthalpy flow, since the increase of temperature is more significant than the decrease of mass flow. Nevertheless – as it will be shown in section 3.4 in detail – compared to a reduction of effective expansion, the enthalpy flow gain resulting from an adaption of cylinder charge is small. Of course the mentioned above secondary effect, relevant for strategies resulting in an efficiency decrease, has to be taken into account also in this context. Since VVT methods keeping constant EVO only adjust low pressure cylce, also the secondary effect will be less significant compared to a reduction of effective expansion.

When it comes to exhaust temperature and not enthalpy flow the effect of mass reduction due to an temperature increase is no longer a drawback but becomes a benefit. This could be shown by means of the energy balance referred to the high pressure cycle (closed system):

$$Q_{\mathrm{Fuel}} - Q_{\mathrm{W,HP}} - \int_{\mathrm{SHP}}^{\mathrm{EVO}} p\,\mathrm{d}V = \int_{\mathrm{SHP}}^{\mathrm{EVO}} \mathrm{d}U \tag{3.5}$$

Assuming constant specific heat capacities and neglecting the increase of cylinder mass due to injected fuel mass delivers

$$T_{\mathrm{EVO}} = T_{\mathrm{SHP}} + \frac{Q_{\mathrm{Fuel}} - Q_{\mathrm{W,HP}} - \int_{\mathrm{SHP}}^{\mathrm{EVO}} p\,\mathrm{d}V}{c_v \cdot m_{\mathrm{SHP}}} \tag{3.6}$$

Of course, the equation of state could be used to eliminate the mass

$$T_{\mathrm{EVO}} = T_{\mathrm{SHP}} + \frac{R \cdot T_{\mathrm{SHP}}}{c_v \cdot p_{\mathrm{SHP}} \cdot V_{\mathrm{SHP}}} \cdot \left(Q_{\mathrm{Fuel}} - Q_{\mathrm{W,HP}} - \int_{\mathrm{SHP}}^{\mathrm{EVO}} p\,\mathrm{d}V\right) \tag{3.7}$$

Studying equation 3.7 makes obvious that an increase of cylinder charge temperature results in a higher temperature at EVO due to two effects. First a higher start temperature leads to a higher end temperature, based on the assumption that this effect is not compensated by higher wall heat losses (direct effect). Second, a higher temperature in combination with constant pressure declines mass and hence absolute heat capacity of the cylinder charge (indirect effect).

Besides an increase of cylinder charge temperature, a higher T_{EVO} could be achieved also by means of a pressure decrease, which leads also to a decline of the absolute heat capacity.

This is worth mentioning not at least since a pressure reduction results in a decrease of enthalpy flow as shown in equation 3.4.

Since the effect of cylinder charge heat capacity on exhaust temperature depends on supplied fuel energy and hence on fuel mass, the figure charge fuel ratio (CFR) should be introduced. As shown in equation 3.8, the CFR is defined as ratio of total cylinder mass (m_{SHP}) to fuel mass (m_{Fuel}). The total cylinder mass comprises air as well as external ($m_{\mathrm{EGR,\,ext}}$) and internal ($m_{\mathrm{EGR,\,int}}$) exhaust gas.

$$\mathrm{CFR} = \frac{m_{\mathrm{SHP}}}{m_{\mathrm{Fuel}}} = \frac{m_{\mathrm{Air}} + m_{\mathrm{EGR,\,ext}} + m_{\mathrm{EGR,\,int}}}{m_{\mathrm{Fuel}}} \tag{3.8}$$

Using the CFR in equation 3.7 leads to

$$T_{\mathrm{EVO}} = T_{\mathrm{SHP}} + \frac{1}{c_v} \cdot \frac{1}{\mathrm{CFR}} \cdot \frac{Q_{\mathrm{Fuel}} - Q_{\mathrm{W,\,HP}} - \int_{\mathrm{SHP}}^{\mathrm{EVO}} p\,\mathrm{d}V}{m_{\mathrm{Fuel}}} \tag{3.9}$$

Equation 3.9 makes clear that a decrease of CFR – by an increase of T_{SHP} and/or a decrease of p_{SHP} – enables a gain in T_{EVO} without raising fuel energy or decreasing power output. Hence it has the theoretical potential for a BSFC-neutral exhaust temperature gaining. Of course, this is based on the assumption that wall heat losses remain constant. Furthermore it must be taken into account that T_{EVO} and not the exhaust temperature directly upstream catalyst is considered. Hence a maybe higher temperature decrease after EVO – e.g. due to higher heat losses in exhaust ports and pipes – is also neglected in this fundamental view. Of course, these losses are also relevant for VVT methods based on a reduction of effective expansion. Thus, VVT methods adjusting cylinder charge seem to be more efficient than those based on an early exhaust valve opening, since the latter lead to a decreasing power output as a matter of principal. However, this efficiency benefit applies only as far as exhaust temperature and not enthalpy flow is concerned.

Not at least it should be mentioned that the consideration of consequences resulting from an adjustment of cylinder charge is valid not only for a single cylinder, but also for the whole engine. Hence also a cylinder deactivation – by switching off injection and keeping close both intake and exhaust valves – is treated as VVT method for adjustment of aspirated cylinder charge.

To sum up considerations aimed to classify VVT strategies for exhaust thermomanagement, it can be stated that a discrimination in two groups seems to be reasonable. Methods of the first group achieve an exhaust temperature increase without reduction of aspirated cylinder mass and hence exhaust mass flow. As a result, the enthalpy flow increases in the same way as the temperature. This means, the amount of energy exhausted by the engine in each working cycle increases. Hence it seems to be clear that these methods lead to an increase of fuel consumption or a decrease of power output. Exhaust thermomanagement strategies, which belong to the second group, are based mainly on reduction of cylinder mass. Due to the lower heat capacity of cylinder charge, these methods are able to achieve an exhaust temperature increase without raising fuel energy. However, the exhaust enthalpy flow does not increase or only in a minor way compared to the temperature.

3.4 VVT Strategies for Exhaust Thermomanagement

The following subsections provide a discussion of different VVT strategies which are of particular interest for exhaust thermomanagement. Compared to section 3.3, which was focussed on the fundamental basics, this section makes a step toward realization of discussed effects in engine. For this purpose various valve timing strategies should be evaluated by means of the engine model introduced in section 2.1. Hence also effects which were neglected in section 3.3, like impact on wall heat losses, could be considered.

Since the need for heat up methods mainly belong to low load operation, the subsequently discussed evaluation of VVT strategies refers to an operation point at 1500 min^{-1} and a BMEP of 2 bar.

Keeping constant injected fuel mass was considered as well as maintaining engine load. In the latter case, it has to be taken into account that methods with an efficiency penalty lead to the mentioned above secondary heat up effect (gain of exhaust temperature due to increase of injected fuel mass).

When defining air management boundary conditions, it has to be kept in mind that the engine works more or less naturally aspirated in the considered engine operation area. Thus, keeping constant both air excess ratio and rate of EGR could be achieved only if the injected fuel mass remains constant. In other words, maintaining engine load while applying an VVT strategy which leads to an increase of fuel consumption requires a cut of air excess ratio and/or EGR. In case of low pressure EGR, both intake air and recirculated exhaust gas are cooled by the CAC. Hence, in the considered operation range, it nearly does not matter for exhaust thermomanagement, whether air excess ratio or EGR will be declined. Thus, both EGR and air excess ratio will be reduced.

Of course, when it comes to the combustion process, the share of air and EGR in the overall cylinder mass does matter of course. Nevertheless, for the subsequently discussed simulations the relative rate of heat release was kept constant, which has several reasons. The most relevant one is that a variation of heat release has a considerable effect on exhaust temperature. Hence, it would mean the focussed exhaust thermomanagement method – variation of valve timing – is manipulated by another exhaust temperature gaining method, what is problematic for evaluation. Apart from that, it has to be kept in mind that an adaption of the injection strategy provides a way for maintaining the relative heat release of combustion or at least the $\mathrm{MFB}_{50\%}$. Thus, using a constant rate of heat release is definitely legitimate.

3.4.1 Early Exhaust Valve Opening

Figure 3.9 shows the exhaust valve lift curves, which were used for simulation of an early exhaust valve opening (EEVO). It can be seen that only EVO is advanced while EVC and the maximum valve lift remain constant.

At first, a variation of EVO at a constant injected fuel mass and hence a declining engine load (efficiency penalty) should be discussed. Keeping constant fuel mass and hence supplied energy is easier for understanding in case of analysing energy flows. However, at the beginning, not energy flows, but the effect of EEVO on exhaust temperatures should be considered, see figure 3.10. For this purpose, the variation of exhaust temperatures upstream exhaust manifold (ΔT_{EX}) and downstream turbine (ΔT_{41}) are plotted versus variation of EVO. In

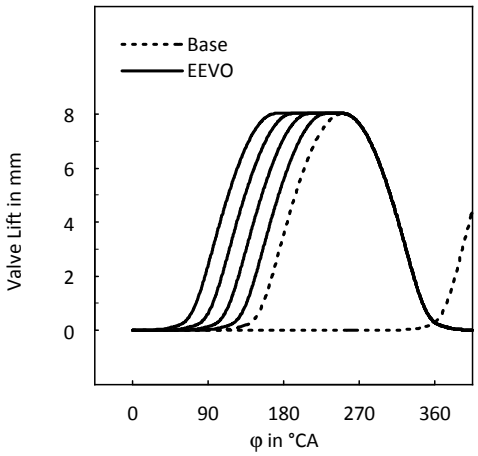

Figure 3.9: Valve lift curves used for simulation of an early exhaust valve opening (EEVO)

addition also the variation of the cylinder temperature at EVO ($\Delta T_{\mathrm{Cyl,\,EVO}}$) is considered. The increase of T_{EX} and T_{41} is up to about 60 and 45 °C respectively (at $\Delta\varphi_{\mathrm{EVO}}$=80 °CA). The increase of $\Delta T_{\mathrm{Cyl,\,EVO}}$ is significantly higher, what means, the difference between cylinder temperature at EVO and exhaust temperatures becomes the higher, the earlier the exhaust valves open. In this context it is worth mentioning that the plotted exhaust temperatures (T_{EX} and T_{41}) are mass flow averaged temperatures and hence representative for the energy content of exhaust gas. The increase of time averaged exhaust temperatures is lower, in particular for the more upstream measuring point (T_{EX}).

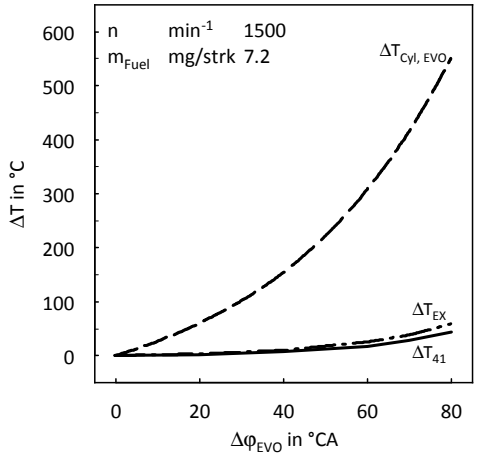

Figure 3.10: Increase of exhaust temperatures due to EEVO at 1500 min^{-1} and a constant injected fuel mass of 7,2 mg/strk

To find out the reason for the high difference between exhaust temperatures and cylinder temperature at EVO, the energy balance should be analysed. For this purpose not the whole engine but a single cylinder inclusive exhaust ports is considered. Figure 3.11 gives a survey of energy flows in this system, which is splitted in two parts – cylinder and exhaust port.

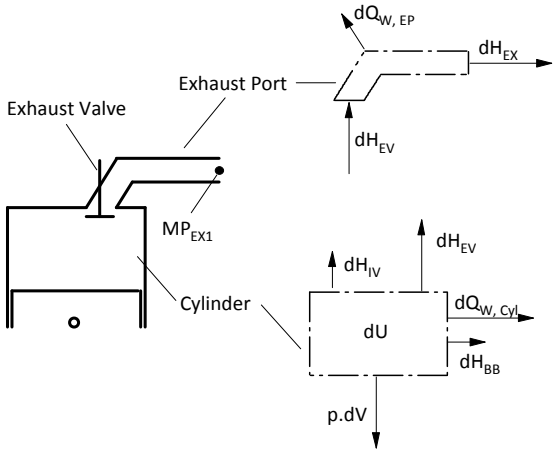

Figure 3.11: Enthalpy and heat flows in cylinder and exhaust ports

The discrimination – cylinder and port – is reasonable when it comes to define the integration limits of the energy balances. In case of the cylinder, the most convenient way is considering only the section of working cycle between EVO and EVC. Doing so delivers the energy balance shown in equation 3.10. The most relevant figures are the variation of internal energy in the cylinder ($\mathrm{d}U$), the delivered volume work ($p \cdot \mathrm{d}V$), the cylinder wall heat flow ($\mathrm{d}Q_{\mathrm{W,\,Cyl}}$) and the enthalpy flow through exhaust valves ($\mathrm{d}H_{\mathrm{EV}}$). The enthalpy flow through the blowby gap ($\mathrm{d}H_{\mathrm{BB}}$) and the intake valves ($\mathrm{d}H_{\mathrm{IV}}$) – during valve overlap – are of secondary importance, in general.

$$-\int_{\mathrm{EVO}}^{\mathrm{EVC}} \mathrm{d}U = \int_{\mathrm{EVO}}^{\mathrm{EVC}} p \cdot \mathrm{d}V + \int_{\mathrm{EVO}}^{\mathrm{EVC}} \mathrm{d}Q_{\mathrm{W,\,Cyl}} + \int_{\mathrm{EVO}}^{\mathrm{EVC}} \mathrm{d}H_{\mathrm{BB}} + \int_{\mathrm{IVO}}^{\mathrm{EVC}} \mathrm{d}H_{\mathrm{IV}} + \int_{\mathrm{EVO}}^{\mathrm{EVC}} \mathrm{d}H_{\mathrm{EV}} \tag{3.10}$$

For analysing the enthalpy and heat flows of the exhaust port (equation 3.11), the whole engine cycle (0 ... 720 °CA) is taken into account. This is necessary since the unsteady flow regime in ports means that a mass flow and hence an enthalpy flow between port and manifold ($\mathrm{d}H_{\mathrm{EX}}$, figure 3.11) could occur also when exhaust valves are closed. However, due to continuity, this is not true for the flow between cylinder and ports ($\mathrm{d}H_{\mathrm{EV}}$). In other words, the integration of $\mathrm{d}H_{\mathrm{EV}}$ over the whole working cycle leads to the same results as the integration between EVO and EVC.

$$\int_{\mathrm{EVO}}^{\mathrm{EVC}} \mathrm{d}H_{\mathrm{EV}} = \int_{0\,°CA}^{720\,°CA} \mathrm{d}H_{\mathrm{EV}} = \int_{0\,°CA}^{720\,°CA} \mathrm{d}Q_{\mathrm{W,\,EP}} + \int_{0\,°CA}^{720\,°CA} \mathrm{d}H_{\mathrm{EX}} \tag{3.11}$$

Combining both equations (3.10 and 3.11) and solving the integrals delivers

$$-\Delta U_{\mathrm{oEV}} = W_{\mathrm{oEV}} + \underbrace{Q_{\mathrm{W,\,oEV}} + Q_{\mathrm{W,\,EP}} + H_{\mathrm{BB,\,oEV}} + H_{\mathrm{IV,\,oEV}} + H_{\mathrm{EX}}}_{H_{\mathrm{EX,\,ideal}}} \tag{3.12}$$

The figures resulting from integration between EVO and EVC are labelled with the index oEV (open Exhaust Valve). The sum of exhaust enthalpy (H_{EX}), heat ($Q_{\mathrm{W,\,oEV}}$, $Q_{\mathrm{W,\,EP}}$) and enthalpy losses ($H_{\mathrm{BB,\,oEV}}$, $H_{\mathrm{IV,\,oEV}}$) delivers the enthalpy of an idealised blow down and exhaust stroke ($H_{\mathrm{EX,\,ideal}}$).

To examine the dependency from EVO, for the parameters discussed in context of the energy balance, figure 3.12 should be analysed. The left chart shows the increase of internal energy variation during open exhaust valves ($-\Delta U_{\mathrm{oEV}}$) and the exhaust enthalpy (H_{EX}) versus variation of EVO. It can be seen that ($-\Delta U_{\mathrm{oEV}}$) exceeds H_{EX}. The difference clearly increases versus $\Delta\varphi_{\mathrm{EVO}}$, which is due to the very low gradient of H_{EX} compared to ($-\Delta U_{\mathrm{oEV}}$). For a $\Delta\varphi_{\mathrm{EVO}}$ below about 40 °CA, a relevant increase of H_{EX} can not be observed. The reason for this effect should be analysed in the right chart. Besides the curves already known from the left chart – ($-\Delta U_{\mathrm{oEV}}$) and H_{EX} – also the exhaust enthalpy of the idealised exhaust flow ($H_{\mathrm{EX,\,ideal}}$, see equation 3.12) is plotted. As discussed in equation 3.12, the difference between the actual and the idealised enthalpy is determined by heat and enthalpy losses in the cylinder and the exhaust ports. Hence, considering the ideal case, for a $\Delta\varphi_{\mathrm{EVO}}$ smaller than about 20 °CA, the discussed difference between ($-\Delta U_{\mathrm{oEV}}$) and $H_{\mathrm{EX,\,ideal}}$ becomes even negative.

Studying equation 3.12 makes clear that the difference between these curves – ($-\Delta U_{\mathrm{oEV}}$) and $H_{\mathrm{EX,\,ideal}}$ – is the volume work delivered during open exhaust valves (W_{oEV}). More exactly, the volume work between EVO and EVC is positive and hence delivered only for EVO advancements higher than about 20 °CA. Otherwise, the supplied volume work during exhaust stroke exceeds the volume work delivered during expansion after EVO, what means a negative W_{oEV} and hence an idealised exhaust enthalpy which is higher than the decrease of internal energy between EVO and EVC. In other words, using base valve timing or moderate EEVO means that the exhaust enthalpy comes not only from decrease in internal energy but also from volume work. For more advanced EVO timings, this – concerning exhaust enthalpy – positive effect becomes smaller and even reverses in a drawback. The most relevant reason for the increase of W_{oEV} due to earlier EVO is the fact that opening of exhaust valves does not lead to a prompt drop of cylinder pressure to the pressure level downstream exhaust valves, but to a decrease which is defined by the characteristic of valve lift curves. Higher friction losses due to higher flow velocities lead to an additional decrease of mass flow rate and hence a delay in cylinder pressure reduction. However, not only the cylinder pressure, but also the variation of cylinder volume is relevant for W_{oEV}. The gradient of cylinder volume versus crank angle at EVO becomes higher due to EEVO, what is another reason for the discussed increase of W_{oEV} versus $\Delta\varphi_{\mathrm{EVO}}$.

Making a further step of idealisation – assumption of a rectangular valve lift characteristic and an isentropic flow through exhaust valves – means a reduction of volume work (W_{oEV}) to a value, which is negligible compared to ($-\Delta U_{\mathrm{oEV}}$) and $H_{\mathrm{EX,\,ideal}}$. Hence, it could be written

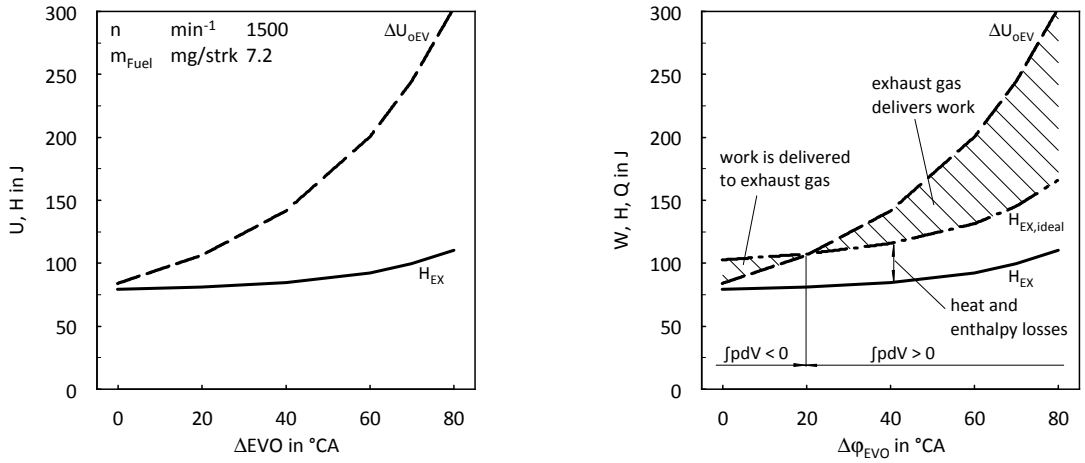

Figure 3.12: Effect of EEVO on internal energy, volume work and enthalpy at 1500 min^{-1} and a constant injected fuel mass of 7,2 mg/strk

$$-\Delta U_{\mathrm{oEV}} = H_{\mathrm{EX,\,ideal}} \quad \Leftrightarrow \quad -\int_{\mathrm{EVO}}^{\mathrm{EVC}} \mathrm{d}U_{\mathrm{Cyl}} = \int_{0\,°CA}^{720\,°CA} \mathrm{d}H_{\mathrm{EX}} \tag{3.13}$$

Assuming that the whole cylinder charge is expelled (compression volume is zero) means U_{EVC} disappears. Assuming further, constant values of heat capacities (c_p, c_v) delivers following interaction between cylinder temperature at EVO ($T_{\mathrm{Cyl,\,EVO}}$) and exhaust temperature (T_{EX}):

$$T_{\mathrm{EX}} = \frac{c_v}{c_p} \cdot T_{\mathrm{Cyl,\,EVO}} \quad \Leftrightarrow \quad T_{\mathrm{Cyl,\,EVO}} - T_{\mathrm{EX}} = T_{\mathrm{Cyl,\,EVO}} \cdot \left(1 - \frac{c_v}{c_p}\right) \tag{3.14}$$

The difference of cylinder and exhaust temperature, illustrated by means of the heat capacities, points out the energy required for expansion of exhaust gas. Compared to the variation of $T_{\mathrm{Cyl,\,EVO}}$ resulting from EEVO, the relation of c_p and c_v remains nearly constant. Hence EEVO means not only an increase of cylinder temperature at EVO but also an increase of difference to the theoretical achievable exhaust temperature (T_{EX}). Thus, the difference of cylinder and exhaust temperature observed in figure 3.10 is not only due to enthalpy losses, heat losses and the delivered volume work but also due to the fact that the expansion of exhaust gas – resulting from pressure difference between cylinder an exhaust duct – is not for free.

After demonstration of theoretical potentials by means of several idealisations, subsequently the original engine model – taking into account heat and pressure losses – should be considered. Moreover, not fuel mass but engine load will be maintained while EVO variation.

The left chart in figure 3.13 points out, what this means for the exhaust temperature downstream turbine (T_{41}). It can be seen that the temperature gain at this position is up to about 50 °C higher when engine load and not injected fuel mass is kept constant. The most

relevant reason for this significant difference could be found in analysing the characteristics of charge fuel ratio (CFR), which are plotted in the same chart. As obvious, keeping constant fuel mass, means also a nearly constant CFR. This is due to maintaining the VNT position – fully opened – during variation of EVO, what results in a more or less constant boost pressure and hence a nearly constant mass of aspirated cylinder charge (air and EGR). Thus, it is clear that the CFR decrease in case of a constant BMEP comes from the increase in injected fuel mass, or in other words from the decreasing efficiency. This efficiency penalty could be seen also by considering the BSFC curves in the right chart. For keeping constant fuel mass, the BMEP characteristic plotted below is a more meaningful figure.

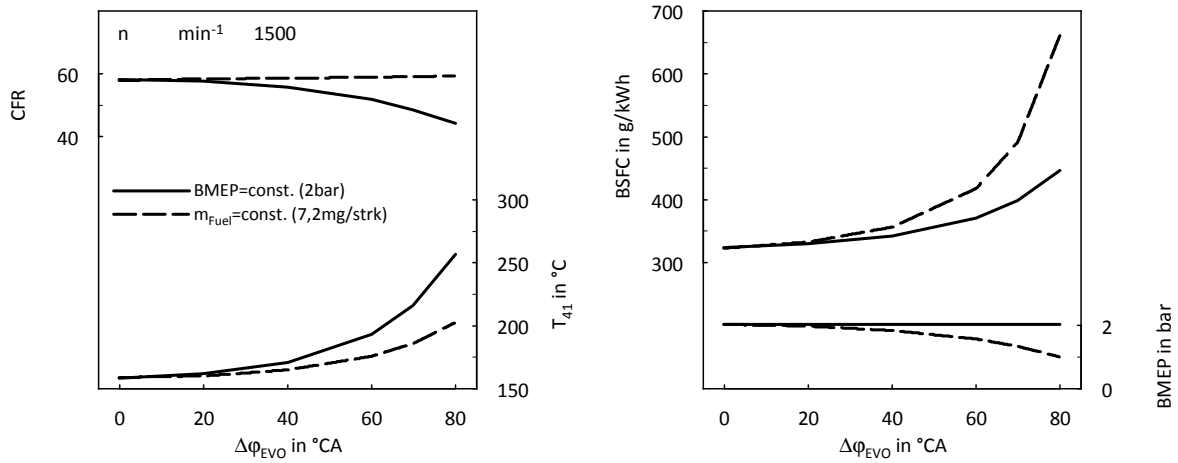

Figure 3.13: Comparison between keeping constant fuel mass and engine load – while applying EEVO – concerning charge fuel ratio, exhaust temperature, specific fuel consumption and BMEP at 1500 min^{-1}

More detailed information concerning exhaust thermomanagement efficiency of EEVO could be found in studying energy flows. For this purpose, the left chart in figure 3.14 shows the distribution of supplied energy – fuel energy (Q_{Fuel}) and intake enthalpy flow (H_{in}) – to effective work (W_{eff}), friction losses (W_{f}), heat losses ($Q_{\mathrm{W,\,Cyl}}$, $Q_{\mathrm{W,\,Exh+In}}$) and exhaust enthalpy ($H_{\mathrm{exh\,41}}$). The right hand side of figure 3.14 provides the engine layout with the corresponding system boundary and energy flows. Considering the variation of supplied energy ($Q_{\mathrm{Fuel}} + H_{\mathrm{in}}$), a characteristic similar to this observed in figure 3.13 for the BSFC (for constant BMEP) can be observed. In this context it is worth mentioning that the share of H_{in} in variation of overall energy supply ($Q_{\mathrm{Fuel}} + H_{\mathrm{in}}$) is not more than about 1 %. Analysing friction losses, the assumption of a constant FMEP can be identified. The cylinder heat losses ($Q_{\mathrm{W,\,Cyl}}$) comprise wall heat flow (piston, head and liner) as well as the blowby enthalpy flow. $Q_{\mathrm{W,\,Exh+In}}$ takes into account the heat flow in ports, manifolds, turbine, CAC and pipes (inside system boundary). The increase of $Q_{\mathrm{W,\,Exh+In}}$ versus $\Delta\varphi_{\mathrm{EVO}}$ comes mainly from the exhaust ports, the exhaust manifold and the turbine.

The relation of the discussed energy flows to the the supplied energy delivers the relative shares, see figure 3.15. Attention has to be paid to the arrangement. In contrast to the

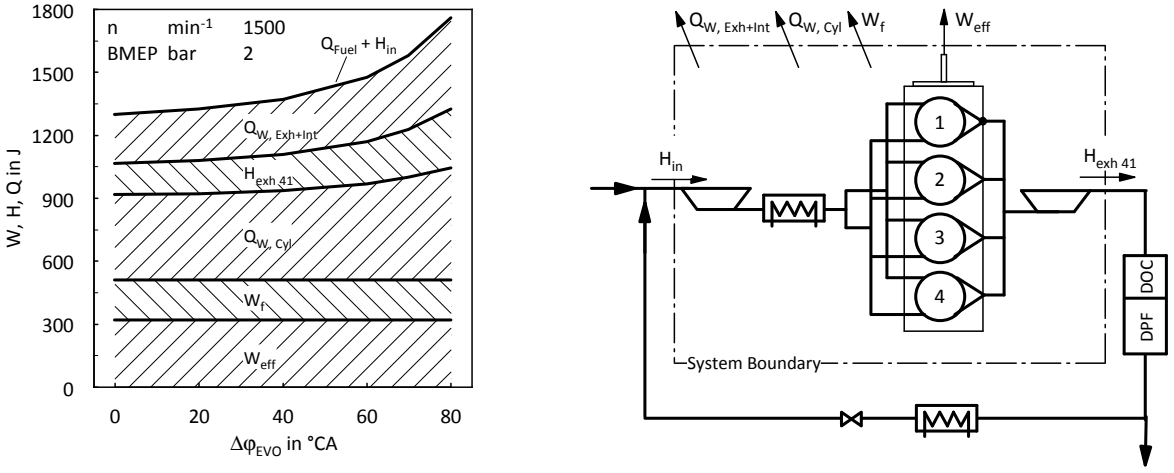

Figure 3.14: Energy flow analysis of EEVO at 1500 min^{-1} and a BMEP of 2 bar

illustration of absolute values in figure 3.14, for the relative split, the exhaust enthalpy is added to effective work before friction and heat losses. Due to this, it is obvious that the relative share of overall heat losses ($Q_{\mathrm{W,\,Cyl}} + Q_{\mathrm{W,\,Exh+In}} + W_{\mathrm{f}}$) remains nearly constant. In other words, applying EEVO means shifting relative share of effective work (W_{eff}) to relative share of exhaust enthalpy ($H_{\mathrm{exh\,41}}$). Having a more detailed look on heat losses, an increase of $Q_{\mathrm{W,\,Exh+In}}$ and a decrease of $Q_{\mathrm{W,\,Cyl}}$ could be identified. This is reasonable since the exhaust temperature becomes higher and the interval between IVC and EVO – mainly relevant for cylinder wall heat flow – becomes shorter. As already observed in figure 3.14, this more or less constant relative share of overall heat losses means an increase of absolute heat losses. Analysing the distribution of additional supplied energy – necessary for maintaining engine load while advancing EVO – should be done by means of the evaluation chart introduced in section 3.1.1, see figure 3.15 (right). Plotting the gain of exhaust enthalpy ($\Delta H_{\mathrm{exh\,41}}$) versus the increase of heat losses (ΔQ_{Loss}) makes obvious a gradient lower than 1. This means that the increase of heat losses (ΔQ_{Loss}) – comprising change in $Q_{\mathrm{W,\,Cyl}}$; $Q_{\mathrm{W,\,Exh+In}}$ and W_{f} – exceeds the increase of enthalpy ($\Delta H_{\mathrm{exh\,41}}$).

As already mentioned, in case of dynamic flow regimes, the time and the mass flow averaged temperature are not identical. An advanced EVO leads to a higher pressure gradient between cylinder and exhaust ports at the beginning of the blow down. This means a more dynamic characteristic of mass flow and hence a higher difference of time and mass flow averaged temperature, at least directly downstream exhaust valves.

The exhaust temperatures considered above for evaluation of EEVO were mass flow averaged temperatures. This is reasonable since the focus was on energy balance and hence on exhaust enthalpy flow. Nevertheless, when it comes to effects of exhaust gas on catalyst, it is not that clear, whether the mass flow or the time averaged temperature is more relevant. Figure 3.16 shows both mass flow and time averaged exhaust temperatures upstream (T_{31}) and downstream (T_{41}) turbine. Considering T_{31}, a significant increase of difference between mass flow and time averaged temperature versus $\Delta\varphi_{\mathrm{EVO}}$ can be seen. At the position relevant

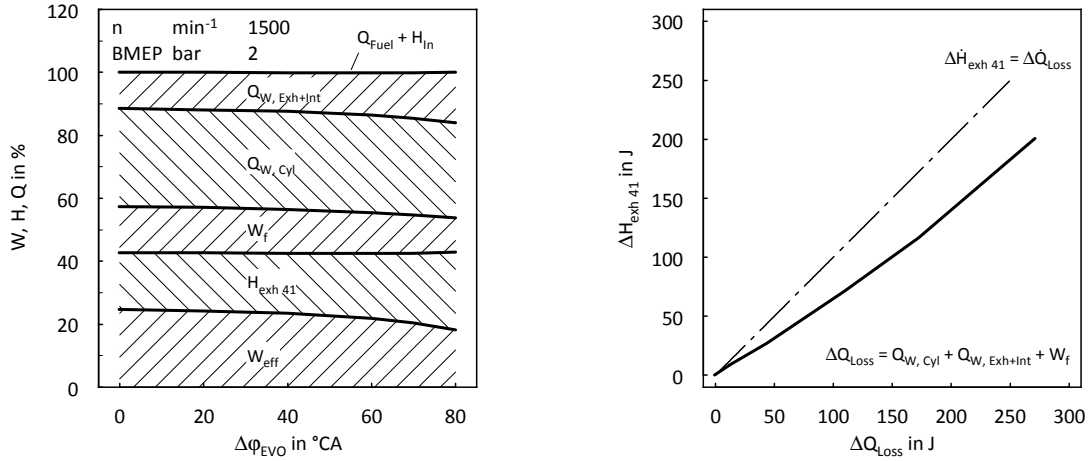

Figure 3.15: Effect of EEVO on relative energy flows (left) and exhaust enthalpy gain versus increase of heat losses (right)

for exhaust thermomanagement – downstream turbine (T_{41}) – the difference between time and mass flow averaged temperature is negligible. Thus, detailed investigations of mass flow characteristic on thermal behaviour of the catalyst seem to be not necessary. The elimination of the difference between time and mass flow averaged temperature comes mainly from the turbine, which cuts enthalpy peaks due to conversion in mechanical work (delivered to compressor).

So far, early EVO was considered as a variability applied to both exhaust valves. Of course advanced opening of only one exhaust valve is relevant too, not at least in combination with a rotated valve layout, which enables combination of variable exhaust and intake valve timings with one cam shaft [29]. Figure 3.17 shows the difference between applying EEVO only to one and to both exhaust valves at 1500 min^{-1} and a BMEP of 2 bar.

In the left chart the fuel consumption (BSFC) and the exhaust temperature downstream turbine (T_{41}) are plotted versus variation of EVO.

As expected, EEVO of only one valve leads to a less increase of both fuel consumption and exhaust temperature. Considering efficiency of these concepts by means of the well known evaluation chart (right) makes obvious a slight advantage of applying EEVO to only one exhaust valve.

The reason for this difference in efficiency could be found in studying wall heat losses. Figure 3.18 illustrates wall heat losses in cylinder and exhaust ports versus exhaust temperature downstream turbine (T_{41}). While cylinder wall heat losses are more or less identical, port wall heat losses are smaller in case of applying EEVO to only one valve. This could be explained by a smaller overall port surface during blow down phase.

As already mentioned, the adaption of valve timings is not the only way for gaining exhaust temperature and enthalpy flow. Thus, a comparison with alternative exhaust thermomanagement methods is reasonable. For this purpose a retarded combustion, the application of an electrical heater as well as a reduction of the geometrical compression ratio (ε) should be

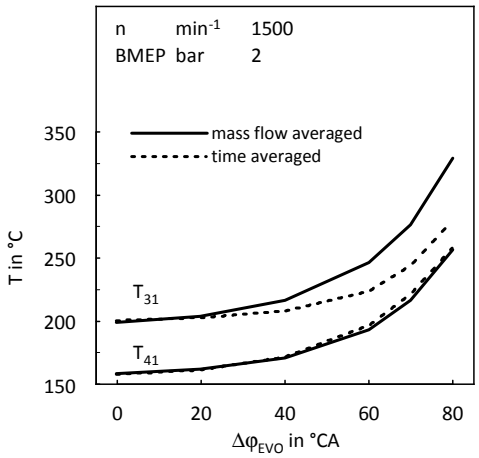

Figure 3.16: Difference of time averaged and mass flow averaged exhaust temperatures upstream (T_{31}) and downstream (T_{41}) turbine when applying EEVO at 1500 min^{-1} and a BMEP of 2 bar

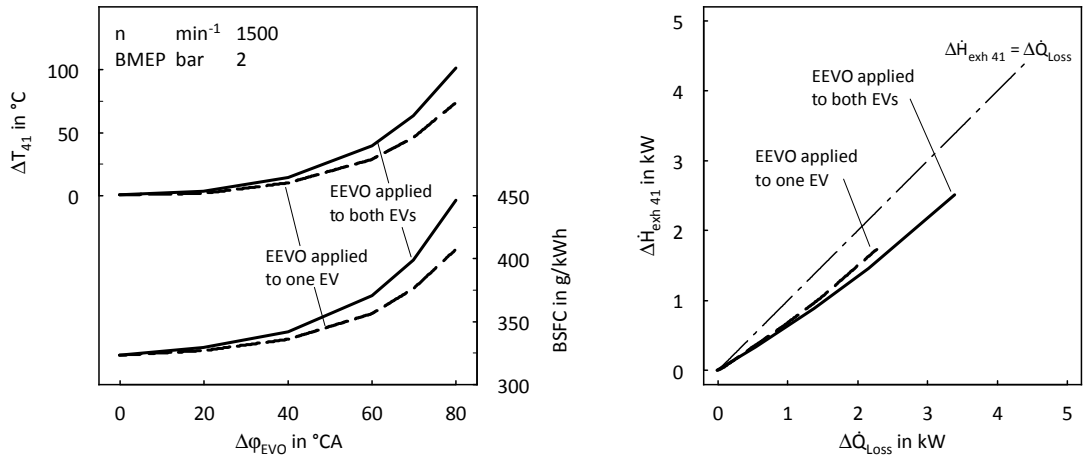

Figure 3.17: Comparison of applying EEVO to one and to both exhaust valves concerning exhaust temperature and efficiency at 1500 min^{-1} and a BMEP of 2 bar

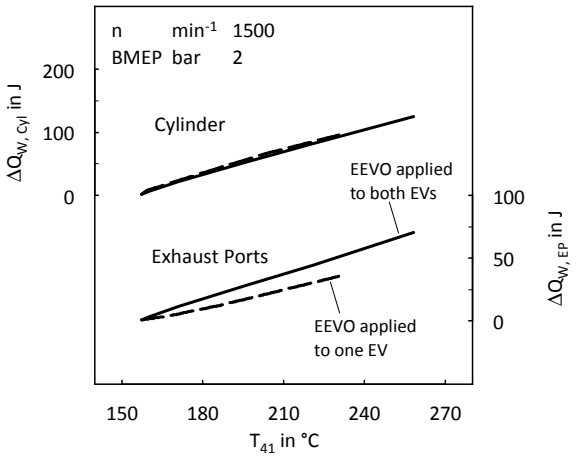

Figure 3.18: Comparison of applying early exhaust valve opening to one and to both exhaust valves concerning wall heat flow in cylinders and exhaust ports at 1500 min^{-1} and a BMEP of 2 bar

considered. These methods were selected because of their characteristic – gaining exhaust temperature without reduction of mass flow – which is similar to this of EEVO.

The retarded combustion was modelled by a variation of $\mathrm{MFB}_{50\%}$ while the shape of the relative rate of heat release was kept constant. The electrical heater was realized in the simulation model by a heat supply directly upstream catalyst. Hence the electrical heater does affect T_{41} (downstream turbine, directly upstream catalyst) but not T_{31} (upstream turbine). The required electrical energy is provided by the generator of the combustion engine. Thus, the activation of the electrical heater means an increase of IMEP and hence FMEP. The assumed overall efficiency of the electrical heater – taking into account losses of the generator and heat which is transferred not to the exhaust gas but to the ambient – is 50 %. This assumption is based on measurement data.

Figure 3.19 shows the comparison of EEVO with the mentioned alternative methods – retarded combustion ($\mathrm{MFB}_{50\%}$ Var.), electrical heater (EHeater) and reduction of geometrical compression ratio (ε Var.). In the left chart the BSFC and the exhaust mass flow ($\dot{m}_{\mathrm{exh}\,41}$) are plotted versus exhaust temperature downstream turbine (T_{41}). The $\dot{m}_{\mathrm{exh}\,41}$ characteristics confirm that neither of the considered methods leads to a reduction of exhaust mass flow. The mass flow even increases more or less, what is due to an increase of boost pressure, which results from a constant – fully opened – VNT position and an increase of exhaust enthalpy. Since EEVO means not only an increase of temperature but also of kinetic energy upstream turbine, it results in the most significant $\dot{m}_{\mathrm{exh}\,41}$ increase. Considering the BSFC plotted above, nearly identical characteristics of EEVO and the EHeater can be observed. The retarded combustion ($\mathrm{MFB}_{50\%}$ Var.) achieves a clearly lower fuel consumption penalty. The exhaust temperature gain by means of a compression ratio (ε Var.) reduction is even slightly more efficient. However, defining a lower ε limit of 9 – what is an unrealistic low value for diesel engines, anyway – does not allow an T_{41} increase of more than about 30 °C.

The right chart illustrates the most relevant heat losses – cylinder ($Q_{\mathrm{W,Cyl}}$), exhaust duct ($Q_{\mathrm{W,Exh}}$) – and the EHeater loss versus the exhaust temperature T_{41}.

Analysing the EHeater, it is obvious that the cylinder wall heat losses are nearly identical to these of EEVO. The heat losses in exhaust duct – comprising ports, manifold and turbine housing – are clearly lower, what is reasonable since the EHeater increases the exhaust enthalpy directly upstream the catalyst. Increasing exhaust enthalpy more or less at the same location where it is required, of course, is beneficial. Referring to the BSFC characteristics this benefit – compared to EEVO – is not apparent. This could be explained by the losses resulting from an overall efficiency of the electrical heater which is 50 % and hence clearly lower than 100 %. More exactly the defined EHeater efficiency of 50 % means that the increase of indicated work has to be twice the enthalpy increase. The difference between increase in indicated work and exhaust enthalpy increase could be considered as EHeater loss.

The retarded combustion leads to a similar increase of heat losses in exhaust duct as EEVO. However, the retarded heat release means a lower cylinder pressure and temperature and hence a lower cylinder wall heat flow, which is the main reason for the lower penalty in fuel consumption. A reduction of compression ratio results in cylinder wall heat losses which are even lower than these of the retarded combustion. The exhaust duct wall heat losses of the ε reduction are on the same level as for EEVO and the retarded combustion.

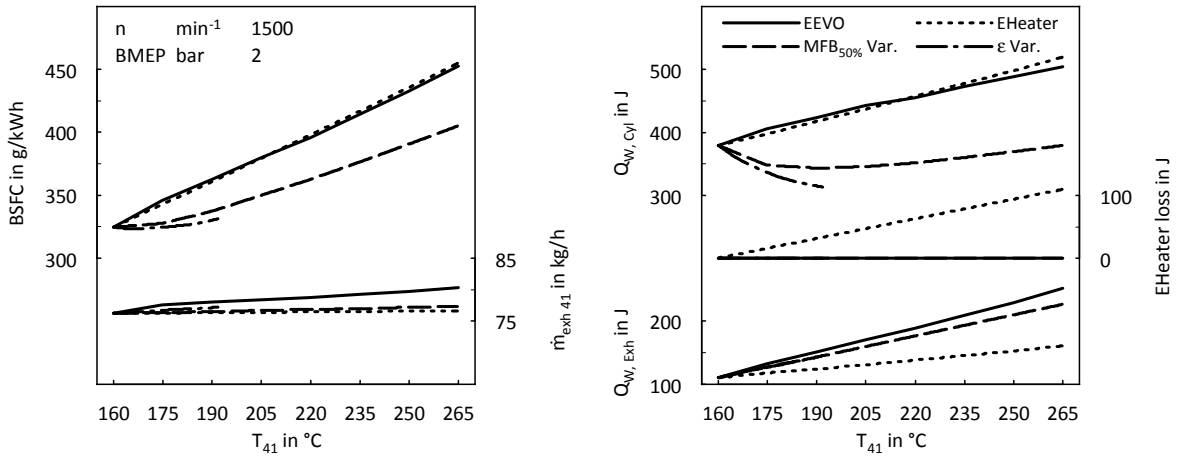

Figure 3.19: Comparison of EEVO with alternative exhaust thermomanagement methods concerning fuel consumption, mass flow and heat losses at 1500 $\mathrm{min^{-1}}$ and a BMEP of 2 bar

In figure 3.20 the comparison of EEVO with the alternative exhaust thermomanagement methods should be discussed by means of the characteristics of exhaust enthalpy change ($\Delta\dot{H}_{\mathrm{exh\,41}}$) versus change in heat losses ($\Delta\dot{Q}_{\mathrm{Loss}}$). Similar to the BSFC versus T_{41} illustration considered above, EEVO and the EHeater are nearly identical for low and moderate gains of $\dot{H}_{\mathrm{exh\,41}}$. For a higher increase, EEVO shows advantages which come from the more significant increase of mass flow ($\dot{m}_{\mathrm{exh\,41}}$, see figure 3.19) and hence enthalpy flow. Nevertheless, both methods EEVO and the EHeater are characterized by an increase of the exhaust enthalpy flow ($\dot{H}_{\mathrm{exh\,41}}$) which is lower than this of the heat losses ($\dot{Q}_{\mathrm{Loss}}$). As obvious, the retarded

combustion ($MFB_{50\%}$ Var.) achieves more or less the opposite – an increase of $\dot{H}_{\mathrm{exh}\,41}$ which exceeds this of $\dot{Q}_{\mathrm{Loss}}$. A moderate retarding of combustion even achieves a simultaneous increase of $\dot{H}_{\mathrm{exh}\,41}$ and decrease of $\dot{Q}_{\mathrm{Loss}}$, which lead to a position at the left hand side of the starting point. This means that not only the entire amount of additional supplied fuel energy, but also a part of the energy originally spent to heat losses is used for the increase of enthalpy flow. As obvious, the relation of increase in $\dot{H}_{\mathrm{exh}\,41}$ and $\dot{Q}_{\mathrm{Loss}}$ becomes less beneficial for a higher increase of exhaust enthalpy. This behaviour corresponds with the analysed above cylinder wall heat flow characteristic ($Q_{\mathrm{W,\,Cyl}}$, figure 3.19). The reduction of compression ratio (ε) achieves increasing $\dot{H}_{\mathrm{exh}\,41}$ in an even more efficient way than the retarded combustion. For low ε reductions the characteristic is more or less identical with the plotted reference line '$\Delta\dot{H}_{\mathrm{exh}\,41} - -\Delta\dot{Q}_{\mathrm{Loss}} = 0$'. This means, the enthalpy flow increase is achieved only due to a reduction of heat losses and hence without an increase of supplied fuel energy. Nevertheless, due to the already mentioned reason, the achievable $\dot{H}_{\mathrm{exh}\,41}$ is small.

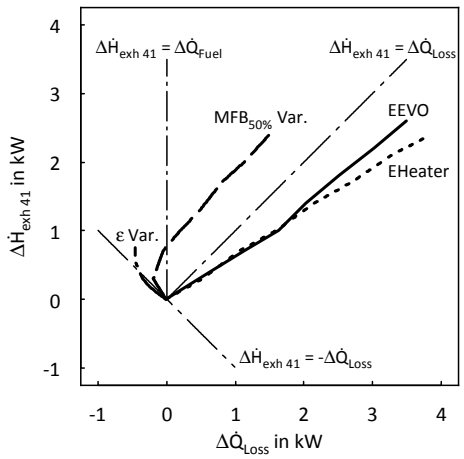

Figure 3.20: Comparison of EEVO with alternative exhaust thermomanagement methods concerning variation of exhaust enthalpy flow versus variation of heat losses at 1500 min^{-1} and a BMEP of 2 bar

Figure 3.21 illustrates the variation of exhaust valve opening (Δ $EVO_{1\mathrm{mm}}$), $MFB_{50\%}$, enthalpy flow increase by the EHeater ($\dot{Q}_{\mathrm{EH}}$) and the compression ratio (ε) versus exhaust temperature (T_{41}). As obvious, the advancement of EVO is up to 80 °CA.

Analysing the $MFB_{50\%}$ plotted below, it can be seen that a retarding from about 10 up to nearly 40°CA is necessary to achieve the considered exhaust temperatures (T_{41}). It is evident that variations of $MFB_{50\%}$ as significant as these can not be achieved by keeping constant the shape of relative rate of heat release. Retarding combustion about 30 °CA is even challenging by means of post injections. Assuming a combustion heat release, which affects the exhaust temperature in the same way as the considered idealised $MFB_{50\%}$ variation, could be achieved, another problem will occur. As known from experimental investigations, retarding combustion in general means an increase of HC and CO emissions, what applies in particular for cold engine conditions. Of course, a relevant increase of HC and CO emissions before catalyst

light off is absolutely unwanted. Hence, taking into account effects on emissions, a retarded combustion in terms of exhaust thermomanagement, applied directly after engine cold start, seems to be not that promising as it can be assumed by studying figure 3.20. Moreover, it is worth mentioning in this context that the increasing losses of incomplete combustion – which is the reason for increasing HC and CO emissions – mean also a penalty in efficiency.

Coming to the right chart in figure 3.21, it can be seen that the necessary heat added by the EHeater ($\dot{Q}_{\mathrm{EH}}$) increases steadily versus T_{41}, what is reasonable due to the nearly constant exhaust mass flow. As obvious, for a gain in T_{41} of 100 °C an increase of $\dot{Q}_{\mathrm{EH}}$ from about 1,4 kW is necessary.

As already mentioned the lower compression ratio (ε) limit was set to 9, what is of course unrealistic low for a diesel engine. However, for discussion of fundamental effects by means of a simulation this is absolutely reasonable.

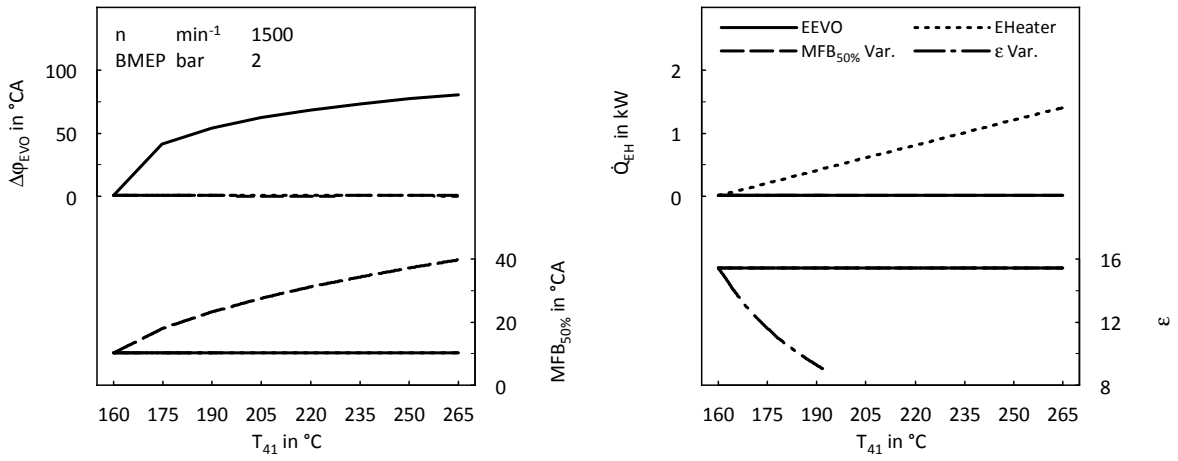

Figure 3.21: Variation of EVO, $\mathrm{MFB}_{50\%}$, heat delivered by EHeater and compression ratio versus exhaust temperature downstream turbine at 1500 min^{-1} and a BMEP of 2 bar

Due to the reasons mentioned above, the EHeater seems to be the most relevant alternative to EEVO in terms of increasing exhaust temperature without a reduction of mass flow. Thus, the effect resulting from an increase in the overall efficiency of the EHeater should be discussed, see figure 3.22. The plotted $\Delta\dot{H}_{\mathrm{exh}\,41}$ versus $\Delta\dot{Q}_{\mathrm{Loss}}$ characteristics of EEVO is already known from figure 3.20. The same applies for the characteristic of the EHeater which corresponds to an overall EHeater efficiency of 50 % ($\eta_{\mathrm{EH}} = 50\,\%$). In addition an efficiency increase up to 100 % is considered. As apparent, using an idealised EHeater – $\eta_{\mathrm{EH}} = 100\,\%$ – means an increase of exhaust enthalpy flow $\dot{H}_{\mathrm{exh}\,41}$ which is higher than the increase of $\dot{Q}_{\mathrm{Loss}}$. Nevertheless as clearly obvious an η_{EH} of 100 % does not mean that the whole additional supplied energy is spent to the exhaust gas. This is of course due to the fact that the electrical energy is provided by the combustion engine, which is characterized by an efficiency clearly lower than 100 %.

To overcome the negative effect of low engine efficiency on exhaust thermomanagement efficiency, the fuel energy has to be converted directly into heat without the intermediate

step of power generation in cylinders. Using a burner which is located in the exhaust system directly upstream the catalyst, as recommended by [33], may be a way for doing so. However, the idealised case of converting the entire additionally supplied fuel energy in exhaust enthalpy ($\Delta\dot{H}_{\mathrm{exh\,41}} = \Delta\dot{Q}_{\mathrm{Fuel}}$) is only the theoretical potential of a burner. In a real application the energy for providing the compressed air, incomplete combustion and wall heat losses lead to an overall efficiency of the burner which is smaller than the theoretical potential. Nevertheless, compared to an electrical heater a burner is promising in terms of efficiency. The drawback of a burner is the high demand of installation space. Hence an application upstream a close coupled catalyst is almost not achievable. Furthermore the complexity of a burner caused by the air and fuel supply has to be considered.

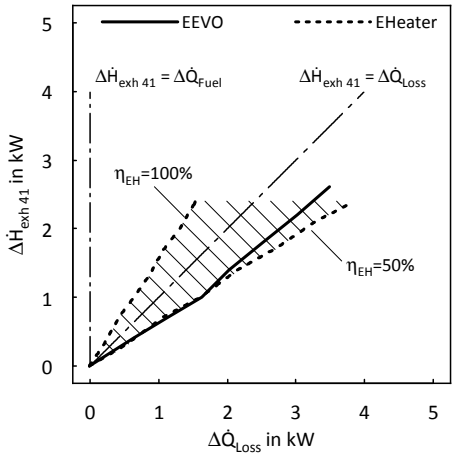

Figure 3.22: Effect of overall effiecieny of the electrical heater on comparison with EEVO concerning variation of exhaust enthalpy flow versus variation of heat losses at 1500 min^{-1} and a BMEP of 2 bar

3.4.2 Variable Intake Valve Timings

As discussed in section 3.3.2, one way for gaining exhaust temperature is a reduction of the cylinder charge heat capacity related to fuel energy. For characterisation of this exhaust temperature gaining effect, the charge fuel ratio (CFR), which was introduced in section 3.3.2, will be considered. The variation of the intake valve lift provides several strategies for a reduction of aspirated mass of cylinder charge. Two of them – late intake valve closing (LIVC) and late intake valve opening (LIVO), see figure 3.23 (right) – will be discussed subsequently. The wide spread method of cylinder mass reduction by means of an intake throttle – located between compressor and intake manifold – will serve as reference.

The left chart in figure 3.23 represents the impact of LIVO, LIVC and throttling on fuel consumption (BSFC), exhaust mass flow ($\dot{m}_{\mathrm{exh}\,41}$) and CFR. The results are plotted versus exhaust temperature downstream turbine (T_{41}). LIVO leads to a significant increase of fuel consumption. Compared to this, the penalty of throttling is clearly lower. Using LIVC, a moderate exhaust temperature increase – up to about 200 °C – could be achieved without a drawback in BSFC. For higher exhaust temperatures a slight increase could be observed. However, LIVC remains clearly more efficient than throttling and LIVO. The reason for this should be discussed later.

Considering the exhaust mass flow ($\dot{m}_{\mathrm{exh}\,41}$), a reduction versus exhaust temperature can be observed for all considered strategies, what is typical for methods using a reduction of CFR for gaining exhaust temperature. The mass flow difference of the considered methods has two reasons. First, the different efficiency and hence the different increase of injected fuel mass. In other words, a strategy with a low efficiency and hence a high amount of injected fuel mass requires a higher cylinder mass for the same CFR than a more efficient method (less injected fuel mass). Second, as the bottom graphs illustrate, the CFR differs. This is because the reduction of CFR is not the only exhaust temperature gaining effect which is relevant for the considered methods. The exhaust temperature is also influenced by the temperature of aspirated cylinder charge (see equation 3.7), which is not identical for the considered methods. Due to this a reduction of cylinder mass by means of raising cylinder charge temperature leads to a higher exhaust temperature and hence a higher enthalpy flow than the same decrease of cylinder mass achieved by a reduction of cylinder charge pressure (refer to direct and indirect effect discussed in section 3.3.2). Thus, it can be assumed that LIVO, which has the highest CFR at a given exhaust temperature, achieves also the highest temperature of aspirated cylinder charge at start of combustion (SOC).

Having a detailed look on the BSFC and $\dot{m}_{\mathrm{exh}\,41}$ curves of LIVO, a unsteady characteristic can be observed. More exactly the BSFC increase becomes lower at an exhaust temperature (T_{41}) of about 220 °C, simultaneously the mass flow reduction becomes more significant. The reason for this unsteadiness will be explained later.

Figure 3.24 shows the crank angle based characteristics of cylinder pressure (left) and temperature (right). The illustrated curves are related to an exhaust temperature of 210 °C. Studying the cylinder temperature characteristics in the right chart confirms that LIVO achieves the highest temperature of aspirated cylinder charge. The reason for this could be derived from the cylinder pressure curves during gas exchange, which are plotted in the left chart. Since LIVO means that the intake valves remain closed at the beginning of the intake stroke, a depression in cylinder occurs. Hence, opening of intake valves – clearly after TDC –

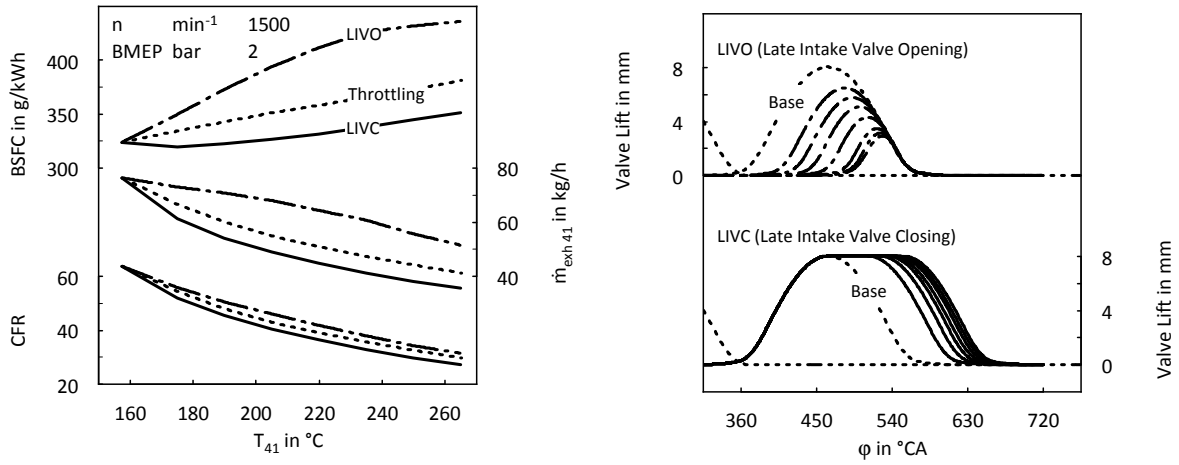

Figure 3.23: Effect of late intake valve closing (LIVC), throttling and late intake valve opening (LIVO) on fuel consumption, exhaust mass flow and CFR at 1500 min^{-1} and a BMEP of 2 bar

results in a high velocity of in cylinder flowing gas. The dissipation of this kinetic energy in cylinder causes the discussed temperature increase.

Analysing the cylinder pressure curves during gas exchange provides also the most relevant reason for the effect of LIVC, throttling and LIVO on fuel consumption, observed in figure 3.23. As obvious, the mentioned cylinder depression of LIVO during gas exchange results in a extremely negative PMEP, what means an according increase in BSFC. A similar effect – albeit to a lesser extent – could be observed for throttling. LIVC leads to the lowest pumping losses, which explains the relatively low penalty in fuel consumption.

The left chart in figure 3.25 shows the wall heat losses via cylinders ($Q_{\mathrm{W,\,Cyl}}$) and the exhaust duct ($Q_{\mathrm{W,\,Exh}}$). The latter comprises exhaust ports, the exhaust manifold and the turbine housing. Analysing cylinder wall heat losses, makes obvious a significant increase due to LIVO. Also throttling and LIVC lead to an increase. This is mainly due to the higher temperatures during combustion and expansion. In case of LIVO, also a higher wall heat flow during compression stroke – resulting from the increase in temperature of aspirated cylinder charge – has to be considered. Moreover, it has to be kept in mind that the lower cylinder pressure resulting from throttling and LIVC means a partly compensation of the wall heat flow increase coming from the higher cylinder temperatures. In case of LIVO, which achieves the reduction of aspirated cylinder charge more or less without a pressure decrease, this effect does not occur. Studying the characteristics of wall heat losses in the exhaust duct plotted above, attention has to be paid to the scaling of axis, which differs from scaling used for cylinder wall heat losses. Nevertheless, the increase – mainly caused by the increase of exhaust temperature – is considerable.

The right chart shows the already known illustration of change in exhaust enthalpy flow ($\Delta\dot{H}_{\mathrm{exh\,41}}$) plotted versus change in heat losses ($\Delta\dot{Q}_{\mathrm{Loss}}$). It can be seen that throttling and in particular LIVC lead to a decrease of exhaust enthalpy flow, what surprises at first glance,

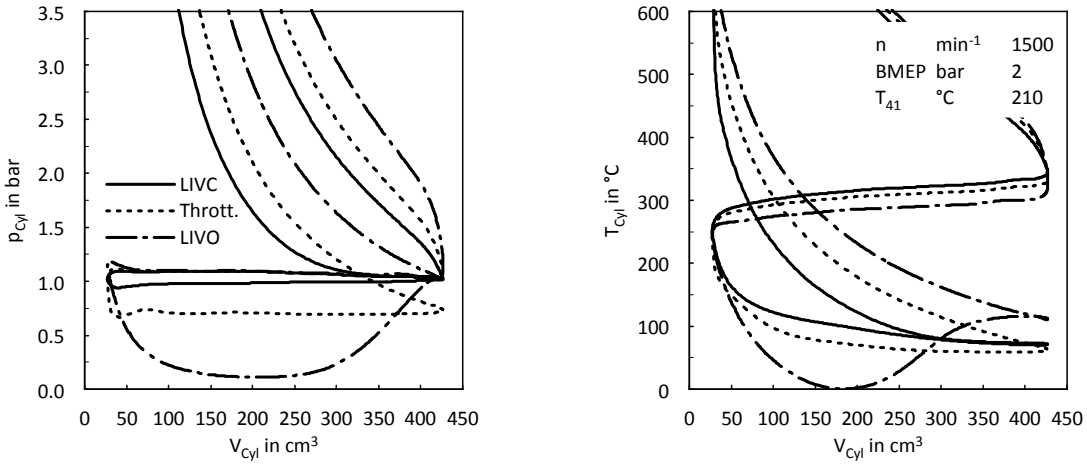

Figure 3.24: Comparison of LIVC, throttling and LIVO concerning characteristic of cylinder pressure and temperature versus cylinder volume at 1500 min^{-1} and a BMEP of 2 bar, referring to the same exhaust temperature

since both throttling and LIVC lead to an increase of exhaust temperature. However, the temperature increase is overcompensated by the reduction of mass flow. LIVO achieves a higher gradient of $\dot{H}_{\mathrm{exh}\,41}$ versus $\dot{Q}_{\mathrm{Loss}}$, what means – referring to the evaluation strategy introduced in section 3.1.1 – a higher exhaust thermomanagement efficiency, although the BSFC is higher at a given exhaust temperature (see figure 3.23). This could be explained by the fact that LIVO achieves the same exhaust temperature increase by means of a less dramatic mass flow reduction compared to LIVC and throttling. Keeping in mind that the gradient of the EEVO characteristic is only slightly lower than 1 ($\dot{H}_{\mathrm{exh}\,41} = \dot{Q}_{\mathrm{Loss}}$), also LIVO seems to be not recommendable for gaining exhaust enthalpy flow. This confirms that methods achieving an increase of exhaust temperature by a decrease of CFR are not adequate when it comes to gaining exhaust enthalpy flow, what was already assumed in section 3.3.2. Nevertheless, as examined also in section 3.3.2, there are also applications, which do not require a high mass flow or even benefit from a mass flow reduction.

The left chart in figure 3.26 illustrates the effect of LIVC, LIVO and throttling on pressure ($p_{\mathrm{Cyl,\,SOC}}$) and temperature ($T_{\mathrm{Cyl,\,SOC}}$) of aspirated cylinder charge at start of combustion (SOC). A decline in pressure particularly in combination with a decline in temperature is critical in terms of ignition and combustion stability. This applies all the more for the low cylinder wall temperatures during warm up. Hence, the application of throttling and in particular LIVC for rapid heat up of a catalyst directly after engine cold start is not recommended without detailed experimental investigations of this effect. LIVO means an increase of $T_{\mathrm{Cyl,\,SOC}}$ at a more or less constant $p_{\mathrm{Cyl,\,SOC}}$ what seems to be beneficial in context of cold start behaviour. This benefit – as well as the drawback concerning fuel consumption – was also identified by [36] by means of experimental investigations.

Besides deriving findings relevant for cold start behaviour, analysig $p_{\mathrm{Cyl,\,SOC}}$ and $T_{\mathrm{Cyl,\,SOC}}$ enables also explaining the reason for the unsteady characteristics of LIVO. Doing so will be

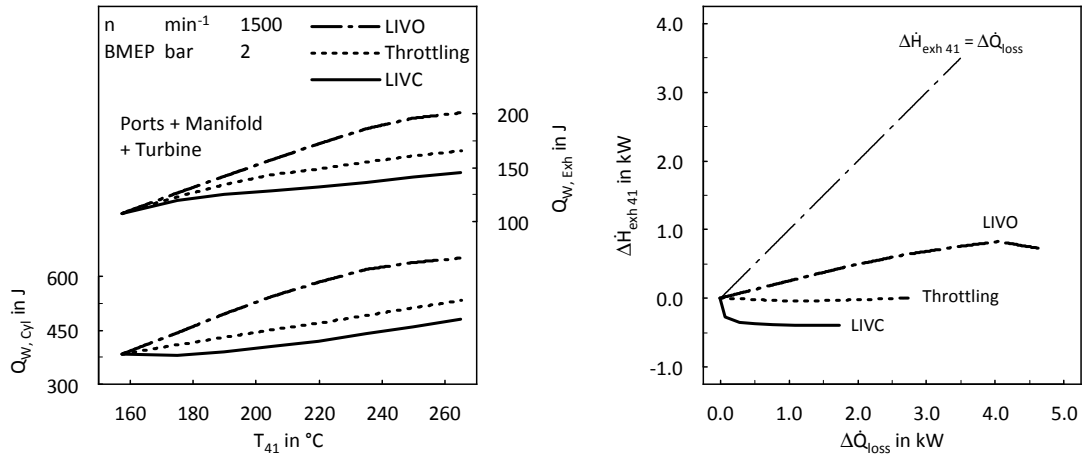

Figure 3.25: Effect of LIVC, throttling and LIVO on wall heat losses and variation of exhaust enthalpy flow versus heat losses at 1500 min^{-1} and a BMEP of 2 bar

supported by considering also the cylinder pressure versus volume curves of LIVO (figure 3.26, right chart). More exactly these curves are plotted for a retarding of IVO which leads to an exhaust temperature (T_{41}) of 210 (1) and 260°C (2). Relative to the base (0), which is also illustrated, this means an exaust temperature increase of 50 and 100 °C. The corresponding values of $p_{\mathrm{Cyl,SOC}}$ and $T_{\mathrm{Cyl,SOC}}$ are shown in the left chart by means of markers. Thus, it is obvious that the exhaust temperature of 210 °C (1) was selected since it indicates more or less exactly the break of the LIVO versus T_{41} characteristics. Considering 0 and 1 concerning cylinder pressure versus volume, it can be seen that the cylinder pressures at the compression stroke are nearly identical. Thus, LIVO achieves the CFR reduction necessary for exhaust temperatures up to 210 °C almost without a decrease of cylinder charge pressure and hence only by an increase of cylinder charge temperature. However, a further increase of 50 °C in exhaust temperature (260 °C, 2) requires retarding IVO in a degree that does not allow a pressure equalization between intake ports and cylinders. As a consequence of this, the cylinder charge pressure decreases, which can be identified by the negative offset of the corresponding cylinder pressure volume characteristic (2) during compression stroke. Having a closer look on the low pressure cycle makes obvious that the increase of pumping losses between 0 and 1 is far higher than this between 1 and 2. That explains why the gradient of BSFC versus T_{41} becomes lower for high exhaust temperatures (refer to figure 3.23).

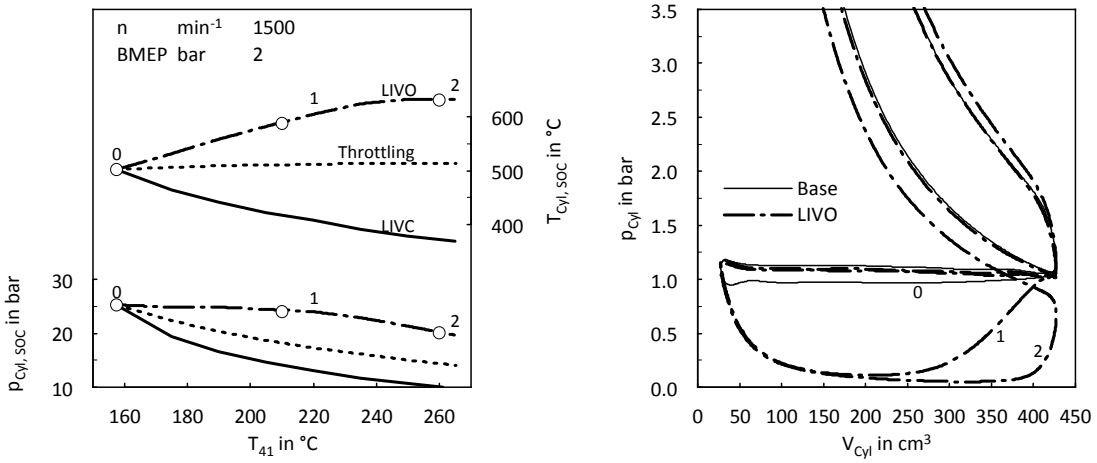

Figure 3.26: Comparison of LIVC, throttling and LIVO concerning effect on pressure and temperature of cylinder charge at start of combustion at 1500 min^{-1} and a BMEP of 2 bar (left). Effect of LIVO on cylinder pressure versus cylinder volume characteristic (right).

3.4.3 Internal Exhaust Gas Recirculation

As already explained, gaining exhaust temperature by means of a CFR reduction is achieved mainly due to a cut of overall aspirated cylinder mass (air and EGR). Besides the alternative intake valve timings discussed above (LIVC and LIVO), also a replacement of cooled external EGR by means of hot internal EGR enables a decrease of cylinder charge density and hence a mass reduction. Subsequently three potential strategies for internal EGR should be discussed. The corresponding valve lift curves are plotted in the left chart of figure 3.27. One way for achieving an internal EGR is by an advanced closing of exhaust valves, what could be realized by a phasing of exhaust camshaft – Early Exhaust (EE) camshaft timing. The second internal EGR strategy considered in detail – Early Exhaust Late Intake (EELI) camshaft timing – uses the same principle for recirculation of exhaust gas. However, EELI is featured in addition with a phasing of the intake camshaft, which enables retarding intake valve timing in the same degree as the exhaust valve timings is advanced. Of course, both EE and EELI lead not only to an internal EGR but also to an advanced EVO. Hence the achieved exhaust temperature increase comes not only from a reduction of CFR but also from a decrease in effective expansion. Another way for realization of internal EGR is an additional opening of exhaust valves during the intake stroke (2^{nd} Event).

The right chart in figure 3.27 provides the characteristics of the overall rate of EGR ($\mathrm{EGR}_{\mathrm{Cyl,\,tot}}$) and the low pressure rate of EGR (LPEGR) plotted versus exhaust temperature downstream turbine (T_{41}). $\mathrm{EGR}_{\mathrm{Cyl,\,tot}}$ is the the total residual gas concentration identified at the start of high pressure cycle. In other words, the sum of external and internal EGR. As explained at the beginning of section 3.4, the EGR controlling was defined for all methods, considered by simulation, in a way that a reduction of the charge fuel ratio (CFR) leads to a reduction of both air excess ratio and EGR. More exactly the low pressure EGR valve is controlled in order to achieve a relative change in total residual gas concentration in cylin-

der ($EGR_{Cyl,\,tot}$) which is identical to the relative change in the charge fuel ratio. Taking into account that the exhaust temperature gaining effect of the considered strategies (EE, EELI and 2nd Event) is based mainly on a reduction of overall cylinder mass, the decrease of $EGR_{Cyl,\,tot}$ versus T_{41} is reasonable. Hence, the relatively low decrease of $EGR_{Cyl,\,tot}$ resulting from EE indicates a lower reduction of CFR compared to EELI and 2nd Event. This effect will be discussed later in detail. Considering the curves of external EGR (LPEGR) it becomes clear that the replacement of external EGR by internal EGR, required for a given exhaust temperature, depends on the EGR strategy. Internal EGR realized by a second exhaust valve lift event (2nd Event) leads to the lowest rates of external and hence to the highest rates of internal EGR. This could be explained by the fact that the replacement of cooled by hot EGR is more or less the only exhaust temperature gaining effect of 2nd Event. In case of EE and EELI, the exhaust temperature increase is also supported by the advanced EVO. Thus, it is also clear that the limit of exhaust temperature increase – defined by a closed low pressure EGR valve – for 2nd Event is lower than these of EE and EELI. Exceeding the T_{41} limit of about 195 °C by means of 2nd Event could be achieved only by increasing the overall rate of EGR ($EGR_{Cyl,\,tot}$).

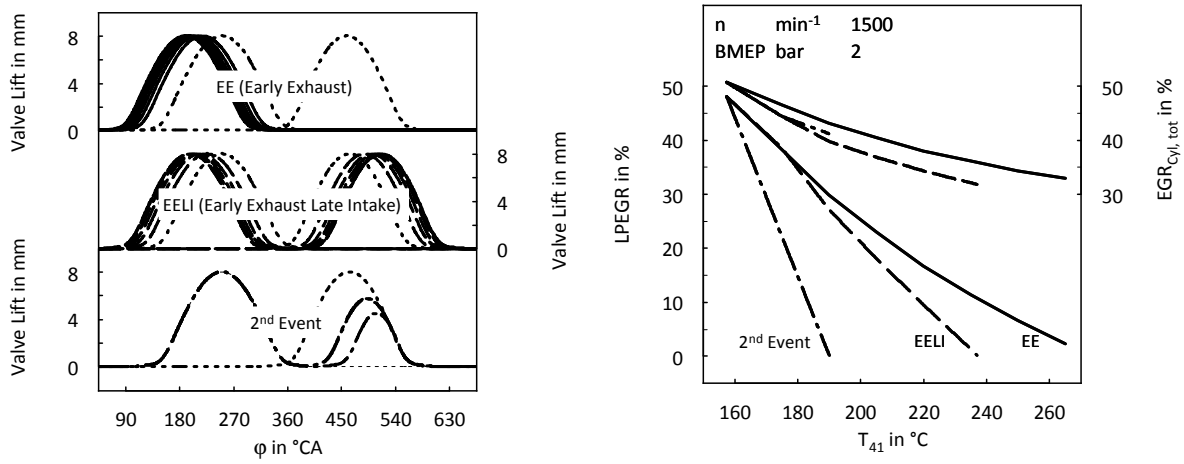

Figure 3.27: Replacement of low pressure EGR by internal EGR using various valve timing strategies

In the left chart of figure 3.28 the interaction of exhaust temperature (T_{41}) with fuel consumption (BSFC) and charge fuel ratio (CFR) is shown for the considered internal EGR strategies – EE, EELI and 2nd Event. While the 2nd Event enables a nearly BSFC-neutral exhaust temperature increase, internal EGR based on exhaust phasing (EE, EELI) leads to a considerable penalty, what has mainly two reasons. First, the advanced EVO causes a decrease of effective expansion. Second, the residual gas compression resulting from an advanced closing of exhaust valves means an increase of pumping losses. The reason for the difference of EE and EELI will be discussed later.

The characteristics plotted below – CFR – point out the ratio of overall cylinder mass (air, external and internal EGR) to fuel mass. The difference between EE and EELI could

be explained by the fact that phasing only exhaust cam shaft (EE) by a given angle means a less significant reduction of volumetric efficiency than phasing both (EELI) by the same angle (of course in opposite directions). Thus, for achieving the same exhaust temperature, phasing has to be done for EE in a more extensive way than for EELI. Hence, also the share of advanced EVO in exhaust temperature increase is higher, which is also a reason for the mentioned difference of EE and EELI concerning fuel consumption. Analysing 2nd Event makes clear that the CFR reduction required for a given exhaust temperature (T_{41}) is nearly identical or even slightly lower than this of EELI. Keeping in mind that EELI is featured with an exhaust temperature gaining early exhaust valve opening and 2nd Event not, this may be surprising at first sight. However, as pointed out in section 3.3.2, not only the mass of cylinder charge and the CFR (indirect effect), but also the cylinder charge temperature (direct effect) is relevant when it comes to exhaust temperature. The nearly identical CFR of 2nd Event and EELI – although EELI is featured with an early exhaust valve opening – could be explained by a higher cylinder charge temperature of 2nd Event, which comes from the higher share of internal EGR (see figure 3.27). The right chart in figure 3.28 provides the change in overall cylinder mass ($m_{\mathrm{Cyl,\,HP}}$) and exhaust mass flow ($\dot{m}_{\mathrm{exh\,41}}$) versus exhaust temperature (T_{41}). For engine operation without internal EGR the relative variation of these characteristics would be identical. As obvious, in case of the considered internal EGR strategies, considerable differences occur. Analysing EE, a nearly constant mass of cylinder charge ($m_{\mathrm{Cyl,\,HP}}$) can be seen. Thus, the CFR reduction of EE observed in the left chart is more or less only due to the increase of fuel mass. Although the overall mass of cylinder charge remains constant for EE, the exhaust mass flow ($m_{\mathrm{exh,\,41}}$) declines, what comes from the partly replacement of external EGR (low pressure EGR, recirculated via EAS and hence via measuring point '41') by internal EGR. Of course this effect is also relevant for EELI and 2nd Event. Comparing EELI and 2nd Event concerning CFR and $m_{\mathrm{Cyl,\,HP}}$ makes clear that 2nd Event results in a lower CFR reduction although the reduction of cylinder mass is more significant. This could be explained by the higher efficiency and hence lower increase of fuel mas in case of 2nd Event. The higher difference of 2nd Event and EELI concerning $\dot{m}_{\mathrm{exh\,41}}$ compared to this concerning $m_{\mathrm{Cyl,\,HP}}$ comes from differences in the mechanism of $m_{\mathrm{Cyl,\,HP}}$ reduction. While 2nd Event achieves the low cylinder mass mainly due to a replacement of external by internal EGR and hence an increase of cylinder charge temperature, a considerable share of cylinder mass reduction resulting from EELI is due to the late IVC and hence a reduction of cylinder charge pressure.

In figure 3.29 the engine operation cycle of EE, EELI and 2nd Event should be discussed in detail by referring to an exhaust temperature (T_{41}) of 190 °C. The considered cylinder pressure (left) and temperature (right) characteristics are plotted versus cylinder volume. Analysing the pressure curves, one reason for the lower fuel consumption penalty of EELI compared to EE could be identified. Both EE and EELI lead to a considerable increase of cylinder pressure at the end of the exhaust stroke, which comes from residual gas compression due to the advanced closing of exhaust valves. While a conventional intake camshaft timing (EE) means a high pressure gradient between cylinder an intake ports at IVO and hence an expansion of compressed residual gas into the intake ports, this could be – at least partly – avoided by a retarded intake camshaft timing (EELI). The retarded IVO leads to an expansion of compressed residual gas in cylinder and hence enables recovering a part of the energy spent in residual gas compression. To prevent the flow of hot compressed exhaust gas into the intake

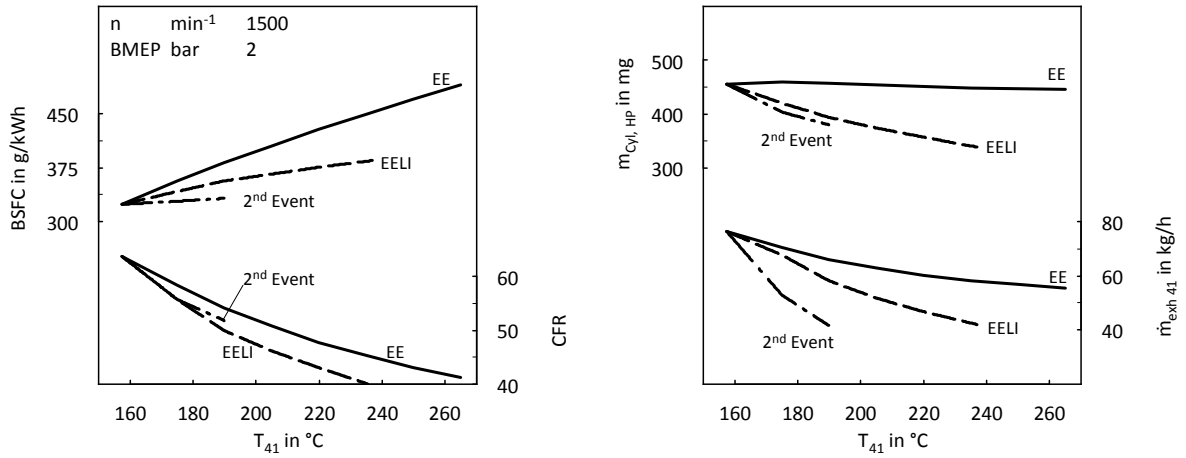

Figure 3.28: Effect of various internal EGR strategies on fuel consumption, charge fuel ratio, cylinder mass and exhaust mass flow at 1500 min^{-1} and a BMEP of 2 bar

ports means also a reduction of heat losses. Both energy recovery by in-cylinder expansion of compressed residual gas and lower wall heat losses in intake ports contribute to the higher efficiency of EELI compared to EE. Moreover it is worth mentioning that [22] had observed an acoustic drawback of compressed residual gas expansion into the intake ports (EE) by means of experimental investigations.

Having a closer look on EE and EELI during compression stroke, a later increase in case of EELI can be identified. The reason is that an retarded intake camshaft timing means not only a retarded opening but also a retarded closing of intake valves. Hence a part of the already aspirated cylinder charge is expelled back into the intake ports, which explains the mentioned above less significant CFR reduction of EE compared to EELI.

Analysing the temperature characteristics in the right chart of figure 3.29, makes obvious the internal EGR mechanism of 2^{nd} Event. Due to the additional exhaust valve lift during intake stroke, a part of the already expelled exhaust gas is aspirated. This could be identified by an increase of cylinder temperature during the intake stroke which results in the highest temperature of considered internal EGR strategies at the beginning of the compression stroke.

In the left chart of figure 3.30 the wall heat flow in the exhaust duct ($Q_{\mathrm{W,\,Exh}}$) – ports, manifold and turbine housing – and these in the intake ports (Q_{IP}) is plotted versus exhaust temperature (T_{41}). Considering the heat losses in the exhaust duct, a clear drawback of EE and EELI can be seen, which is mainly due the early exhaust valve opening. Of course also 2^{nd} Event leads to an increase of cylinder temperature at EVO and hence to an increase of wall heat losses in exhaust duct. However, due to the conventional exhaust camshaft timing, the pressure gradient between cylinders and exhaust ports at EVO and hence the flow velocities of cylinder outflow are lower than in case of EE and EELI, what is beneficial concerning wall heat flow.

The characteristics of the intake port wall heat flows plotted below, point out the explained above disadvantage of EE. In case of EELI and 2^{nd} Event heat is transferred from port to

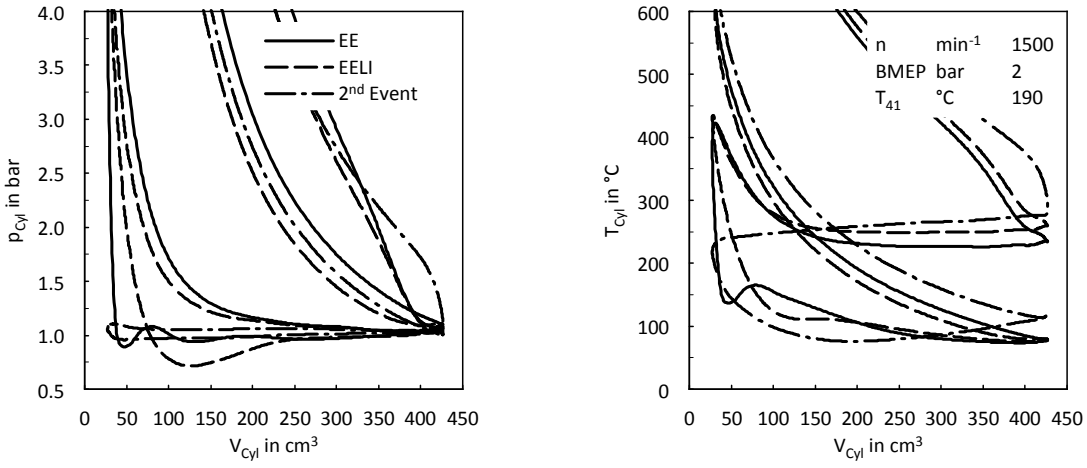

Figure 3.29: Comparison of various internal EGR strategies concerning cylinder pressure and temperature versus volume characteristic at 1500 min^{-1}, a BMEP of 2 bar and an exhaust temperature of 190 °C

gas. For EE this transfer reverses, what is due to the outflow of hot compressed residual gas after opening of intake valves.

Analysing the change in exhaust enthalpy flow ($\Delta\dot{H}_{\mathrm{exh\,41}}$) versus the change in heat losses ($\Delta\dot{Q}_{\mathrm{Loss}}$) – figure 3.30, right – leads to the same finding as it was derived from analysing LIVC, LIVO and throttling by means of this evaluation chart: Exhaust temperature gaining methods mainly based on a CFR reduction seem to be not adequate for increasing exhaust enthalpy flow, what is due to the reduction of exhaust mass flow. Hence it is not surprising that the strategy with the lowest exhaust mass flow reduction (EE) leads to the best performance, although it has the highest heat losses. Here it is worth mentioning that the reason for the higher $\Delta\dot{Q}_{\mathrm{Loss}}$ are not only the heat flows discussed in the left chart (exhaust duct, intake ports), but also these in the cylinders (not illustrated).

As already mentioned in the discussion of alternative intake valve timings, besides fuel consumption, exhaust temperature and enthalpy flow, also the effect on cylinder pressure and temperature at start of combustion ($p_{\mathrm{Cyl,\,SOC}}$, $T_{\mathrm{Cyl,\,SOC}}$) has to be considered in evaluation of exhaust thermomanagement methods. A decrease of these parameters is critical concerning cold start ignitability and combustion stability. Thus, the variation of $p_{\mathrm{Cyl,\,SOC}}$ and $T_{\mathrm{Cyl,\,SOC}}$ versus exhaust temperature (T_{41}) should be analysed also for the internal EGR strategies, see figure 3.31. It can be seen that EE leads to a clearly increase of $T_{\mathrm{Cyl,\,SOC}}$ at a nearly constant $p_{\mathrm{Cyl,\,SOC}}$, what means by trend a benefit concerning the mentioned issues. EELI shows a decrease of pressure, while temperature remains more or less constant. This is reasonable, since it is known from analysing alternative intake valve timings that a late IVC leads to a decrease of $p_{\mathrm{Cyl,\,SOC}}$ and $T_{\mathrm{Cyl,\,SOC}}$. In case of EELI the temperature decrease could be avoided by a higher temperature of aspirated cylinder charge (internal EGR).

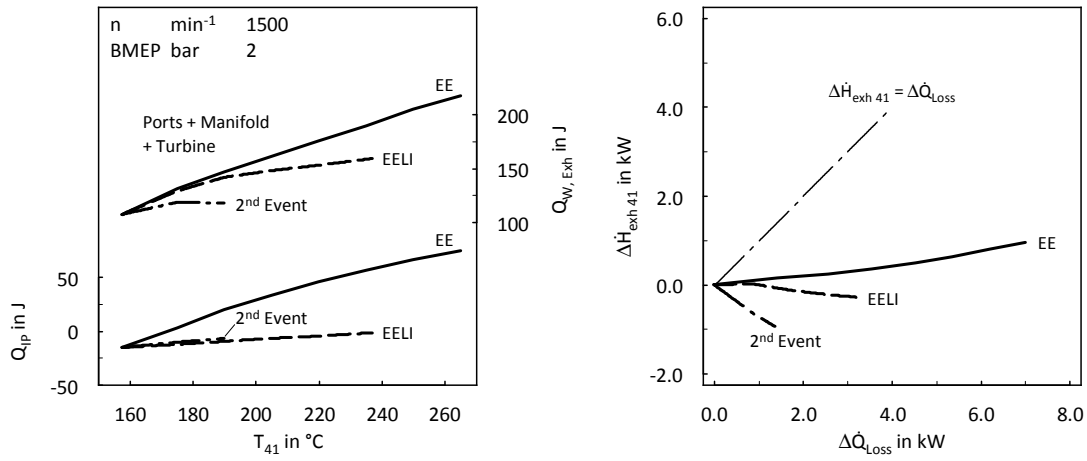

Figure 3.30: Effect of various internal EGR methods on wall heat losses and enthalpy flow versus heat losses at 1500 min^{-1} and a BMEP of 2 bar

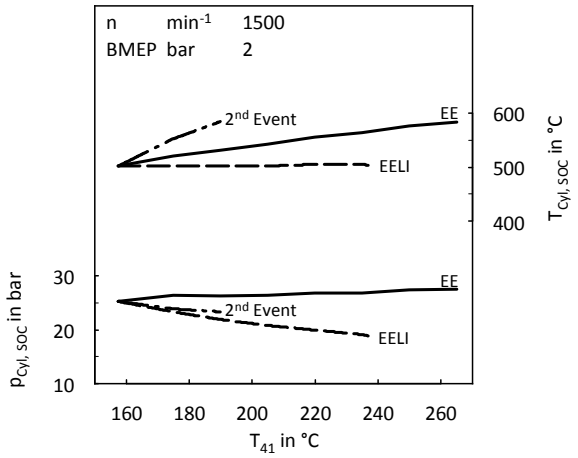

Figure 3.31: Effect of various internal EGR methods on pressure and temperature of cylinder charge at start of combustion at 1500 min^{-1} and a BMEP of 2 bar

Also for the 2nd Event a slight decrease of $p_{\mathrm{Cyl,SOC}}$ can be identified, however $T_{\mathrm{Cyl,SOC}}$ shows a clear increase. The decrease of pressure at start of combustion results from higher wall heat losses during compression stroke. Taking into account both increase of $T_{\mathrm{Cyl,SOC}}$ and decrease of $p_{\mathrm{Cyl,SOC}}$ does not allow a simple diagnosis concerning effect on cold start ignitability and combustion stability in case of the 2nd Event.

Another relevant issue in terms of internal EGR is the effect on in-cylinder swirl-motion. [14] has shown that the flow of internal EGR has to be adapted to the swirl motion which is provided by the in-cylinder flow through the intake ports. Otherwise a reduction of swirl motion and hence a drawback concerning NO_x/soot trade-off may appear.

3.4.4 Cylinder Deactivation

Cylinder deactivation as it is discussed in this work is characterized by keeping closed both intake and exhaust valves as well as by switching off injection. This could be applied for one or more cylinders. In the considered operation area which is characterized by a more or less naturally aspiration, it is obvious that doing so will lead to a reduction in overall cylinder mass. Contrary to methods considered above, this is achieved neither by an increased temperature nor by a decreased pressure of aspirated cylinder charge, but by declining the effective displacement. While the VVT methods for exhaust thermomanagement discussed above could be applied more or less continuously, this is of course not possible in case of cylinder deactivation. When it comes to realization, another limitation results from the total number of cylinders. More exactly, cylinder deactivation is only relevant for engines with an even number of cylinders. This enables switching off half of the cylinders, while maintaining a regular firing interval, what is necessary for achieving a good NVH behaviour. In case of simulation also irregular firing intervals could be considered. Hence, in case of the known 4-cylinder engine model, besides the 4-cylinder mode (original), both operation with 2 and 3 cylinders was considered. In figure 3.32 the effect of cylinder deactivation on the most relevant parameters concerning exhaust thermomanagement is shown. For this purpose the characteristics are plotted versus the number of active cylinders. The considered operation point is identical to this considered in discussion of the VVT strategies analysed above. Keeping in mind the variable overall displacement of active cylinders, declaration of engine load by means of effective torque (τ_{eff}) is clearer than by means of BMEP. It can be seen that switching off one cylinder rises the exhaust temperature downstream turbine (T_{41}) about 30 °C. Cutting an additional one – 2-cylinder operation – leads even to an increase of about 105 °C. Considering the exhaust mass flow ($\dot{m}_{\mathrm{exh\,41}}$) plotted below, makes obvious a linear decrease. Keeping in mind the more or less naturally aspirating engine operation and hence a nearly constant pressure of aspirated cylinder charge, this is not surprising. Analysing the exhaust enthalpy ($H_{\mathrm{exh\,41}}$) – which takes into account both exhaust temperature and mass flow – a slight decrease due to cutting the first cylinder can be seen. This means, the temperature increase is overcompensated by the mass flow decrease. Switching from 3 to 2 cylinder does not mean a further enthalpy decrease, what is due to the fact that the mass flow reduction remains constant, while temperature gain becomes higher. The BSFC characteristic in the right chart shows that the analysed exhaust temperature increase is achieved almost without a drawback concerning fuel consumption. Thus, the CFR reduction plotted above is more or less only due to the decrease of aspirated mass flow (air and EGR). In other

words, the contribution of increase in fuel mass could be neglected. At first sight, it may be not reasonable why a linear decrease of CFR leads to a progressive exhaust temperature increase. However, as shown in equation 3.9, the exhaust temperature increase is not directly but inversely proportional to CFR. For a better illustration of this interaction also 1/CFR is plotted.

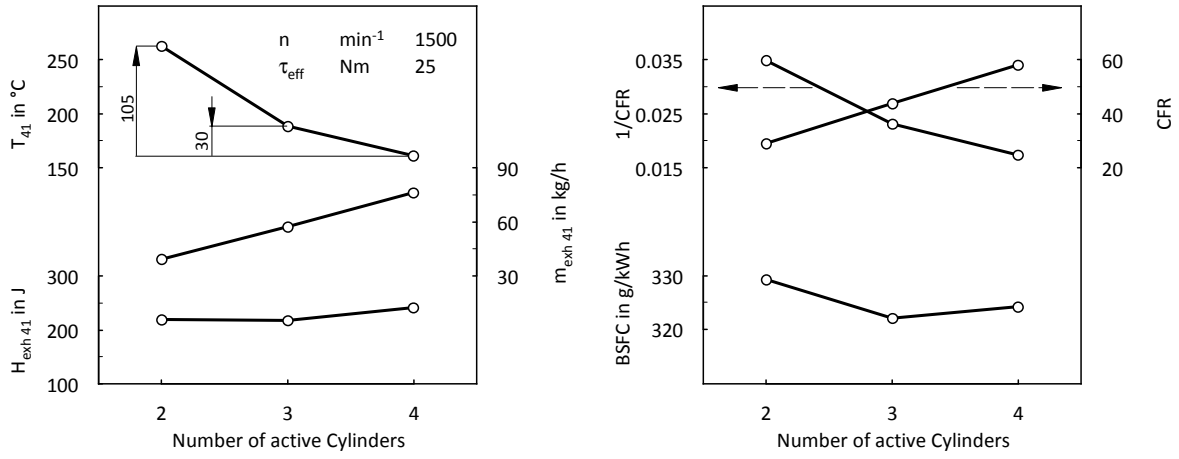

Figure 3.32: Effect of cylinder deactivation on exhaust gas parameters, fuel consumption and charge fuel ratio at 1500 min^{-1} and an engine torque of 25 Nm

As shown in figure 3.32, the variation of fuel consumption due to cylinder deactivation is small. Nevertheless, slight variations can be seen. Considering the overall cylinder wall heat flow plotted in figure 3.33, a characteristic similar to this of the BSFC – a slight decrease due to switching from 4 to 3 cylinders and a slight increase when switching from 3 to 2 cylinders – can be seen. Besides the overall cylinder wall heat flow also the contribution of every single cylinder is obvious. Due to this, it becomes clear that the fall away of wall heat flow in deactivated cylinders is more or less compensated by an increase of the still active cylinders. In this context it is worth mentioning that the wall heat flow in deactivated cylinders is very low but not zero. This means, wall heat flow occurring while compression and expansion is taken into account by the model. In addition to cylinder wall heat losses, figure 3.33 points out also the effect of cylinder deactivation on wall heat flow in the exhaust duct ($Q_{\mathrm{W,\,Exh}}$), which comprises the exhaust ports, the exhaust manifold and the turbine housing. It is apparent that this heat flows increase due to switching off one or two cylinders, which comes from the higher exhaust gas temperature.

For the considered above VVT strategies pressure and temperature at start of combustion ($p_{\mathrm{Cyl,SOC}}$, $T_{\mathrm{Cyl,SOC}}$) were analysed. Considering the aspirated mass (air + EGR) of one single cylinder it does almost not matter if one ore more of the other cylinders is deactivated – neither concerning pressure nor concerning temperature. Thus, also pressure and temperature at start of combustion is nearly independent from cylinder deactivation.

After the analysis of most relevant effects occurring due to switching off one or more cylinder, some further issues relevant for cylinder deactivation should be discussed by a

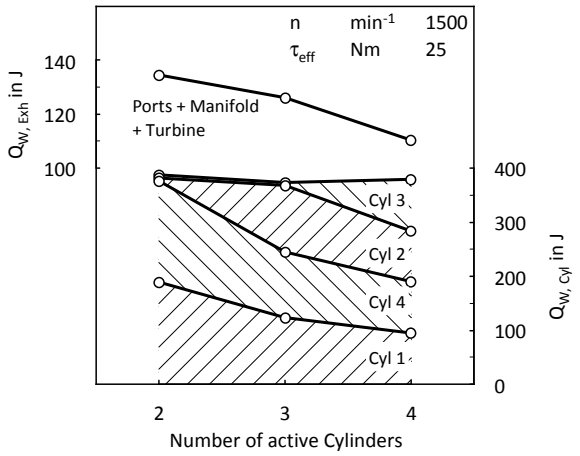

Figure 3.33: Effect of cylinder deactivation on wall heat losses in the cylinders and the exhaust duct at 1500 min^{-1} and an engine torque of 25 Nm

comparison of 4- (original) and 2-cylinder operation. This takes into account that a 2-cylinder operation is also relevant for experimental investigations on a 4-cylinder engine.

Figure 3.34 shows a comparison of 2- and 4-cylinder operation at 1500 min^{-1} and an engine torque (τ_{eff}) up to about 50 Nm. The considered parameters – BSFC, exhaust temperature (T_{41}) and charge fuel ratio (CFR) – are plotted versus the engine torque. In the left chart it can be seen that the increase of T_{41} resulting from switching off 2 cylinders becomes higher versus τ_{eff}. This could be explained by the fact that the CFR reduction which results from cutting 2 cylinders means a relative increase of exhaust temperature, refer to equation 3.9. Thus, applying this relative increase at a higher load operation point and hence a higher base (4-cylinder) exhaust temperature, the absolute amount of exhaust temperature increase is also higher compared to doing the same at a lower load operation point.

Analysing the characteristics of fuel consumption (BSFC) plotted above, a benefit at low engine torques and a drawback at higher torques can be seen. Both could be explained mainly due to differences in overall cylinder wall heat flow.

The right chart in figure 3.34 shows a comparison between 2- and 4-cylinder operation concerning CFR. Of course the main effect for CFR reduction resulting from 2-cylinder operation comes from cutting overall aspirated cylinder charge to half of the 4-cylinder value. However, the differences in BSFC lead to a relation of 4- and 2-cylinder CFRs which is slightly lower than 2 at low engine torque (BSFC benefit of 2-cylinder) and slightly higher than 2 at higher engine torques (BSFC penalty of 2-cylinder).

Moreover the illustration of CFR versus engine load points out the limitation of available engine output by the lower limit of air excess ratio (λ). This issue is of particular interest for cylinder deactivation, since switching off cylinders could be applied not continuously – in contrast to most other VVT strategies. Thus, in case of a 4-cylinder engine which is operated temporarily with 2 cylinders, a desired torque which is higher than the available torque requires switching back in 4-cylinder operation mode. Hence, for a given torque character-

istic of a driving cycle, the available torque in 2-cylinder mode defines how many times it is necessary to switch between 2- and 4-cylinder mode. Of course a high number of changes is disadvantageous and may be a reason that speaks against an application of cylinder deactivation. Thus, besides the exhaust thermomanagement performance also the available engine output is relevant when considering cylinder deactivation.

As apparent in figure 3.34 (right chart), taking into account a λ limit of 1,2 and a deactivated EGR leads to a maximum torque of slightly less than 50 Nm. Here it should be kept in mind that the results are based on a fully opened VNT position and hence on engine operation almost without boost pressure. This is reasonable for exhaust thermomanagement methods which are based mainly on a reduction of CFR.

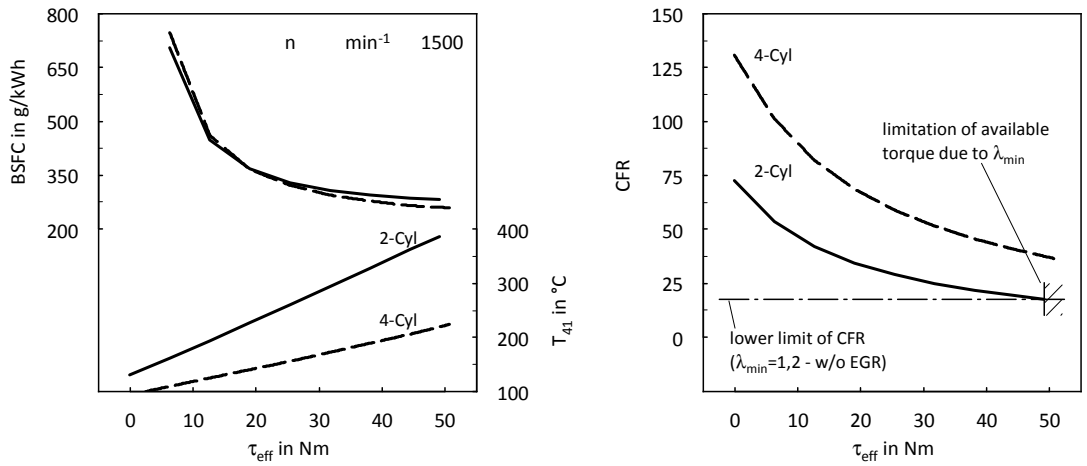

Figure 3.34: Comparison of 2- and 4-cylinder operation concerning fuel consumption, exhaust temperature and charge fuel ratio at 1500 min^{-1} and low engine torque

When it comes to find out the maximum available engine output, boosting nevertheless is reasonable. Due to this, in figure 3.35 a variation of the VNT position should be discussed.

For this purpose the characteristics of engine torque (τ_{eff}), boost pressure (p_{IM}) and compressor mass flow ($\dot{m}_{\mathrm{Comp}}$) are plotted versus the VNT position. A VNT value of 100 % corresponds to the vane position with the maximum flow cross section.

Due to the objective of maximizing the engine output, EGR was deactivated and fuel injection was controlled in order to achieve the defined lower λ limit of 1,2.

As obvious closing VNT increases boost pressure and hence compressor mass flow in a way that an engine torque of almost 70 Nm could be achieved. However, this applies only when the compressor surge limit is ignored. Taking into account the compressor surge line, means a significant cut in boost pressure and hence in mass flow, which leads to an actually available torque of less than 60 Nm.

The right chart shows the compressor map of the considered turbo charger. In addition also the swallowing capacity curves of the engine – in 2- and 4-cylinder operation mode – at 1500 min^{-1} are plotted. While the 4-cylinder curve is covered by the compressor operation map up to a compressor pressure ratio (π_{Comp}) of more than 2, the 2-cylinder curve exceeds

the surge line and hence the operation area of the compressor at a π_{Comp} of about 1,3. This illustration points out, why the surge limit of the compressor in 2-cylinder operation mode is far more critical than in operating the engine with 4 cylinders. Of course, an engine speed of 1000 min^{-1} means an operation curve which is located even more at the left hand side of the surge line.

In context of boosting in 2-cylinder operation mode, it is also worth mentioning that the higher value of firing interval leads to a more unsteady flow regime in compressor and turbine. Consequences on actual efficiency of turbine and compressor could be not excluded. For detailed investigation of this issue experimental investigations are necessary.

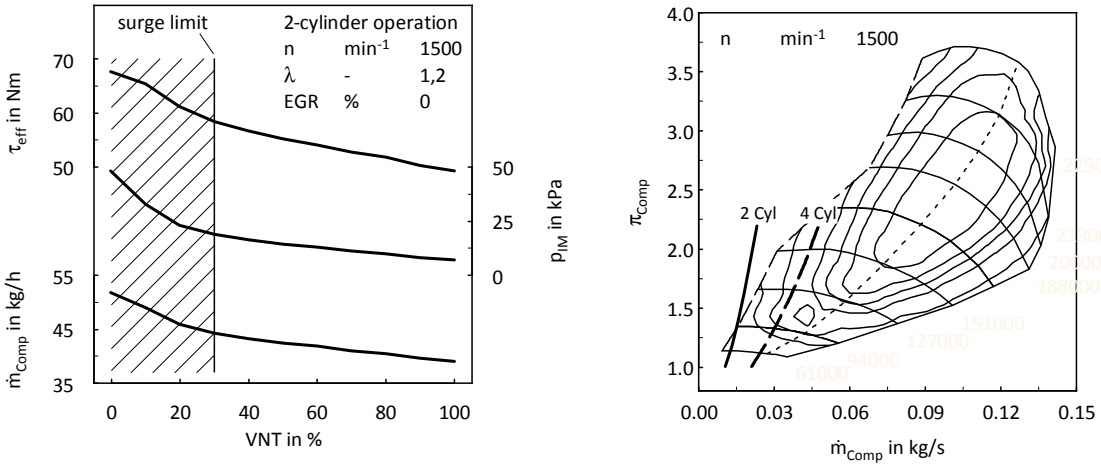

Figure 3.35: Effect of a VNT position variation in 2-cylinder mode on boost pressure, compressor mass flow and engine torque (left). Comparison of 2- and 4-cylinder operation concerning swallowing capacities and hence position of operation curves in compressor map at 1500 min^{-1} (right).

3.5 Comparison of VVT strategies

Subsequently the VVT methods considered above in detail should be compared to each other concerning their effect on most relevant parameters for exhaust thermomanagement. For this purpose, the left chart in figure 3.36 shows the characteristics of fuel consumption (BSFC) versus exhaust temperature downstream turbine (T_{41}) for all methods considered above. It can be seen that, apart from switching off one single cylinder (3Cyl) and a moderate application of LIVC, an increase in exhaust temperature leads to an increase in BSFC.

In the right chart the exhaust enthalpy flow ($\dot{H}_{\mathrm{exh}\,41}$) is plotted versus exhaust temperature for the same methods. Analysing the characteristics of both BSFC and enthalpy flow makes clear that methods achieving a given exhaust temperature with a relatively low fuel consumption do not result in an increase of enthalpy flow. This is reasonable since the exhaust temperature gain of these methods is mainly due to a reduction of overall aspirated cylinder mass, what is critical in terms of exhaust mass flow and hence enthalpy flow (for more details refer to section 3.3). Taking into account this interaction, early exhaust camshaft timing (EE) seems to be not attractive compared to EEVO, since it leads to a higher fuel consumption but a lower enthalpy flow than EEVO. Nearly the same as for EE applies also for LIVO. The BSFC of LIVO is lower than this of EEVO only for retarding IVO in a degree which leads not only to an increase of cylinder charge temperature but also to a decrease of cylinder charge pressure (refer to section 3.4.2). Although this effect – which could be identified by the unsteadiness in LIVO curves – causes a lower fuel consumption, it does not mean a benefit of LIVO compared to EEVO in general. This is because the mentioned decrease of pressure leads also to a decrease of enthalpy flow ($\dot{H}_{\mathrm{exh}\,41}$, right chart) and hence a becoming higher penalty of LIVO compared to EEVO in this context. To sum up, both EE and LIVO are disadvantageous compared to EEVO. To keep in mind this drawback also in subsequently discussed charts, EE and LIVO are illustrated by thin curves. Anyway, based on this illustration it is not possible to say if EEVO or one of the methods characterized by a lower BSFC – e.g. LIVC – is more efficient. It depends on application – whether only a high exhaust temperature or also a high mass flow and hence a high enthalpy flow is required.

In figure 3.37 the already known methods are compared concerning charge fuel ratio (CFR) and exhaust mass flow ($\dot{m}_{\mathrm{exh}\,41}$) versus exhaust temperature (T_{41}). Considering the CFR versus T_{41} characteristics, points out that CFR reduction is not the only effect for exhaust temperature gain. Not even if EEVO, EELI and EE (reduction of effective expansion) are excluded from consideration. Comparing e.g. LIVC and LIVO, makes obvious that the CFR reduction required for a given exhaust temperature is smaller in case of LIVO. This could be explained by the fact that a CFR reduction is achieved by LIVO mainly due to an increase of temperature while the main effect in case of LIVC is a pressure reduction. Of course, the first mentioned way is more beneficial when it comes to increasing exhaust temperature (refer also to discussion of direct and indirect effects in section 3.3.2). Considering both CFR and exhaust mass flow ($\dot{m}_{\mathrm{exh}\,41}$) enables pointing out the most relevant characteristic of internal EGR. For this purpose internal EGR by means of a 2^{nd} Event should be compared with LIVC. Doing so makes obvious that the exhaust temperature increase of 2^{nd} Event is higher than this achieved by LIVC for the same CFR. The reason for this difference is the higher temperature of cylinder charge in case of 2^{nd} Event which results from internal EGR. However, referring not to the same CFR but to the same exhaust mass flow ($\dot{m}_{\mathrm{exh}\,41}$, right chart), leads to a

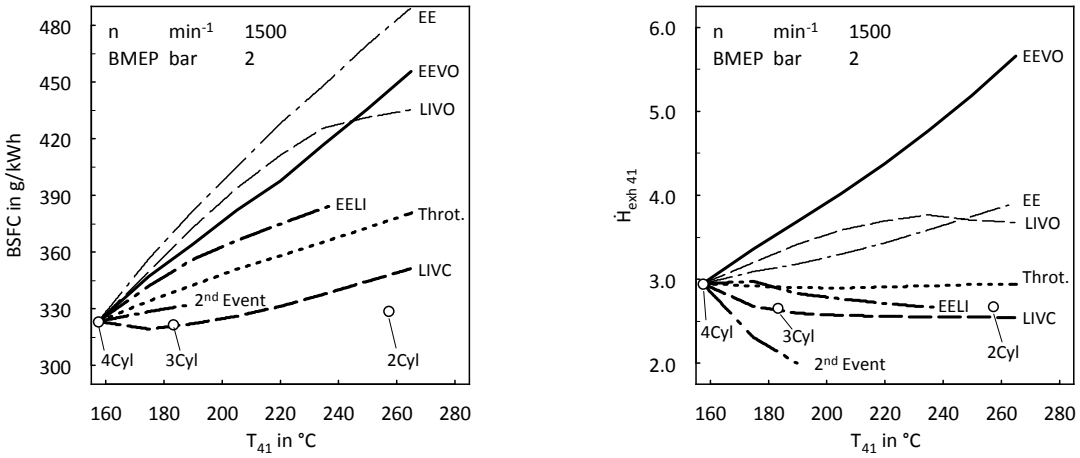

Figure 3.36: Comparison of various VVT strategies concerning BSFC and exhaust enthalpy flow versus exhaust temperature at 1500 min^{-1} and a BMEP of 2 bar

higher exhaust temperature of LIVC compared to this of 2nd Event. This is due to the fact that $\dot{m}_{\mathrm{exh}\,41}$ considers external but not internal recirculated mass of exhaust gas. Thus, the T_{41} penalty of 2nd Event – compared to LIVC, at the same $\dot{m}_{\mathrm{exh}\,41}$ – is mainly due to the fact that 2nd Event has to heat up not only the mass of aspirated air and external EGR (relevant for $\dot{m}_{\mathrm{exh}\,41}$) but also the mass of internal EGR. Hence taking into account both comparisons – referring to the same CFR and to the same mass flow – it seems to be clear that a replacement of external EGR by internal EGR is beneficial concerning exhaust temperature. Nevertheless, even more beneficial is achieving the same reduction of mass flow in a way that declines the cylinder mass in the same degree as the mass flow, hence without internal EGR (e.g. LIVC).

Analysing the characteristics of EEVO, it is obvious that the CFR decreases although the mass flow increases, what is due to a decline in efficiency and hence a rise of injected fuel mass. The slight increase of ($\dot{m}_{\mathrm{exh}\,41}$) comes mainly from a higher boost pressure resulting from an increase in exhaust enthalpy flow and a constant – fully opened – VNT position.

Studying the characteristics of LIVO makes clear that the mentioned unsteadiness – resulting from a cylinder charge pressure decrease which occurs only when retarding of IVO exceeds a critical degree – can be identified in the characteristic of $\dot{m}_{\mathrm{exh}\,41}$ but not in this of CFR. The reason is that the pressure decline means not only a higher gradient of decrease in mass flow ($\dot{m}_{\mathrm{exh}\,41}$) and hence in mass of cylinder charge, but also a less increasing injected fuel mass (see BSFC, figure 3.36).

For taking into account effects of considered exhaust thermomanagement methods on cold start ignitability and combustion stability, the change in pressure and temperature at start of combustion ($p_{\mathrm{Cyl,SOC}}$, $T_{\mathrm{Cyl,SOC}}$) versus exhaust temperature (T_{41}) should be analysed, see figure 3.38. As mentioned above, a decrease of these parameters is critical, which applies in particular for cold engine conditions. Hence, LIVC, which causes a significant decrease of both cylinder pressure and temperature at SOC, shows the clearest drawback. Besides LIVC also EELI is featured with a late IVC which results in a decrease of effective compression ratio

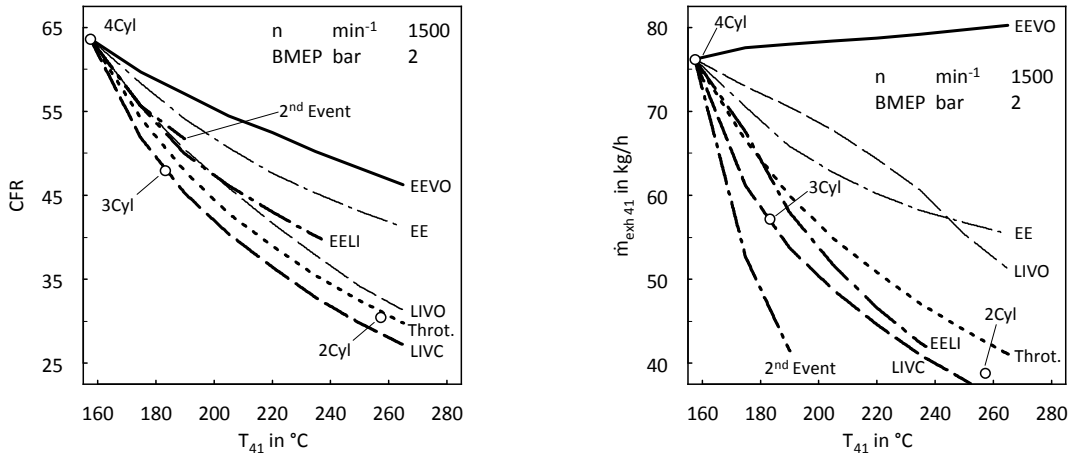

Figure 3.37: Comparison of various VVT strategies concerning charge fuel ratio and exhaust mass flow versus exhaust temperature at 1500 min^{-1} and a BMEP of 2 bar

and hence a decrease of both cylinder pressure and temperature. However, in case of EELI the internal EGR compensates the temperature decrease. Moreover, EELI leads to a higher increase of BSFC compared to LIVC, which supports CFR reduction and hence means a lower required decrease of aspirated cylinder mass. In summary, methods achieving a reduction of CFR mainly by temperature increase and not by pressure decrease are beneficial concerning $p_{\mathrm{Cyl,SOC}}$ and $T_{\mathrm{Cyl,SOC}}$. Hence keeping in mind that LIVO leads to a relevant decrease of cylinder charge pressure only for high degrees of retarding IVO, it is reasonable that also the $p_{\mathrm{Cyl,SOC}}$ characteristic resulting from LIVO becomes critical for high degrees of retarding IVO and hence for high exhaust temperatures (T_{41}). Since an EEVO does almost not affect the intake process, the nearly neutral characteristic of pressure and temperature at start of combustion is not surprising. Also cylinder deactivation means neither a relevant effect on $p_{\mathrm{Cyl,SOC}}$ nor on $T_{\mathrm{Cyl,SOC}}$. This is reasonable since the effect resulting from switching off cylinders on gas exchange is more or less negligible in the considered operation area (no boosting, low engine speed). Thus, the intake process of active cylinders is nearly the same as in engine operation without deactivated cylinders. Here it should be pointed out that methods resulting in a decrease of $p_{\mathrm{Cyl,SOC}}$ and/or $T_{\mathrm{Cyl,SOC}}$ are considered as critical concerning the mentioned above issues. However, this is not a final negative evaluation, but arises questions which could be not answered by simulation.

After comparison of potential exhaust thermomanagement VVT methods concerning typical parameters of engine cycle simulation, also the effect on heat up and cool down of exhaust aftertreatment components should be considered. For this purpose the results of engine cycle simulation (section 3.4) and catalyst simulation (section 3.2) will be merged. Here it should be pointed out that the catalyst simulations do not consider any chemical reaction but only the thermal behaviour of the monolith.

One of the most important issues in terms of exhaust thermomanagement is a rapid heat up of the oxidation catalyst (DOC, LNT) after engine cold start. For this purpose exhaust

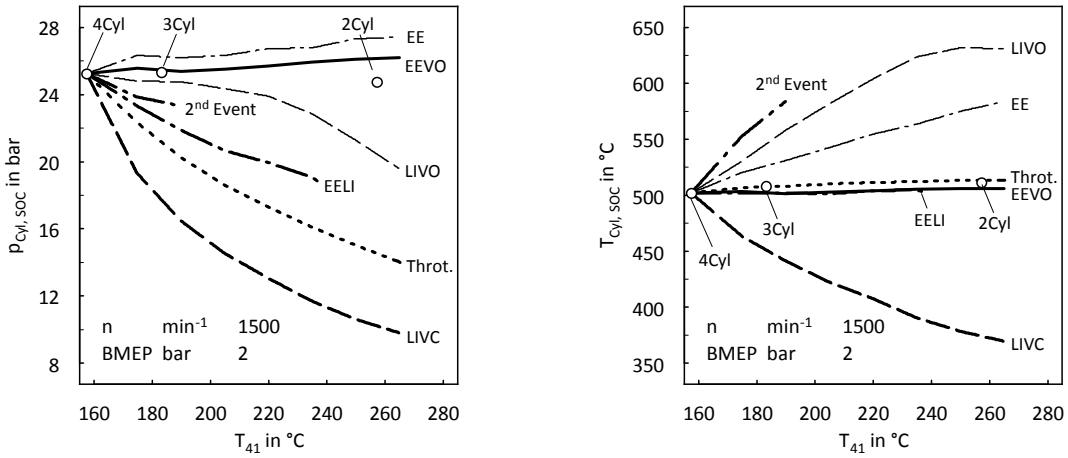

Figure 3.38: Comparison of various VVT strategies concerning pressure and temperature at start of combustion versus exhaust temperature at 1500 min^{-1} and a BMEP of 2 bar

thermomanagement methods must be applied just until the light off temperature in a more or less long section at the upstream end of the catalyst is reached. Afterwards the heat release of the exothermic reactions of HC and CO emissions will heat up the rest of the catalyst. Referring to section 3.2, this means that – contrary to the heat up of a catalyst without exothermic reactions – exhaust mass flow is less important than exhaust temperature. Hence LIVC, internal exhaust gas recirculation by means of 2nd Event and cylinder deactivation should be considered for this task. EEVO – characterized by a nearly constant mass flow – will serve as reference.

The left chart in figure 3.39 shows the characteristics of BSFC and exhaust mass flow ($\dot{m}_{\mathrm{exh}\,41}$) versus exhaust temperature (T_{41}) for the selected methods – EEVO, LIVC, 2nd Event and cylinder deactivation. Having a closer look on the $\dot{m}_{\mathrm{exh}\,41}$ versus T_{41} illustration, in addition to the mentioned characteristics also curves of constant catalyst temperature ($T_{\mathrm{Cat},0\mathrm{mm}}$) – as known from section 3.2 – can be seen. More exactly these constant temperature curves are characteristic for the entry cross section of the catalyst after 10 seconds of a heat up process. As it is pointed out by the vertical characteristic of the $T_{\mathrm{Cat},0\mathrm{mm}}$ curves, the catalyst temperature in the most upstream cross section is nearly independent from mass flow ($\dot{m}_{\mathrm{exh}\,41}$) and hence only a function of exhaust temperature (T_{41}). Thus, the plotted mass flow characteristics of considered exhaust thermomanagement methods do not matter in this context. Concerning efficiency this means that the method achieving the lowest BSFC for a given exhaust temperature (T_{41}) and hence catalyst temperature ($T_{\mathrm{Cat},0\mathrm{mm}}$) is automatically most efficient when it comes to heat up the entry cross section of the catalyst. Due to this, LIVC and cylinder deactivation seem to be in particular convenient for this purpose, while EEVO shows a clear drawback concerning efficiency. Internal EGR by means of 2nd Event leads also to a higher BSFC than LIVC and cylinder deactivation. Nevertheless, it is far more efficient than EEVO. The disadvantage of 2nd Event is the low limit of achievable exhaust temperatures (refer to section 3.4.3). The right chart which provides the characteristics of

pressure and temperature at start of combustion should help to keep in mind that LIVC has a drawback, or at least, leads to questions in this context which could be not answered by simulation.

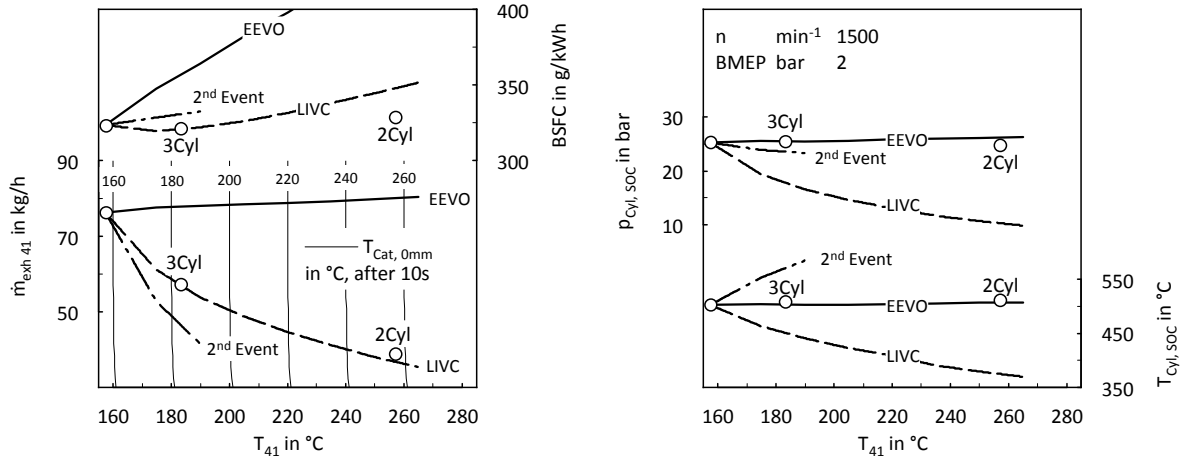

Figure 3.39: Comparison of EEVO, LIVC, internal EGR by means of 2nd Event and cylinder deactivation concerning heat up of the catalyst entry cross section at 1500 min^{-1} and a BMEP of 2 bar

As pointed out above, an exhaust thermomanagement method adequate for heating up an oxidation catalyst has to be focussed on increasing the monolith temperature at the upstream section of the catalyst. Considering the entry cross section – the extreme case of upstream section – does not take into account any thermal inertia of the catalyst. Thus – as shown in figure 3.39 – the catalyst temperature is identical to the exhaust temperature upstream catalyst almost during the whole heat up process. Assuming that also in case of an oxidation catalyst a section with a finite length has to be heated up, considering also a cross section short behind the entry seems to be reasonable. For this purpose figure 3.40 provides the same information as figure 3.39, however, not for the entry but a cross section 5 mm more downstream. Having a look at $\dot{m}_{\mathrm{exh}\,41}$ versus T_{41}, it can be seen clearly that the constant temperature curves ($T_{\mathrm{Cat},5\mathrm{mm}}$) are not vertical, what means a dependency of $T_{\mathrm{Cat},5\mathrm{mm}}$ not only from exhaust temperature (T_{41}) but also from mass flow ($\dot{m}_{\mathrm{exh}\,41}$).

Hence, finding out the most efficient method for achieving a temperature in the considered cross section of e.g. 215 °C is not as easy as it was in case of vertical constant temperature curves (figure 3.39). However, the plotted markers help to find the values of fuel consumption, which correspond to the exhaust temperature and mass flow necessary for achieving a $T_{\mathrm{Cat}\,5\mathrm{mm}}$ of 215 °C. Thus, it is obvious that the required exhaust temperature (T_{41}) of EEVO is clearly lower than these of LIVC and cylinder deactivation. Nevertheless, due to the clearly higher gradient of BSFC versus exhaust mass flow ($\dot{m}_{\mathrm{exh}\,41}$), the fuel consumption penalty of EEVO for achieving a $T_{\mathrm{Cat},5\mathrm{mm}}$ of 215°C after 10 seconds is higher than for LIVC and cylinder deactivation. Comparing LIVC and cylinder deactivation makes obvious an efficiency benefit of cylinder deactivation which comes not only from the lower BSFC at a given T_{41} but also

from a slightly higher mass flow and hence lower required exhaust temperature. This interaction of catalyst temperature ($T_{\mathrm{Cat\,5mm}}$) with exhaust mass flow ($\dot{m}_{\mathrm{exh\,41}}$) and temperature ($T_{41}$) explains also why the maximum achievable catalyst temperature 5 mm downstream entry ($T_{\mathrm{Cat\,5mm}}$) in case of 2nd Event is even lower than the limit observed in the entry cross section (figure 3.39). The right chart in figure 3.40 is nearly identical to figure 3.40, however, in addition to the curves of $p_{\mathrm{Cyl,SOC}}$ and $T_{\mathrm{Cyl,SOC}}$ versus T_{41} also markers for the values which correspond to $T_{\mathrm{Cat\,5mm}} = 215\,^{\circ}\mathrm{C}$ are illustrated. This points out once again the significant decrease of cylinder pressure and temperature at start of combustion resulting from LIVC. EEVO and cylinder deactivation are uncritical in this context.

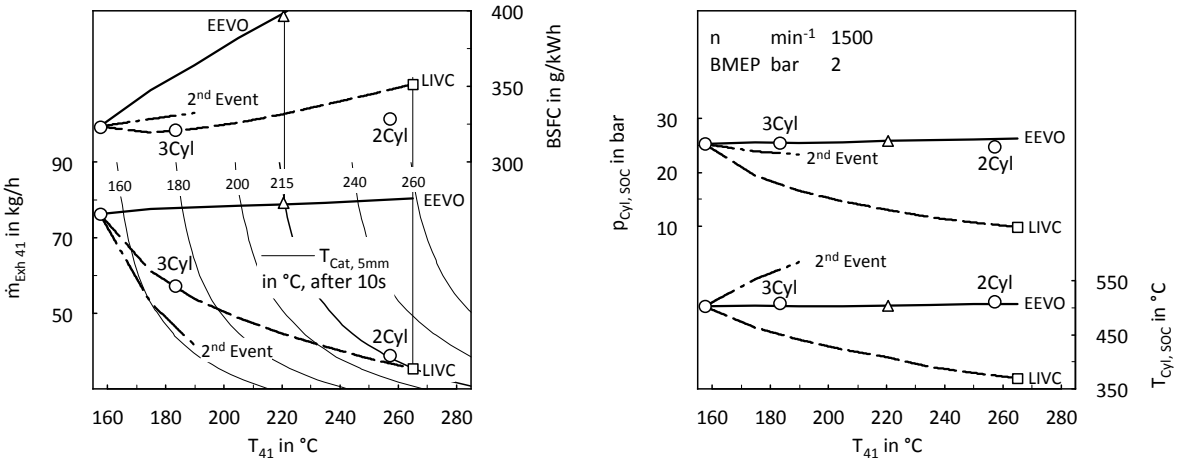

Figure 3.40: Comparison of EEVO, LIVC, internal EGR by means of 2nd Event and cylinder deactivation concerning heat up of the catalyst cross section 5 mm downstream the entry at 1500 min^{-1} and a BMEP of 2 bar

As mentioned in chapter 1, besides the oxidation catalyst also more downstream located EAS components may require a rapid heat up by means of adequate exhaust thermomanagement methods. In case of an exhaust aftertreatment system comprising an SCR catalyst downstream DOC, rapid heat up of both DOC and SCR must be ensured. Hence, a high exhaust temperature downstream DOC is beneficial for the heat up process of the SCR catalyst. Thus, analysing also the heat up process of the catalyst exit cross section – see figure 3.41 – is reasonable. The most relevant parameters for doing so – catalyst temperature ($T_{\mathrm{Cat\,175mm}}$), fuel consumption (BSFC), exhaust temperature (T_{41}) and mass flow ($\dot{m}_{\mathrm{exh\,41}}$) – are considered in the same way as it is already known from the heat up analysis discussed above. With respect to the more downstream located position, the plotted curves of constant catalyst temperature ($T_{\mathrm{Cat\,175mm}}$) refer to a later point in time after start of the heat up process (120 seconds).

As examined in section 3.2, methods generating high exhaust temperatures by means of mass flow reduction result in a higher temperature drop across catalyst than methods providing the same exhaust temperature without a mass flow reduction. Hence strategies with a relatively high enthalpy flow such as EEVO and EE – see figure 3.36 – should be

prefered for this task. The reason for the selection of EE, despite the low efficiency mentioned above, is the easy implementation by means of a simple cam phaser [7]. Also LIVC will be considered in this context, what enables pointing out the drawback resulting from a low exhaust mass flow. Analysing the characteristics of constant catalyst temperature curves ($T_{\mathrm{Cat\,175mm}}$) in the left chart of figure 3.41, makes obvious an even higher dependency of mass flow ($\dot{m}_{\mathrm{exh\,41}}$) than 5 mm downstream entry (after 10 seconds).

For comparison of the selected methods – EEVO, EE and LIVC – concerning efficiency, achieving a temperature in the catalyst exit cross section ($T_{\mathrm{Cat\,175mm}}$) of 180 °C (after 120 seconds) should be considered. By means of markers the effect of the required exhaust temperature increase on specific fuel consumption (BSFC) is pointed out. It can be seen that the relevant BSFC in case of EEVO is clearly lower than in case of EE, what has 2 reasons. First, the BSFC of EEVO is lower than this of EE for all considered exhaust temperatures. Second, the necessary exhaust temperature (T_{41}) for applying EE is higher than for using EEVO which results from the lower mass flow ($\dot{m}_{\mathrm{exh\,41}}$) of EE. Considering the $\dot{m}_{\mathrm{exh\,41}}$ versus T_{41} of LIVC makes obvious a significant decrease. This characteristic explains why LIVC is not able to achieve the considered catalyst temperature of 180 °C after 120 seconds. Not even with an exhaust temperature clearly higher than these necessary in case of EE and EEVO.

As shown, aiming a rapid heat up of the catalyst exit cross section or even of a more downstream located monolith (e.g. SCR) requires the application of exhaust thermomanagement methods over a longer time than it is necessary for heating up only the most upstream end of the catalyst. Thus, the effect of the applied methods on NO_x emissions becomes more relevant. This should be taken into account by analysing the effect of considered methods on charge fuel ratio (CFR), see right chart in figure 3.41. A decrease of CFR means that the air excess ratio, the rate of EGR or both has to be reduced, what is in general critical concerning NO_x and soot emissions. The characteristics of the temperature at start of combustion ($T_{\mathrm{Cyl,\,SOC}}$) plotted above are not only relevant for cold start ability and combustion stability but also for emission formation. A lower $T_{\mathrm{Cyl,\,SOC}}$ and hence lower level of cylinder temperature during combustion is beneficial concerning NO_x. Thus, in case of LIVC the significant decrease of CFR does not mean necessarily a drawback concerning emissions. However, as already pointed out LIVC seems to be not adequate for this exhaust thermomanagement task, anyway. Comparing EEVO and EE, concerning $T_{\mathrm{Cyl,\,SOC}}$ and CFR, it could be assumed that EEVO leads to less disadvantages concerning NO_x and soot emissions. On the one hand the CFR reduction is less significant on the other hand $T_{\mathrm{Cyl,\,SOC}}$ does not increase but remains constant. Of course this is only a rough estimation. For an accurate evaluation of effects on emission formation, experimental investigations are inevitable.

Besides heating up the catalyst after engine cold start also maintaining catalyst temperature during low load operation is an objective of exhaust thermomanagement. Thus, VVT methods should be evaluated also concerning their effect on a cool down process of a catalyst. As known from section 3.2, methods combining an exhaust temperature gain with a decrease in mass flow are particularly beneficial for decelerating the catalyst cool down process. Thus, LIVC and internal EGR by means of a 2^{nd} exhaust valve event should be analysed in this context. Of course, also cylinder deactivation is promising for maintaining catalyst temperature. As shown in figure 3.39, the characteristics of exhaust mass flow and fuel consumption versus exhaust temperature of cylinder deactivation are similar to these of LIVC. Hence find-

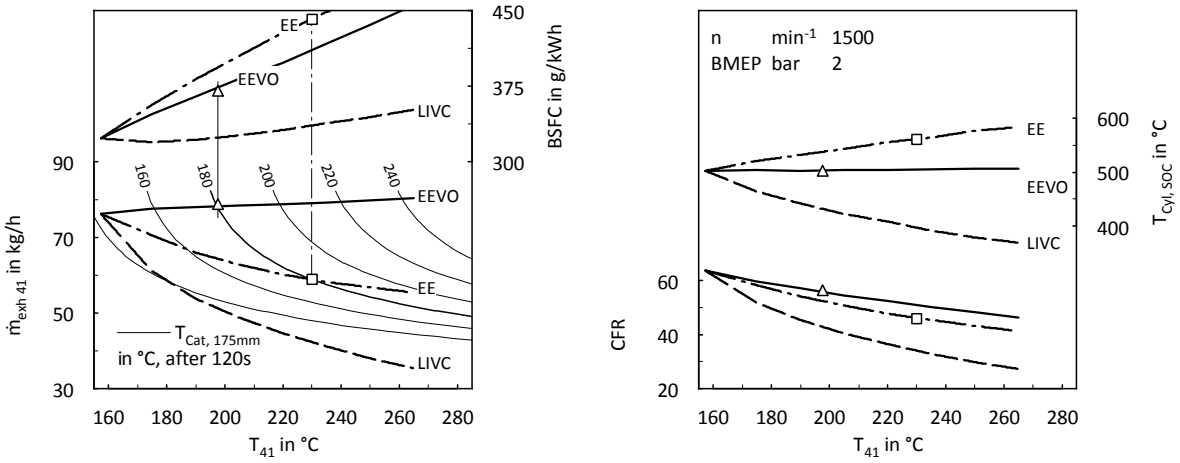

Figure 3.41: Comparison of EEVO, EE and LIVC concerning heat up of catalyst exit cross section at 1500 min^{-1} and a BMEP of 2 bar

ings of LIVC concerning exhaust thermomanagement efficiency do apply more or less also for cylinder deactivation. EEVO serves as a reference for a method without mass flow reduction.

In figure 3.42, the exhaust mass flow ($\dot{m}_{\mathrm{exh}\,41}$) and BSFC characteristics of the selected methods – LIVC, 2$^{\mathrm{nd}}$ Event and EEVO – are plotted versus exhaust temperature (T_{41}). As known from above, the $\dot{m}_{\mathrm{exh}\,41}$ versus T_{41} illustration contains also constant temperature curves of the catalyst ($T_{\mathrm{Cat,\,mean}}$). More exactly these curves refer to the mean temperature of the monolith which is analysed 30 seconds after the start of the cool down process. At the beginning of this process the whole catalyst had a temperature of 300 °C. The characteristic of the $T_{\mathrm{Cat,\,mean}}$ curves confirm that not only a higher exhaust temperature (T_{41}), but also a lower exhaust mass flow ($\dot{m}_{\mathrm{exh}\,41}$) is beneficial concerning maintaining catalyst temperature. This effect is also relevant when it comes to fuel consumption. As illustrated by the plotted markers, the limitation of cool down process to a mean catalyst temperature of 260 °C after 30 seconds can be achieved by LIVC and 2$^{\mathrm{nd}}$ Event in a clearly more efficient way than by means of EEVO. Of course, one reason is the difference in BSFC for the same exhaust temperature (T_{41}). The higher required exhaust temperature (T_{41}) in case of EEVO which results from the higher mass flow ($\dot{m}_{\mathrm{exh}\,41}$) leads to an additional penalty in BSFC.

The right chart in figure 3.42 provides informations of LIVC, 2$^{\mathrm{nd}}$ Event and EEVO concerning temperature at start of combustion ($T_{\mathrm{Cyl,SOC}}$) and the charge fuel ratio (CFR). The performance of LIVC and EEVO regarding this figures was already discussed in context of heating up the catalyst. Analysing the 2$^{\mathrm{nd}}$ Event strategy, an increase of $T_{\mathrm{Cyl,SOC}}$ can be seen, which is advantageous in terms of cold start ignitability and combustion stability, but critical in terms of NO_x emissions. Concerning NO_x emissions, it is also worth having a closer look on CFR which is relevant for combustion and hence emission formation. Although, 2$^{\mathrm{nd}}$ Event leads to a more significant decrease in CFR versus T_{41} than EEVO in general, it can be seen that the CFR values corresponding to a $T_{\mathrm{Cat,\,mean}}$ of 260 °C (illustrated by markers) for EEVO and 2$^{\mathrm{nd}}$ Event are on the same level. The reason for this is a lower exhaust mass

flow ($\dot{m}_{\mathrm{exh}\,41}$) of 2nd Event and hence lower required T_{41}. Nevertheless, taking into account both CFR and $T_{\mathrm{Cyl,\,SOC}}$ a disadvantage of 2nd Event compared to EEVO concerning NO_x/soot trade-off can be assumed. However, keeping in mind that methods aiming a deceleration of the catalyst cool down process will be applied at engine loads which are rather lower than higher compared to the considered BMEP of 2 bar, NO_x emissions are of secondary importance in this context.

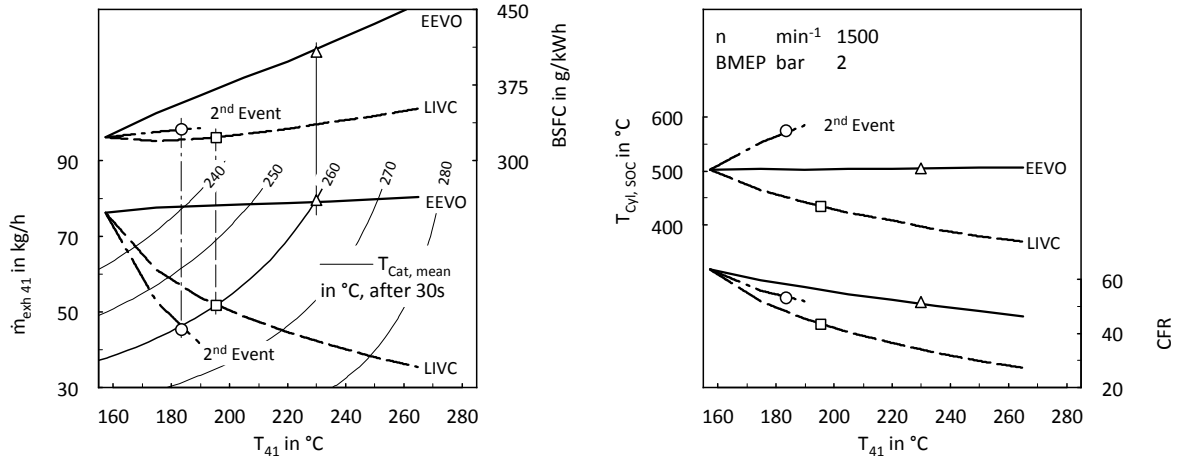

Figure 3.42: Comparison of EEVO, internal EGR by means of 2nd Event and LIVC concerning maintaining catalyst temperature at 1500 min^{-1} and a BMEP of 2 bar

4 Measurement Results

This chapter contains test bed measurement results of engine A which was described in section 1.3. This engine was also used for development of the 1-D engine model. Hence measurement data representing the series configuration of engine A were already considered in section 2.1.2 for model validation purpose.

The measurements were conducted on a dynamic engine test bed, which enables hardware (= engine) in the loop transient test cycle simulations. Besides pressure and temperature sensors for slow measurement data in the intake and exhaust system, the engine was featured also with cylinder pressure indication and an exhaust gas analysis. Positions and labels of all relevant sensors could be found in the measuring point layout illustrated in figure 4.1. Measurement of pollutant emissions (NO_x, soot, HC and CO) was available only upstream EAS (engine out emissions).

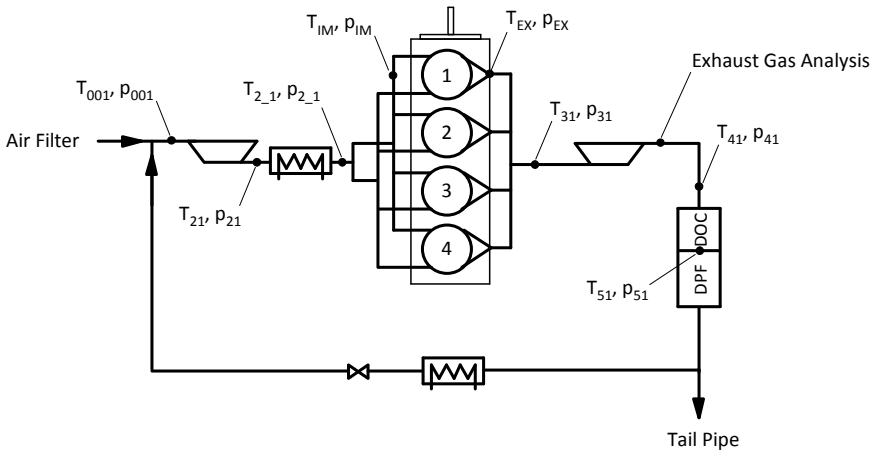

Figure 4.1: Measuring point layout of engine A

The valve timing strategies considered by means of experimental investigations – early exhaust valve opening (EEVO, section 4.1), late intake valve closing (LIVC, section 4.2) and cylinder deactivation (section 4.3) – were selected based on the simulation results discussed in chapter 3. For realisation of these alternative valve timings, the series engine camshafts were replaced. Of course, doing so enables neither a variation of EEVO and LIVC nor considering switching between conventional and alternative valve lift. However, it is an adequate way for fundamental investigations on a series engine. In addition to the VVT strategies also conventional exhaust thermomanagement methods – based on series engine valve lift timings – were considered (section 4.4).

4.1 Early Exhaust Valve Opening

The left chart in figure 4.2 shows the valve lift curves realized on engine A for considering EEVO. As it is pointed out, two alternative exhaust valve lift curves – EEVO_080 and EEVO_-105 – were considered. Both are characterized by a more or less advanced exhaust valve opening compared to the base valve timing. EEVO_080 was achieved by using an exhaust camshaft with modified cam profiles. However, this modification concerns only one valve per cylinder. The cam, actuating the second exhaust valve, has the original characteristic. In other words, EEVO_080 leads to an about 80 °CA earlier exhaust valve opening of only one valve per cylinder. For a better illustration of this unsynchronous exhaust valve actuating, the corresponding valve lift curves – EVL_1 and EVL_2 – are considered separately in the right chart. As obvious, EVL_2 is not concerned by applying EEVO_080 instead of base valve timing. EEVO_105 was achieved by using the same camshaft as it was used for EEVO_080. However, due to mounting the camshaft not in original position, but rotated towards earlier valve timings, a further advancement of the opening event of about 25 °CA was achieved. Of course, as it is also clearly to see in figure 4.2, the rotated camshaft mounting position of EEVO_105 leads not only to an earlier opening but also to an earlier closing of exhaust valves. Since a rotation of the camshaft concerns both exhaust valves of each cylinder, the shift of 25 °CA is relevant also for EVL_2.

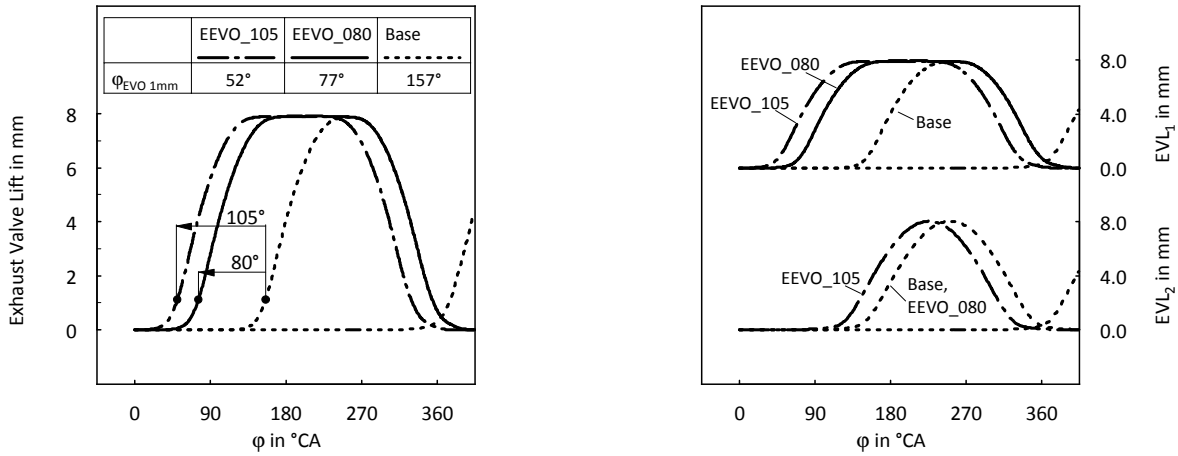

Figure 4.2: Valve lift curves used for experimental investigations on engine test bed concerning early exhaust valve opening

Subsequently the results of engine test bed measurements with the alternative exhaust camshaft, providing the discussed above valve lift curves EEVO_080 and EEVO_105, should be discussed. The main focus is on variation of exhaust temperature and fuel consumption resulting from the advanced exhaust valve opening. Also engine out exhaust gas emissions were considered.

Unless explicitly specified otherwise, the ECU calibration of measurements with EEVO_080 and EEVO_105 was the same as for the base valve timing. This is possible since the considered

EEVO strategies do not cause a variation in aspirated cylinder charge, which requires an adaption of ECU parameters. This is true, although EEVO_105 leads to an advanced closing of exhaust valves and hence to an increase of internal EGR (residual gas compression). Since the ECU controls the low pressure EGR valve in order to achieve the desired air mass flow an increase of internal EGR means only a partly replacement of low pressure EGR by internal EGR. As simulations have shown, the increase of internal EGR due to EEVO_105 does mean only a slight increase of cylinder charge temperature. Hence EEVO_105 leads more or less to the same mass and composition of cylinder charge as EEVO_080 and the base valve timing. Of course, this applies only for comparing operation points with the same injected fuel mass and not with the same BMEP. This is because in the present case the ECU maps – determining main injection timing, boost pressure and so forth – refer to injected fuel mass.

4.1.1 Steady State Operation

The following analysis of steady state operation with alternative exhaust valve lift strategies is concentrated on most relevant operation points for exhaust thermomanagement, characterized by low engine load and speed.

Figure 4.3 shows the exhaust temperatures at 1000 min^{-1} and low engine load achieved with different exhaust valve timings. In the left chart the absolute values of exhaust temperatures – upstream (T_{31}) and downstream (T_{41}) turbine – are plotted. The right chart illustrates the increase of these temperatures relative to the base valve timing. In addition also the increase of T_{EX} – temperature downstream exhaust ports, upstream exhaust manifold – is considered. It is easy to see that the achieved exhaust temperature increase of EEVO_080 is – in this low load operation points – not more than about 20 to 40 °C. Using EEVO_105 leads to a significantly higher temperature gain. This means for instance an increase of the temperature downstream turbine (T_{41}) of about 100 °C in the range close to idle run. At higher loads it is even more.

Concerning the exhaust temperature T_{EX}, some additional remarks are necessary. The illustrated variation of T_{EX} is the average of temperatures delivered by four sensors located at the exhaust manifold entry of each cylinder. Hence each of these sensors is affected only by the exhaust gas expelled by the corresponding cylinder – more or less a quarter of the entire exhaust mass flow. Thus, the more downstream located sensors (T_{31} and T_{41}) are affected by an about 4 times higher mass flow. Taking into account that sensor temperatures are not mass flow averaged, the same value of T_{EX} and T_{31} does not automatically mean an adiabatic flow between these measuring points. The difference between the sensor (thermo couple) temperature and the gas temperature – time or mass flow averaged – will be considered in more detail in section 4.5.1.

The left chart in figure 4.4 shows the exhaust mass flow through the aftertreatment system ($\dot{m}_{\mathrm{exh\,41}}$) as well as the charge fuel ratio ($\mathrm{CFR}_{\mathrm{ext}}$). The subsricpt 'ext' points out that the charge fuel ratio considered in analysing measurement data is not exactly the same as the CFR which was considered in discussion of simulation results. This is because the mass of internal EGR is not available for measurement data and hence could not be taken into account for the calculation of the charge fuel ratio. Thus, $\mathrm{CFR}_{\mathrm{ext}}$ is defined as

$$\mathrm{CFR}_{\mathrm{ext}} = \frac{m_{\mathrm{Air}} + m_{\mathrm{EGR,\,ext}}}{m_{\mathrm{Fuel}}} \tag{4.1}$$

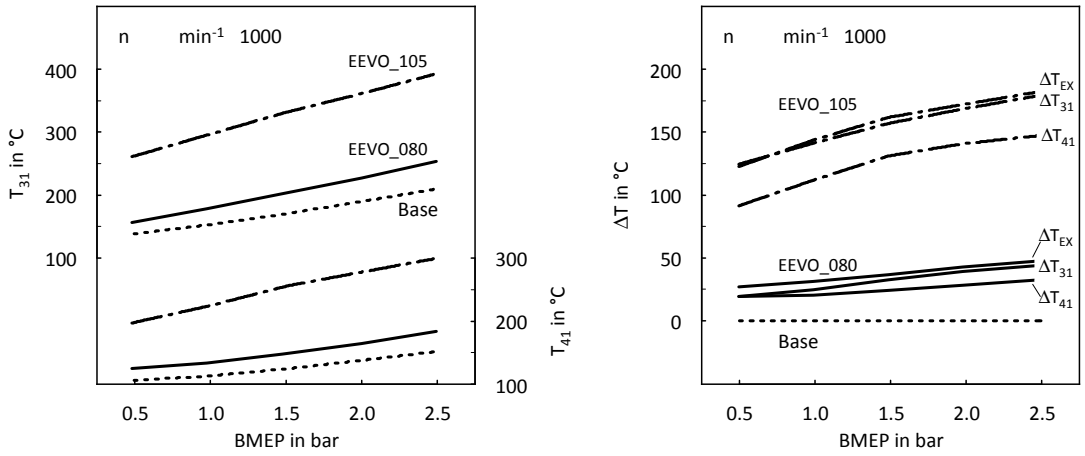

Figure 4.3: Effect of EEVO strategies – EEVO_080 and EEVO_105 – on exhaust temperatures at 1000 min^{-1} and low engine load

Analysing $\mathrm{CFR}_{\mathrm{ext}}$ instead of CFR does not make a relevant difference, since internal EGR is of secondary importance for methods considered by means of measurement. Of course the advanced closing of exhaust valves resulting from EEVO_105 means an increase of internal EGR, however simulations have shown that the difference between CFR and $\mathrm{CFR}_{\mathrm{ext}}$ is small compared to the variation of CFR and $\mathrm{CFR}_{\mathrm{ext}}$ caused by using EEVO_105 instead of EEVO_-080 or base valve timing.

Back to figure 4.4: The mass flow is slightly higher for the EEVO strategies, what has several causes. First, the worse efficiency leads to a shift in ECU maps towards higher injected fuel mass. In the specific case of open loop boost control, this means a variation of VNT position. Second, the higher exhaust temperature upstream turbine leads to a higher enthalpy available for turbine. The sum of these effects causes a higher boost pressure and hence a higher exhaust mass flow ($\dot{m}_{\mathrm{exh}\,41}$).

Despite the higher mass flow, the $\mathrm{CFR}_{\mathrm{ext}}$ is considerably lower for EEVO_080 and in particular for EEVO_105. The reason is a significant increase in fuel consumption, which should be discussed subsequently. As pointed out in chapter 3, not only an advanced exhaust valve opening but also a decrease in charge fuel ratio leads to an increase in exhaust temperature. To separate this effects, the right chart in figure 4.4 considers the exhaust temperature T_{41} versus $\mathrm{CFR}_{\mathrm{ext}}$. By means of this illustration it is easy to see that a considerable part of the temperature gain achieved by EEVO results from lower $\mathrm{CFR}_{\mathrm{ext}}$ or in other words from worse efficiency.

The charts in figure 4.5 provide an efficiency analysis of the considered alternative exhaust valve timings. In the left chart the exhaust temperature (T_{41}) of base valve timing, EEVO_-080 and EEVO_105 is plotted versus BSFC (thin curves). Connecting operation points with the same BMEP (bold curves) shows effects of an exhaust valve timing variation at constant engine load. The lower gradient of these constant BMEP curves for lower load indicates a lower efficiency compared to higher load engine operation points. In the right chart T_{41} versus BSFC

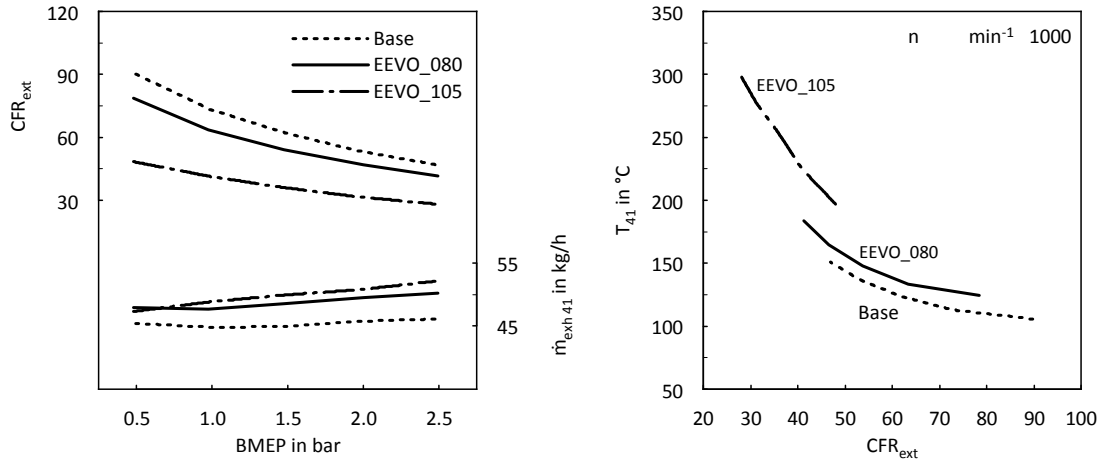

Figure 4.4: Effect of EEVO strategies on charge fuel ratio and consequences for exhaust temperature at 1000 min^{-1} and low engine load

is plotted once more for a BMEP of 1,5 bar. In addition to the warm engine measurement also the results of the same variation measured on a cold engine – oil and coolant temperature of 20 °C – is illustrated. The cold engine condition results in a shift towards higher fuel consumption and lower exhaust temperature, what is mainly caused by higher friction and higher wall heat losses – resulting from lower wall temperatures.

To point out effects of engine load on EEVO strategies, in figure 4.6 operation points with a BMEP of 2 and 10 bar at an engine speed of 1500 min^{-1} are considered. The left chart shows an evaluation of exhaust thermomanagement efficiency by means of analysing the increase of exhaust temperature (ΔT_{41}) versus increase of fuel consumption (ΔBSFC). Since the higher load operation point is characterized by a higher increase in T_{41} and a lower increase in BSFC, it seems to be more efficient than the lower load operation point. However, it has to be taken into account that the absolute values of T_{41} and BSFC – already in case of the base valve timing – are clearly different for a BMEP of 2 and 10 bar. Moreover the exhaust mass flows and their variations due to EEVO are neglected by the considered plot. One way to overcome this problem is analysing heat flows. Thus, in the right chart the variations of supplied fuel energy flow ($\Delta \dot{Q}_{\mathrm{Fuel}}$) and delivered exhaust enthalpy flow ($\Delta \dot{H}_{\mathrm{exh}\,41}$) are plotted versus variation of exhaust valve opening ($\Delta \varphi_{\mathrm{EVO},1}$).

Here it is worth mentioning that the calculation of exhaust enthalpy flow by means of measured exhaust temperatures has to be done carefully. As already explained, the relevant temperature for exhaust enthalpy is the mass flow averaged temperature. The value delivered by a thermo couple sensor in the exhaust system of an internal combustion engine in general is in between of the mass flow averaged and the time averaged temperature. Dependent from flow regime and thermo couple properties, the sensor temperature deviates more or less from the mass flow averaged temperature. According to this, the calculated enthalpy flow deviates more or less from the actual one. However, considering the measuring point downstream turbine means dealing with a nearly steady state flow regime. Thus, the difference between

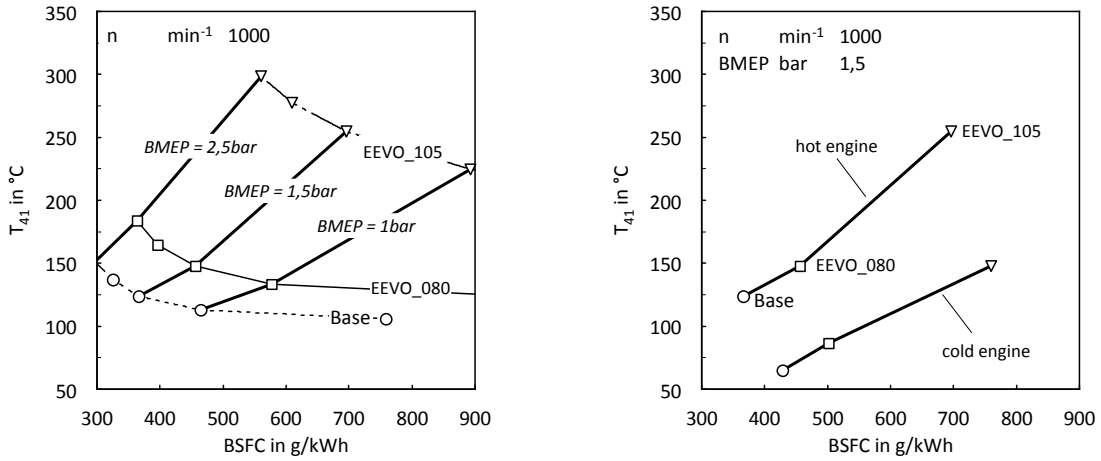

Figure 4.5: Effect of EEVO strategies on exhaust temperature versus fuel consumption characteristics at 1000 min^{-1} and low load operation, considering cold and warm engine conditions

mass flow and time averaged temperature becomes small. Hence the error caused by using the sensor temperature for calculation of enthalpy flow is negligible.

Back to figure 4.6: It can be seen that the higher load operation point leads not only to a higher increase in T_{41} but also to a higher gain in enthalpy flow ($\Delta\dot{H}_{\mathrm{exh}\,41}$). However – contrary to the BSFC – also the increase in supplied fuel energy ($\Delta\dot{Q}_{\mathrm{Fuel}}$) is clearly higher than for the lower load operation point. Hence on the first sight, neither of both operation points could be identified as more efficient. However, this illustration is only an intermediate step towards the evaluation chart known already from discussion of simulation results. Using this chart (figure 4.7) means considering the change of exhaust enthalpy flow ($\Delta\dot{H}_{\mathrm{exh}\,41}$) versus the change of heat losses ($\Delta\dot{Q}_{\mathrm{Loss}}$), which are calculated as difference of increase in supplied fuel energy and increase in exhaust enthalpy. For more details refer to section 3.1.1.

As obvious from figure 4.7, the gradient of $\Delta\dot{H}_{\mathrm{exh}\,41}$ versus $\Delta\dot{Q}_{\mathrm{Loss}}$ – resulting from early exhaust valve opening – is nearly the same for 2 and 10 bar. Hence the share of exhaust enthalpy gain in increase of fuel energy is nearly identical for the considered operation points. Of course the observed independence of exhaust thermomanagement efficiency from engine load is not valid in general. The gradient of $\Delta\dot{H}_{\mathrm{exh}\,41}$ versus $\Delta\dot{Q}_{\mathrm{Loss}}$ is affected by several engine calibration parameters. In particular the main injection timing is relevant for the share of exhaust enthalpy and wall heat losses. Focussing not on the difference between the considered operation points – 2 bar and 10 bar – but on the characteristic of $\Delta\dot{H}_{\mathrm{exh}\,41}$ versus $\Delta\dot{Q}_{\mathrm{Loss}}$ in general, shows that the share of exhaust enthalpy in additional supplied fuel energy, which is necessary for maintaining engine load when applying EEVO, is slightly lower than this of heat losses. This corresponds with simulation results. A comparison of simulation results concerning EEVO with measurement results is done in section 4.5.1.

Besides exhaust enthalpy and efficiency also the effect on pollutant emissions is relevant for the potential of exhaust thermomanagement methods. Figure 4.8 shows that the emissions of EEVO_080 at 1000 min^{-1} and low load operation are nearly neutral compared to these of

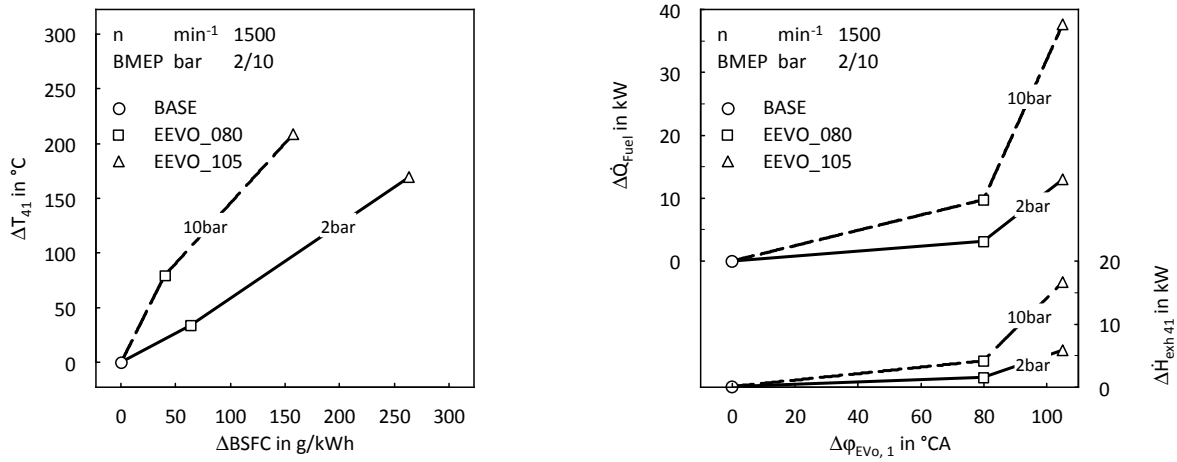

Figure 4.6: Evaluation of exhaust thermomanagement efficiency by considering the exhaust temperature versus BSFC and heat flows resulting from EEVO for a BMEP of 2 and 10 bar at an engine speed of 1500 min^{-1}

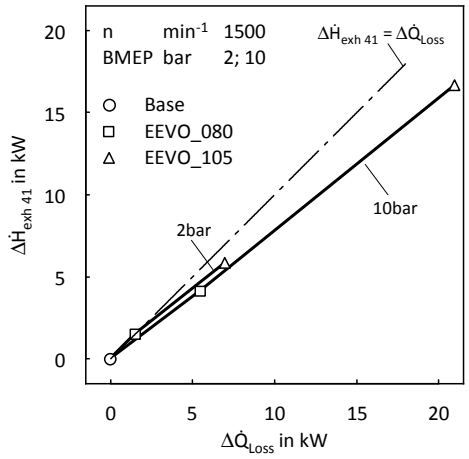

Figure 4.7: Evaluation of exhaust thermomanagement efficiency by considering the effect of EEVO on exhaust enthalpy flow versus heat losses for a BMEP of 2 and 10 bar at an engine speed of 1500 min^{-1}

the base engine. EEVO_105 shows disadvantages in particular concerning NO_x, soot and CO emissions. However, the higher NO_x emissions are not a specific problem of EEVO, at least not in the narrower sense, but a result of decrease in effective efficiency, caused by EEVO. The lower efficiency means a higher injected fuel mass, hence an increase in heat release and thus higher combustion temperatures. Besides this effect with all its consequences for emissions also the shift in ECU maps towards other engine calibration parameter values – e.g. less EGR – is relevant for emissions.

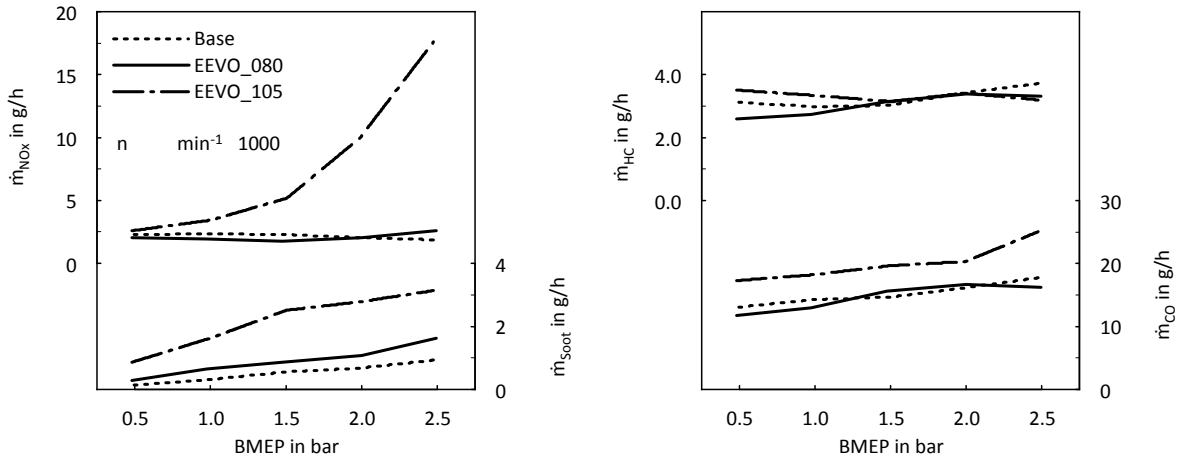

Figure 4.8: Comparison of EEVO strategies with the base engine concerning emissions in low load operation at 1000 min^{-1}

Figure 4.9 shows the same emission readings as figure 4.8. However, they are not plotted versus BMEP, but versus injected fuel mass (m_{Fuel}). The characteristics of the base engine were elongated (thin curves) to higher loads in order to cover the whole m_{Fuel} range of EEVO_105.

Comparing emissions of EEVO_105 with these of the base engine by referring to the same fuel mass, confirms that differences concerning NO_x emissions observed in figure 4.8 are caused mainly by the fuel consumption penalty of EEVO strategies. In other words, using an alternative thermomanagement strategy (e.g. an electrical heater), which has the same consequences for effective efficiency, would lead to nearly the same increase in NO_x emissions. Considering soot and CO emissions a drawback of EEVO_105 could be identified for injection quantities higher than approximately 11 mg/strk. The most probably reason for this effect is a shorter time for the in-cylinder post oxidation process due to the EEVO. In terms of HC emissions, relevant differences between base engine and EEVO strategies can not be seen for the same injection quantity.

In summary, EEVO by itself does not lead to relevant variations of NO_x emissions. However, increasing injected fuel mass in order to maintain engine load does. In the area of higher injection quantities CO and soot emissions are increased compared to the base engine. Of course, an adapted engine calibration used during EEVO operation could provide a degree of freedom. The strategy for such an adaption is significantly dependent from the given exhaust

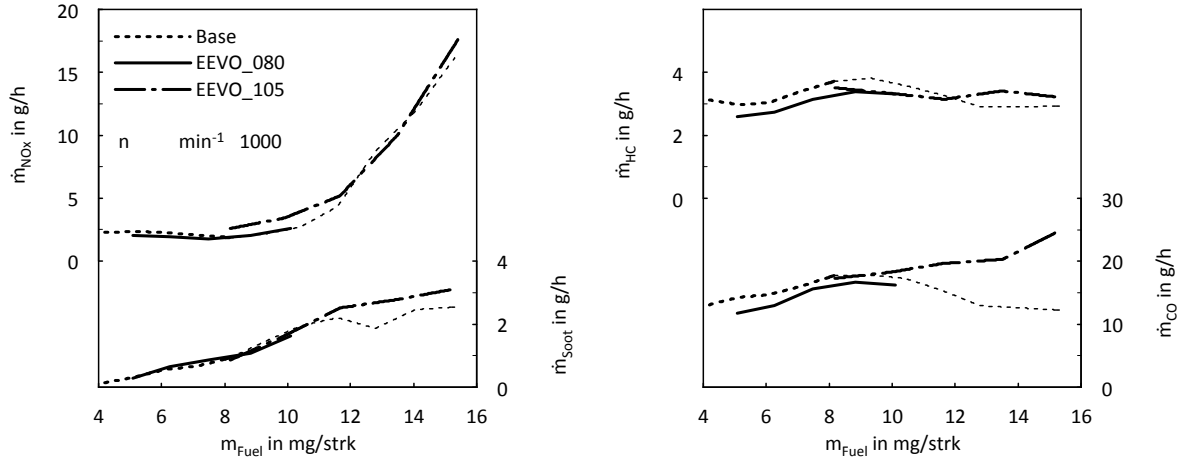

Figure 4.9: Considering emissions of EEVO strategies and the base engine in low load operation at 1000 min^{-1}, referring to the injected fuel mass

aftertreatment system. For instance using a LNT instead of a DOC will relax the demand for low NO_x emissions (due to the low temperature storage capability of a LNT). Hence engine calibration may be adapted towards less EGR, what is promising concerning HC, CO and soot emissions.

Of course early exhaust valve opening may be applied also in combination with other strategies for increasing exhaust temperature.

As shown in figure 4.3, applying EEVO_080 at 1000 min^{-1} and a BMEP of 1,5 bar leads to an increase in exhaust temperature downstream turbine (T_{41}) from 120 to about 145 °C. In order to find out if a further exhaust temperature gain could be achieved, a retarded main injection timing, throttling (downstream compressor) as well as different post injection applications were considered.

Figure 4.10 shows the main effects on fuel consumption (BSFC), exhaust temperatures upstream (T_{31}) and downstream (T_{41}) turbine as well as on exhaust enthalpy flow ($\dot{H}_{\mathrm{exh}\,41}$). The methods are applied additive, that means e.g. application 3 uses EEVO, throttling and a retarded main incection timing. In other words – apart from number 1 – all considered applications are featured with throttling and hence have a reduced mass flow compared to application 1 (EEVO_080 only). This is relevant when it comes to evaluation of fuel penalty (left chart), since it is clear that an increase of exhaust temperature requires less energy if the mass flow is lower. One way to overcome this problem is analysing not only temperatures (T_{31}, T_{41}, right chart) but also the enthalpy flow ($\dot{H}_{\mathrm{exh}\,41}$ – left chart). Doing so makes obvious that EEVO has the highest enthalpy flow. Although the additional thermomanagement methods lead to a further increase in exhaust temperature upstream (T_{31}) and downstream (T_{41}) turbine of 50 and 35 °C respectively, throttling causes a decrease of enthalpy flow even below the level of base valve timing. The additional application of a retarded main injection timing and post injections are necessary to achieve the base level again. In other words, the combination of EEVO, throttling and an adapted injection strategy leads to a fuel penalty

of more than 150 g/kWh without an increase of exhaust enthalpy flow. However, it seems to be clear that for a given enthalpy flow, a higher temperature and hence a lower mass flow is more beneficial for the most exhaust thermomanagement objectives than vice versa. Thus – as already pointed out in chapter 3 – neither only temperature nor only enthalpy flow – is an adequate evaluation figure.

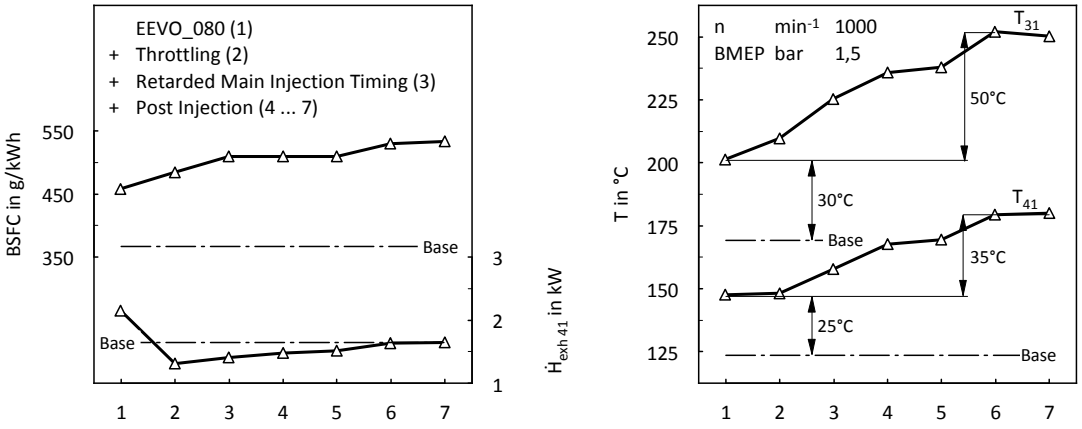

Figure 4.10: Effect of combining EEVO_080 with conventional exhaust thermomanagement methods on fuel consumption, exhaust enthalpy flow and exhaust temperatures at 1000 min^{-1} and a BMEP of 1,5 bar, post injection pattern see figure 4.13

Figure 4.11 shows the effect of the discussed methods on pollutant emissions. Since the exhaust mass flow is not equal for all applications, not only the emission concentrations but also the corresponding mass flows are plotted. It is obvious that almost every method applied in addition to EEVO is disadvantageous concerning HC and CO emissions, what is critical in particular for exhaust thermomanagement methods applied before DOC light off. NO_x emissions are influenced in a relevant way only by throttling and retarded main injection timing. While the reduction of cylinder mass and the cut of EGR caused by throttling lead to a higher peak cylinder temperature and hence higher NO_x emissions, the late combustion caused by the retarded main injection timing has the reverse effect. Soot emissions increase due to throttling, what could be explained above all through to a lower air excess ratio. However, it can be seen that a well adapted post injection is able to cut soot emissions.

In figure 4.12 the methods throttling and retarded main injection timing are considered in detail. The left chart shows effects on cylinder pressure curve (p_{Cyl}) and net rate of heat release ($\mathrm{d}Q_{\mathrm{Fuel,\,net}}$). The right chart illustrates the influence on $\mathrm{MFB}_{50\%}$, intake manifold pressure (p_{IM}) and exhaust mass flow ($\dot{m}_{\mathrm{exh\,41}}$). It is easy to see that throttling leads to a significant reduction in cylinder pressure before start of combustion. That may be the reason for the increase of ignition delay, which could be observed by analysing the heat releases. As obvious both throttling and retarded main injection timing cause a later $\mathrm{MFB}_{50\%}$. The effect of the lower mass flow – resulting from throttling – on enthalpy flow ($\dot{H}_{\mathrm{exh\,41}}$) was already discussed above.

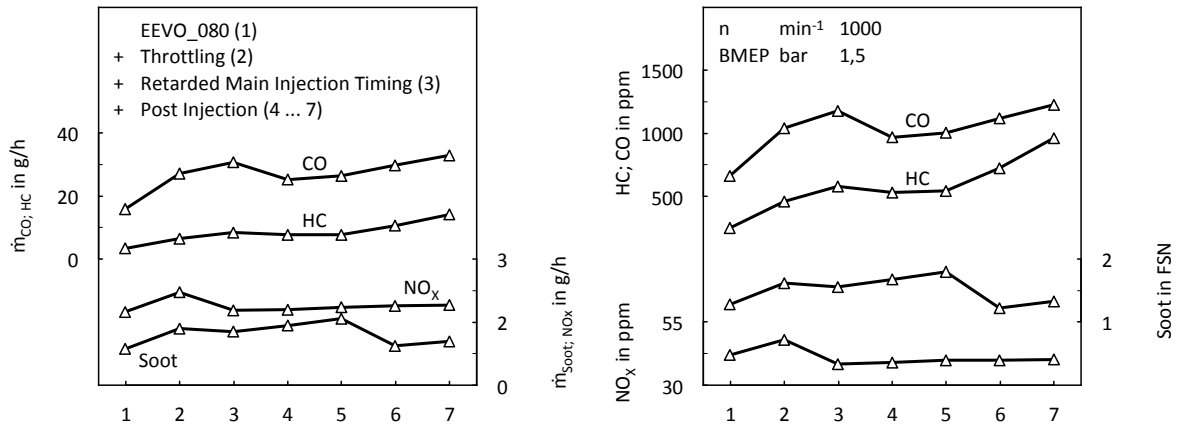

Figure 4.11: Effect of combining EEVO_080 with conventional exhaust thermomanagement methods on emissions at 1000 min^{-1} and a BMEP of 1,5 bar

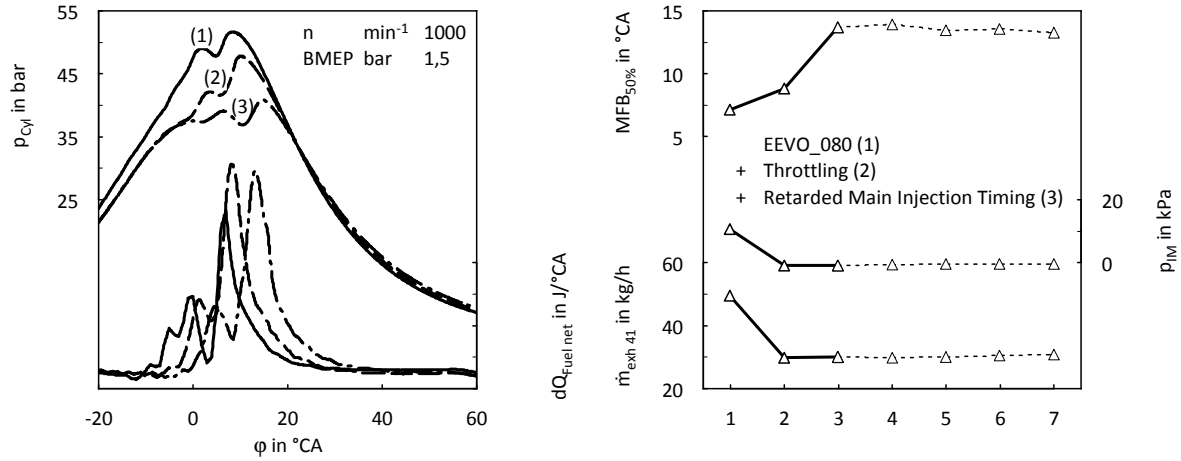

Figure 4.12: Combination of EEVO_080 with throttling and a retarded main injection timing at 1000 min^{-1} and a BMEP of 1,5 bar

The post injection strategies should be discussed by considering the injection pattern and net rate of heat releases (figure 4.13, left). The right chart in figure 4.13 additionally provides timing and quantity of post injection as well as effects on $MFB_{50\%}$ and $MFB_{90\%}$. It can be seen that the quantity of post injection (m_{PoI}) was kept constant while the timing separation (t_{PoI}) was increased, which results in a later $MFB_{90\%}$, nearly without affecting $MFB_{50\%}$. As obvious the latest timing shift of post injection (6 to 7) does not lead to a further retarding of $MFB_{90\%}$. Hence also a further benefit concerning exhaust temperature does not occur. However, HC and CO emissions increase. By studying the heat releases, it can be detected that the combustion of post injection and the decrease of heat release caused by exhaust valve opening (EVO) merges in case of application 7. This characteristic indicates that EVO occurs before combustion is finished – a well known catalyst heat up strategy in terms of spark ignition engines. However, in case of diesel combustion, this strategy seems to be less beneficial.

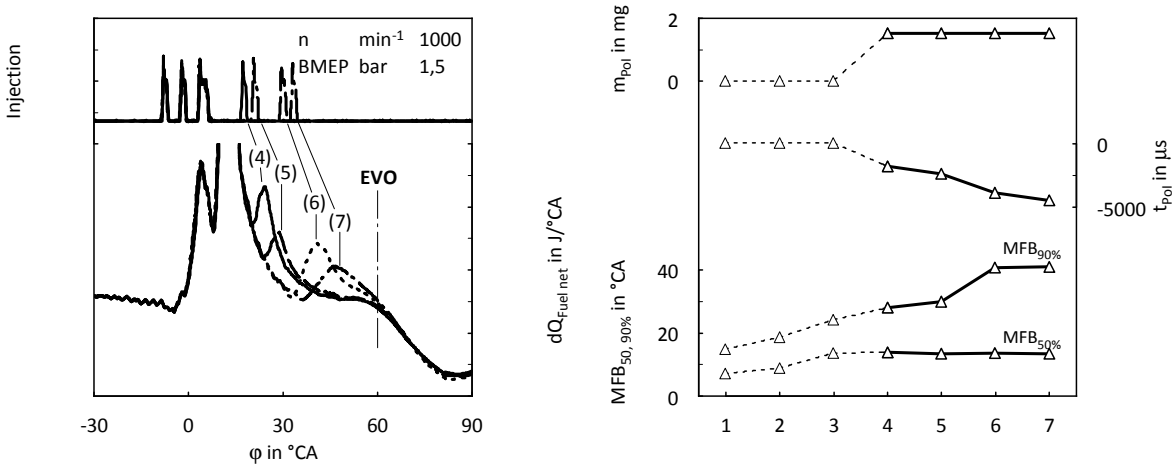

Figure 4.13: Combination of EEVO_080 with various post injection timings at 1000 min^{-1} and a BMEP of 1,5 bar

With regard to the transient tests considered subsequently also the effect of applying EEVO while using high pressure EGR instead of low pressure EGR should be considered. For this purpose figure 4.14 provides measurement data of EEVO_105 with high pressure and low pressure EGR at 1000 min^{-1} and low engine load. As reference also the base engine (low pressure EGR) is considered. Studying the characteristics of fuel consumption and exhaust temperature makes clear that the difference between high pressure and low pressure EGR application of EEVO_105 is small compared to the differences to the base engine measurement. The right chart shows effects on emissions. It is obvious that NO_x emissions are higher when using high pressure instead of low pressure EGR. This is due to the higher temperature of cylinder charge what means a lower rate of EGR, since the air mass flow is the same. Concerning HC emissions EEVO_105 with high pressure EGR shows a benefit, what is most probably because of the higher cylinder charge temperature. When it comes to soot emissions, using high pressure instead of low pressure EGR does not lead to a relevant effect.

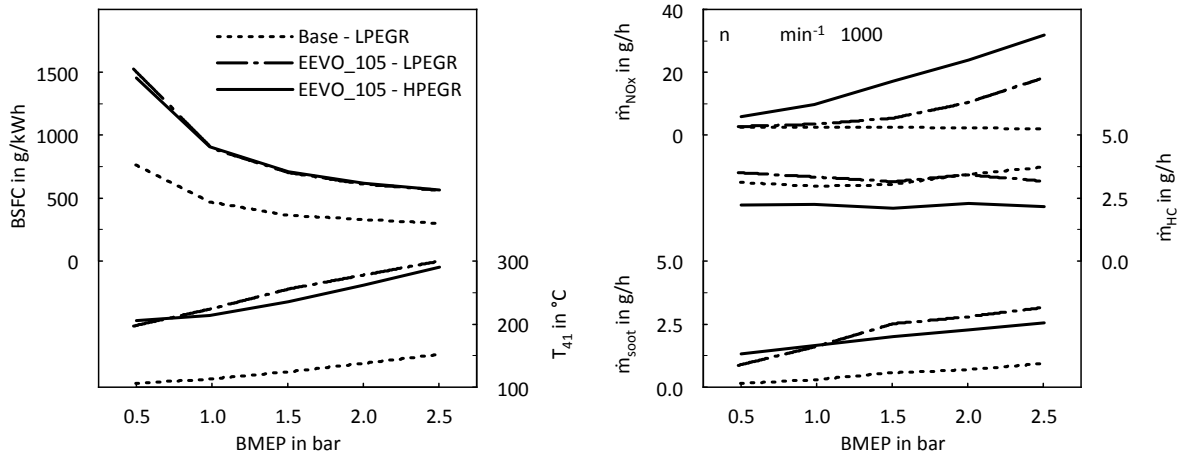

Figure 4.14: Comparison of the base engine and EEVO_105 with high pressure and low pressure EGR – concerning fuel consumption, exhaust temperature and emissions

4.1.2 Transient Operation

For evaluation of EEVO strategies in transient engine operation the most relevant test cycles for present emission legislations in Europe and the USA – NEDC and FTP 75 – were considered. The tests were conducted on a dynamic engine test bed by using engine speed and load characteristics as input data. The calculation of these data by means of a vehicle simulation tool was not part of the present work. The vehicle parameters (mass, transmission ratios, ...) were derived from a medium-sized passenger car, which is the main area of application for the considered engine.

Since exhaust thermomanagement methods will be applied during cold start and the subsequent warm up process, transient tests were done by taking into account cold engine conditions, characterized by an oil and coolant temperature of 20 °C. In order to achieve more than one cold engine test a day, a so-called rapid cool down procedure was applied. The drawback of this method is condensation of air humidity in catalysts and hence a retarded temperature increase downstream catalysts.

Concerning engine calibration it is worth mentioning that the series engine calibration includes the application of high pressure EGR instead of low pressure EGR until the coolant temperature exceeds a defined limit. Since this was not changened, the subsequently discussed very first sections of transient tests refer to high pressure EGR.

Figure 4.15 shows a comparison of the base engine and EEVO valve timings – EEVO_080 and EEVO_105 – in a cold-start NEDC. More exactly only the first 195 seconds (first urban driving cycle, UDC) are considered, since this is the most relevant section for exhaust thermomanagement. The right chart provides information about exhaust temperatures upstream (T_{41}) and downstream (T_{51}) DOC. It can be seen that EEVO_080 achieves after 195 seconds a temperature gain of 25 °C at upstream DOC position (T_{41}). The increase of EEVO_105 is significantly higher (105 °C). Moreover T_{41} of EEVO_105 exceeds the 200°C limit after not more than 60 seconds. The base engine requires for exceeding the same limit 145 seconds, in

case of EEVO_080 it takes about 130 seconds. Considering the temperature downstream DOC (T_{51}), an extremely retarded reaction – compared to the increase in T_{41} – can be identified. The reason is not only the thermal inertia of the DOC but also the condensed water resulting from the rapid cool down procedure. Hence it is expected that the significant increase of EEVO_105 observed after about 120 seconds occurs earlier in case of a dry catalyst. From measurement results conducted with another engine which is featured with a comparable catalyst, it is known that the delay of light off resulting from evaporation of condensed water is about 30 seconds. This information is based on the comparison of two cold-start test cycles. One of them was started after a time-consuming naturally cool down and hence with a dry catalyst while the other ones was started after the mentioned rapid cool down procedure and thereby with condensed water in the catalyst.

The left chart in figure 4.15 shows the characteristics of cumulated fuel mass, which allow an estimation of fuel consumption penalty caused by the EEVO valve timings. Considering only the plotted first 195 seconds of the test, the required fuel mass for EEVO_080 is about 15 % higher compared to the base engine. For EEVO_105 it increases about 70 %. However, it has to be taken into account that thermomanagement methods are applied not during the whole test cycle. Assuming EEVO valve timings will be used until T_{41} exceeds the 200 °C limit and the efficiency in the remaining time is equal to the base engine, the fuel consumption of EEVO_080 and EEVO_105 increases about 1,0 and 2,3 % respectively.

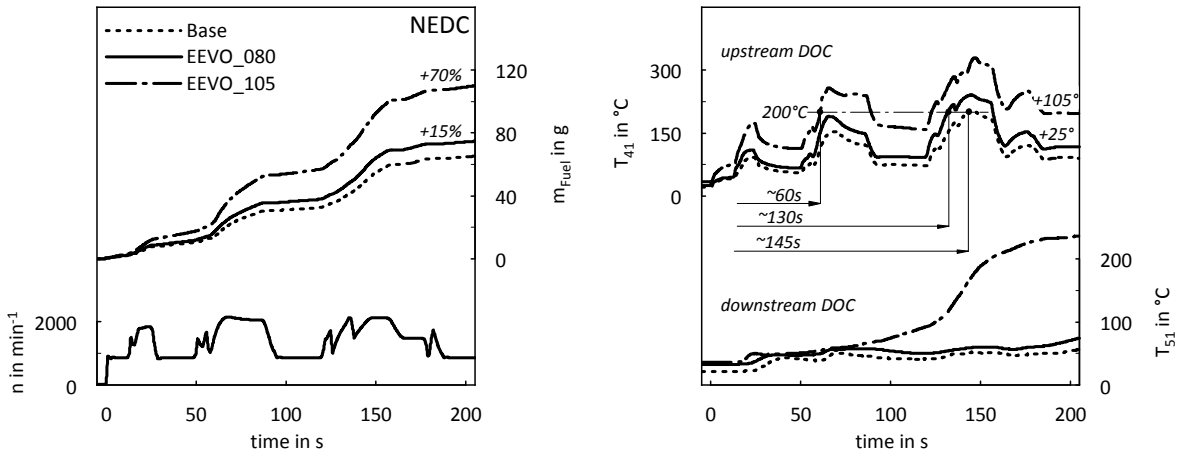

Figure 4.15: Comparison of the base engine with EEVO valve timings concerning fuel consumption and exhaust temperatures during the first 200 seconds of a cold-start NEDC

Figure 4.16 shows the cumulated exhaust enthalpy downstream turbine ($H_{\mathrm{exh}\,41}$) as well as the cumulated heat losses (Q_{Loss}) – attention to the different resolution. Q_{Loss} was calculated by subtracting delivered mechanical work and exhaust enthalpy from supplied fuel energy. One reason for the very high heat losses compared to exhaust enthalpy is the definition of the latter one. For taking into account that energy of exhaust gas could be used only in case of exceeding a defined temperature level, enthalpy is calculated with 0 °C (273,15 K) as reference temperature. Using the absolute zero point (0 K) as reference would lead to a higher

enthalpy and hence lower heat losses. Of course, changes of heat losses and exhaust enthalpy – e.g. resulting from EEVO_080 and EEVO_105 – are not affected by this definition.

Considering the bar chart (figure 4.16, right) makes obvious that the share of supplied energy converted into heat losses (Q_{Loss}) remains nearly constant. Hence only the share of mechanical work (W_{eff}) and exhaust enthalpy ($H_{\mathrm{exh\,41}}$) is affected by EEVO strategies. However, it should be pointed out that this means not a constant absolute value of heat losses, what is illustrated by the curves of cumulated heat losses in the left chart of figure 4.16.

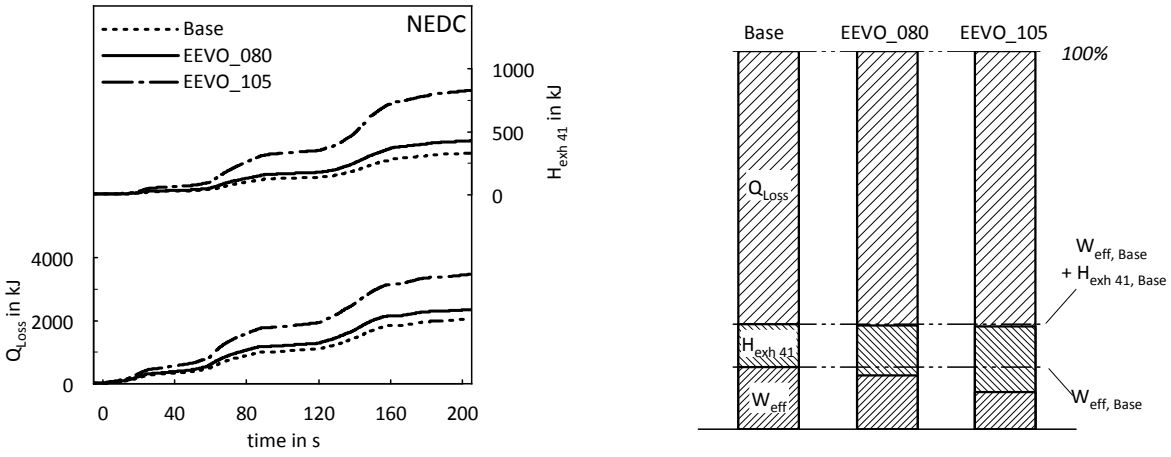

Figure 4.16: Comparison of the base engine with EEVO valve timings concerning energy flows during the first 200 seconds of a cold-start NEDC

Figure 4.17 shows the cumulated characteristics of most relevant engine out emissions. Considering the left chart, a significant increase of NO_x emissions due to EEVO_105 can be seen. The main reason for this is the increased heat release and the lower rate of EGR resulting from the low effective efficiency and hence the higher amount of fuel quantity which is necessary to achieve the desired engine load. In other words, the same effect as it was observed in steady state measurement results. Keeping in mind that the efficiency drop of EEVO_080 is clearly lower than this of EEVO_105 (figure 4.15, left), it is reasonable that also the increase of NO_x emissions resulting from EEVO_080 is far less. When it comes to the difference between EEVO_080 and EEVO_105 in NO_x emissions also another effect has to be considered. Namely the further external EGR reduction of EEVO_105 resulting from internal EGR, which is caused by the early exhaust valve closing. The partly replacement of external EGR by internal EGR in general leads to higher NO_x emissions, what has several causes. First, at a constant overall rate of EGR it leads to a higher cylinder charge temperature. Second, the achievable rate of EGR at a given boost pressure and air mass is lower (lower volumetric efficiency).

Analysing the HC emissions plotted in the right chart of figure 4.17, a clear benefit of EEVO_105 is obvious. This is mainly caused by the higher temperature level of combustion. Hence the same effect, which leads to the increased NO_x emissions. Thus, it is also reasonable that the benefit of EEVO_080 concerning HC emissions after 195 seconds is small compared to

EEVO_105. The CO emissions plotted below show a drawback of EEVO valve timings at the end of the considered time section. However, analysing these characteristics more detailed, makes obvious that the higher values are caused more or less only by a peak of CO emissions at the first acceleration after about 60 seconds. Apart from this event, the CO emissions of EEVO valve timings are neutral (EEVO_080) or even lower (EEVO_105) compared to the base engine. The observed CO peaks of EEVO_080 and in particular of EEVO_105 are caused by the relatively high desired engine load (IMEP $>$ 8 bar) at low engine speed. In interaction with the low efficiency of EEVO valve timings this means a combustion process characterized by a low air excess ratio and high temperatures. Thus, CO emissions are high, while HC emissions are not critical. Similar effects occur with base valve timings in a full load combustion process at low engine speed. It is also worth mentioning that the CO peak does not occur once more in one of the 3 subsequent city cycles of the NEDC, what could be explained by a lower friction and hence a lower required IMEP at the relevant acceleration.

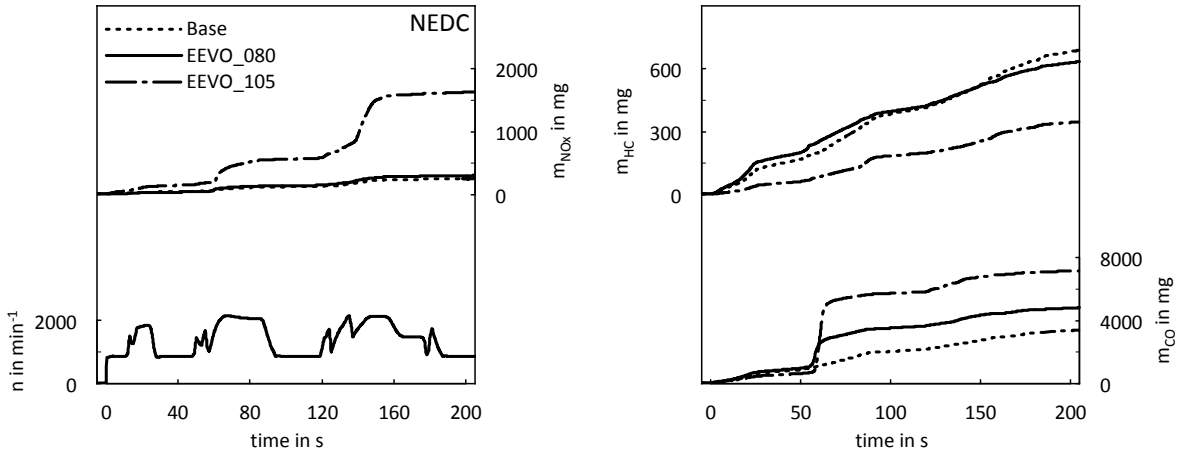

Figure 4.17: Comparison of the base engine with EEVO valve timings concerning engine out emissions during the first 200 seconds of a cold-start NEDC

Besides the NEDC also the FTP 75 was considered. This test cycle is from particular interest since it is relevant for the today's strictest emission legislations. Complying with these limits requires an exhaust aftertreatment system, which achieves high conversion rates already a very short period of time after cold start. This means a special demand for exhaust thermomanagement.

Figure 4.18 provides the most relevant information concerning exhaust temperatures and fuel consumption for the FTP 75. Also for this test cycle only the very first, for thermomanagement purpose relevant section is considered. Analysing the temperatures upstream DOC (T_{41}) in the right chart, it can be seen that applying EEVO_105 enables exceeding the 200 °C limit after not more than half a minute. Taking into account that the base engine achieves the same event after about 200 seconds, this is a really considerable gain. EEVO_080 needs about 65 seconds until T_{41} passes the 200 °C threshold. Referring to the end of the plotted section of time, the achieved temperature gain is 106 °C for EEVO_105 and 33 °C for EEVO_080.

Considering the characteristics of the temperature downstream DOC (T_{51}), the condensed water in catalysts has to be kept in mind. Thus, using a dry catalyst will lead to an earlier temperature increase. The cumulated fuel mass curves in the left chart of figure 4.18 make obvious a clear disadvantage of EEVO valve timings. EEVO_080 requires about 20 % more fuel for the first 130 seconds, in case of EEVO_105 the penalty is about 63 %. Based on the assumption that EEVO will be applied until T_{41} exceeds the 200 °C threshold and the fuel consumption for the rest of the test cycle is equal to the base engine, the increase in fuel consumption referred to the whole cycle for EEVO_080 and EEVO_105 is 0,7 and 1,0 % respectively. Hence the effect on cycle fuel consumption is lower than in case of NEDC, what has several causes. First the FTP 75 is longer than the NEDC. This means less influence of EEVO even if the absolute time of application would be the same. Second the required application time for early EVO is shorter in case of the FTP 75, what is mainly due to the higher load during the first section after cold start.

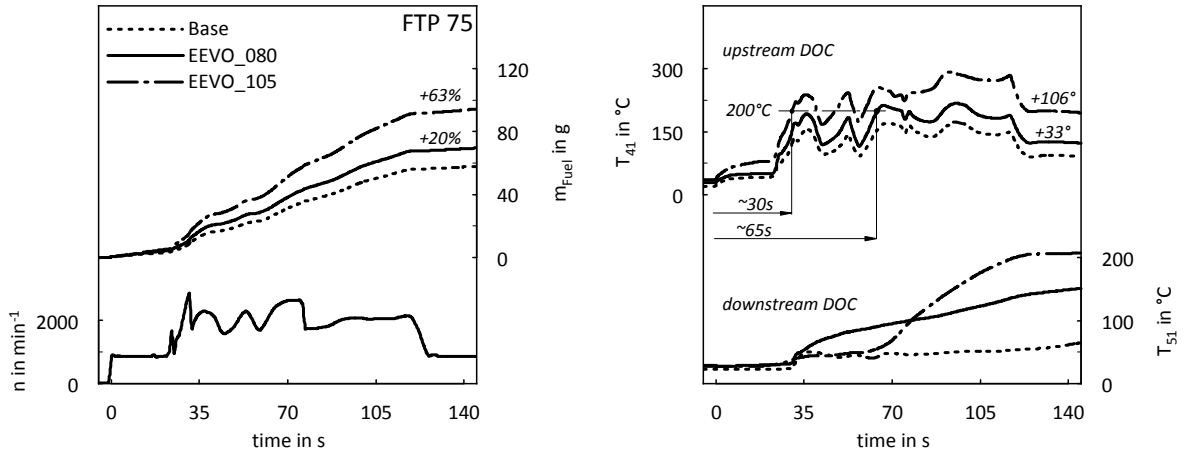

Figure 4.18: Comparison of the base engine with EEVO valve timings concerning fuel consumption and exhaust temperatures during the first 140 seconds of a cold-start FTP 75

The charts plotted in figure 4.19 provide an analysis of energy flows as it was shown already for the NEDC. The characteristics of cumulated exhaust enthalpy and heat losses in the left chart show a slightly higher effect due to EEVO_080 compared to the NEDC. Analysing the relative shares of effective work, exhaust enthalpy and heat losses, which are illustrated by the bars plotted in the right chart of figure 4.19, leads to the same finding as it was derived from the NEDC consideration. Applying an EEVO means increasing the share of exhaust enthalpy mainly by decreasing the share of effective work. In other words the share of heat losses remains nearly constant.

Figure 4.20 points out what this means for the additional supplied fuel energy, which is necessary to maintain engine load when applying EEVO valve timings. Since engine load and hence delivered effective work remains constant, the additional supplied fuel energy is splitted only between exhaust enthalpy flow and heat losses. As obvious the increase of exhaust enthalpy ($\Delta H_{\mathrm{exh}\,41}$) is lower than the increase of heat losses (ΔQ_{Loss}), what means a

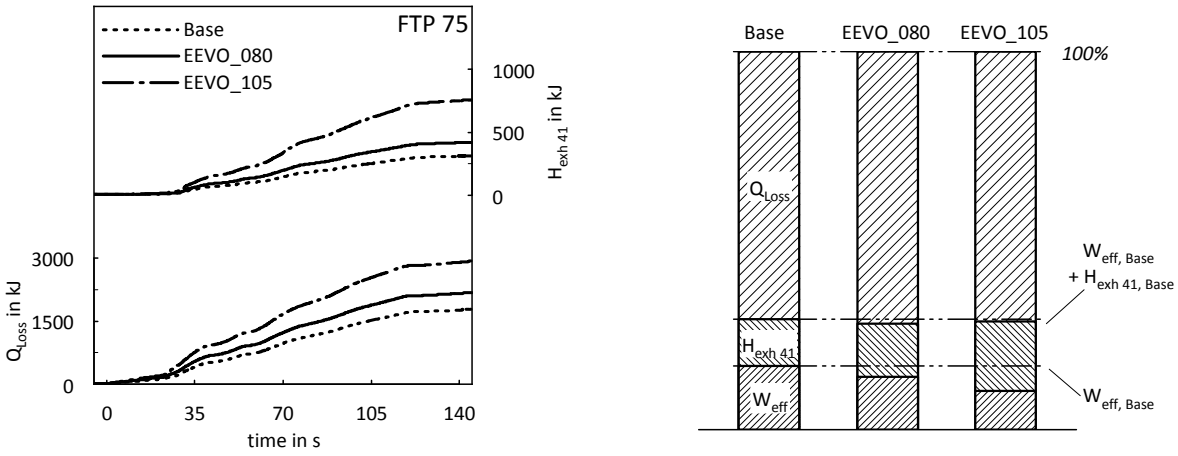

Figure 4.19: Comparison of the base engine with EEVO valve timings concerning energy flows during the first 140 seconds of a cold-start FTP 75

smaller share of exhaust enthalpy on additionally spent fuel energy compared to heat losses. The dash-dotted curve indicates the gradient of a thermomanagement method, which leads to an increase of exhaust enthalpy and heat losses in equal shares. The more or less identical gradient of NEDC and FTP 75 characteristic means that the thermomanagement efficiency of EEVO strategies is nearly the same for the considered test cycle sections.

Keeping in mind evaluation of EEVO strategies in steady state operation points, considered in figure 4.7, makes clear that the gradient of $\Delta\dot{H}_{\mathrm{exh\,41}}$ versus $\Delta\dot{Q}_{\mathrm{Loss}}$ in transient tests (figure 4.20) is clearly lower. When it comes to analyse the reasons for this, several facts must be considered:

- The evaluation of transient tests by considering the cumulated energy flows over a defined section of time covers also operation points, which were not taken into account by evaluation of steady state operation points.
- The considered test cycle sections are not only a range of steady state operation points, but also affected by transient effects. This means e.g. operating at a minimum air excess ratio level (active soot limiter) during acceleration.
- However, the most relevant difference comes from cold engine conditions of the transient test. This means a higher fuel consumption due to a higher friction and higher cylinder wall heat losses. In addition also wall heat losses in exhaust ports, the exhaust manifold and the turbine housing are higher, which results in a lower exhaust temperature and enthalpy flow.

Figure 4.21 gives an survey over most relevant engine out emissions during the first 130 seconds of the FTP 75. The effects of EEVO valve timings on NO_x emissions are the same as observed in analysing the NEDC results (increased heat release, less EGR, for detailed

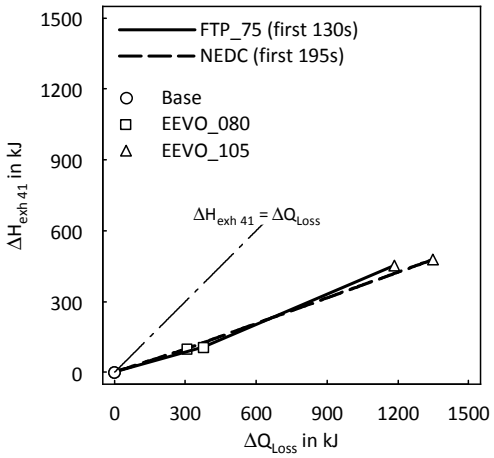

Figure 4.20: Increase of exhaust enthalpy versus increase of heat losses due to EEVO in the first section of a cold-start NEDC and FTP 75

information refer to explaining of figure 4.17). Also the considerably lower HC emissions of EEVO_105 were already observed in the NEDC. The HC emissions of EEVO_080 are comparable to these of the base engine for the main period of considered section of time. However, a peak at the beginning of the cycle leads to a shift of the corresponding curve to a slightly higher level. Concerning CO emissions the same effects observed in the NEDC could be identified. This means a significant increase during the first acceleration, which causes a higher cumulated value at the end of the considered section of time. Nevertheless, after about 30 seconds the CO emissions of both EEVO valve timings – EEVO_080 and EEVO_105 – are lower than these of the base engine, what could be identified by the lower gradient of the cumulated curves.

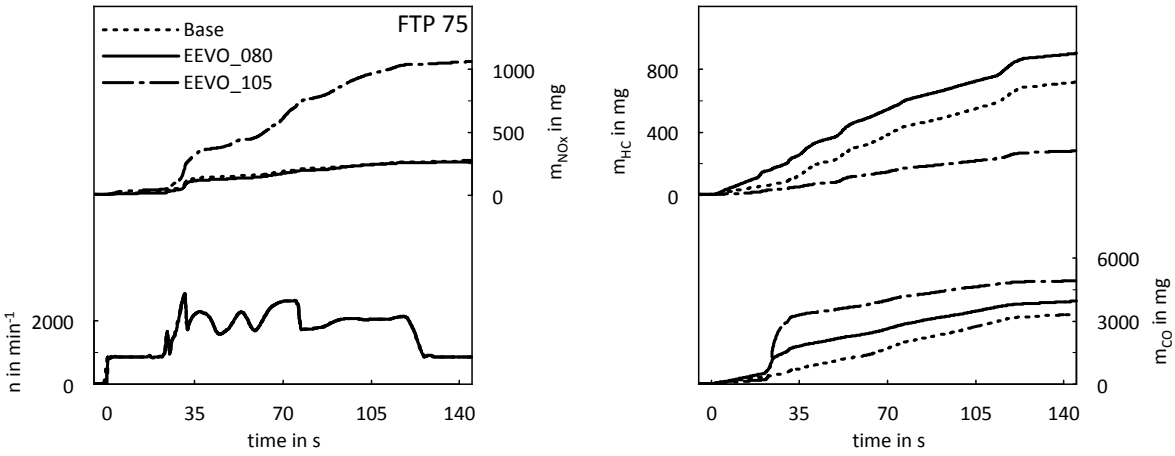

Figure 4.21: Comparison of the base engine with EEVO valve timings concerning engine out emissions during the first 140 seconds of a cold-start FTP 75

4.2 Late Intake Valve Closing

At the beginning of this section it should be pointed out that the main objective of applying late intake valve closing (LIVC) was exhaust thermomanagement. This is worth mentioning once more, since diesel engines with a variable IVC are of particular interest also in terms of in-cylinder NO_x reduction [18, 37, 40].

As pointed out by means of simulation, the exhaust temperature increasing effect of LIVC comes from a decrease in charge fuel ratio, which is mainly caused by a drop in aspirated mass of cylinder charge (air and EGR) and only to a minor degree by an increase of fuel mass (fuel consumption penalty).

Figure 4.22 shows a comparison of the intake valve lift curve used for experimental investigations concerning late intake valve closing – LIVC_063 – with the base. As obvious LIVC_063 is characterized by an about 63 °CA later IVC compared to the base valve timing. The opening event and the maximum valve lift remain constant.

The following analysis comprises steady state measurement data as well as transient tests. Both are based on warm engine conditions. A cold start by using the original starter was not possible with LIVC_063 valve timing. This is because LIVC_063 leads to a lower volumetric efficiency and hence a lower cylinder pressure and temperature at the end of the compression stroke. Of course, this is true also for warm engine conditions. However, cold engine conditions lead to higher wall heat and blowby losses resulting in a further decrease of cylinder pressure and temperature. On engine test bed this effect could be at least partly compensated by motoring the engine at a higher speed, what means a higher volumetric efficiency and thus a higher cylinder pressure and temperature. Nevertheless, the observed drawback concerning cold start ignitability is more or less a criterion for exclusion when it comes to exhaust thermomanagement methods applied at the very first section of a cold-start test cycle.

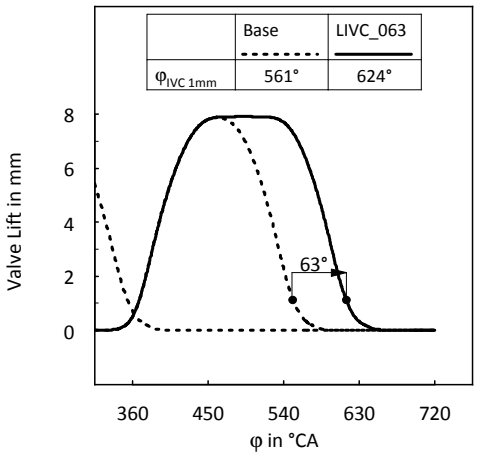

Figure 4.22: Comparison of LIVC_063 – used for experimental investigations of late intake valve closing – with the base intake valve lift curve

4.2.1 Steady State Operation

The reduction of aspirated cylinder mass due to LIVC requires an adaption of EGR. Otherwise, the air management strategy of the ECU will try to achieve the same intake air mass flow as it was reached with the base valve timing. Taking into account the reduction of volumetric efficiency due to LIVC, this would mean a significant cut in EGR and hence an extremely increase in NO_x emissions. As already mentioned, LIVC means also a decrease of cylinder pressure and temperature at the end of the compression stroke, what is in particular relevant for ignition delay and hence for heat release. Thus, also a modification of injection parameters is necessary. In other words, LIVC requires an adaption of the ECU calibration.

Besides the increase of exhaust temperature, the main objective of adapting ECU calibration to LIVC_063 was achieving comparable engine out emissions. Of course also fuel consumption was kept in view. Subsequently the most relevant findings of ECU calibration adaption should be discussed by considering parameter variations at an engine speed of $1000\,\mathrm{min}^{-1}$ and a BMEP of 1,5 bar.

Figure 4.23 shows the fuel consumption (BSFC) and the exhaust temperature downstream turbine (T_{41}) achieved by applying LIVC_063 in a variation of main injection timing. The characteristics are plotted versus $MFB_{50\%}$. As reference also the base engine results are illustrated. Analysing the BSFC, it can be seen that the $MFB_{50\%}$ optimum of LIVC_063 in this operation point is near to this used by the base engine. The absolute value of the lowest BSFC, reached with LIVC_063, is nearly equal to the BSFC of the base engine. The characteristic of the exhaust temperature (T_{41}) plotted below points out that LIVC_063 achieves a gain of about 25 °C compared to the base engine for the same $MFB_{50\%}$. As it is also known from base valve timings, a further exhaust temperature increase could be achieved by using a more retarded main injection timing and hence a later $MFB_{50\%}$.

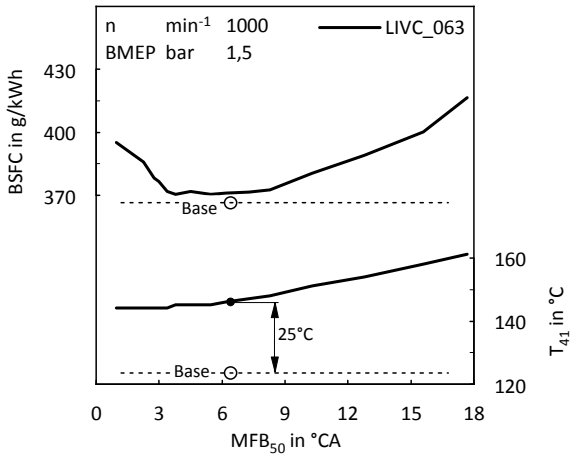

Figure 4.23: Effect of $MFB_{50\%}$ on BSFC and exhaust temperature when applying LIVC_063 at $1000\,min^{-1}$ and a BMEP of 1,5 bar

The right chart in figure 4.24 illustrates effects of $MFB_{50\%}$ on pollutant emissions. It is easy to see that the HC and CO concentrations emitted by LIVC_063 are significantly higher than these of the base engine for the same $MFB_{50\%}$. The most probably reason for this effect is the lower level of cylinder pressure and temperature at start of combustion, what means a higher ignition delay and hence a – concerning HC emissions disadvantageous – higher degree of homogenization. A more detailed discussion of this effect by means of analysing heat releases will be done later. It is also clearly to see in figure 4.24 that a retarded combustion will lead to a further increase of HC and CO emissions. However, not only HC and CO, but also NO_x emissions are clearly higher at the same $MFB_{50\%}$. This is caused mainly by the higher oxygen (O_2) concentration of aspirated cylinder charge, which is shown in left chart. The reason for the higher O_2 concentration is a not yet adapted map of desired air mass flow. Hence air management controlling has to cut EGR in order to compensate the lower volumetric efficiency caused by LIVC_063. The illustrated characteristics of air excess ratio (λ) and rate of EGR give evidence of this strategy for maintaining air mass flow. The slight λ differences result from differences in BSFC.

The output of considering main injection timing variations was the finding that a slightly earlier $MFB_{50\%}$ – compared to base engine calibration – delivers lowest possible HC and CO emissions. The next step of adapting ECU calibration was a modification of desired air mass flow, which means an adaption of EGR. In figure 4.25, this process should be discussed by analysing an EGR swing at the same operation point, which was considered above for variation of $MFB_{50\%}$ ($1500\,min^{-1}$, BMEP $= 1,5$ bar). The results are plotted versus NO_x emissions, what is reasonable, since this parameter is the motivation for increasing EGR. It can be seen in the right chart that the NO_x emissions of the base engine could be achieved by a rate of EGR, which is lower than this of the base engine calibration. However, also the air excess ratio (λ) is lower. Hence the oxygen concentration (not illustrated) of aspirated cylinder charge is at a comparable level. Moreover, the right chart shows that the $MFB_{50\%}$ was kept constant, what

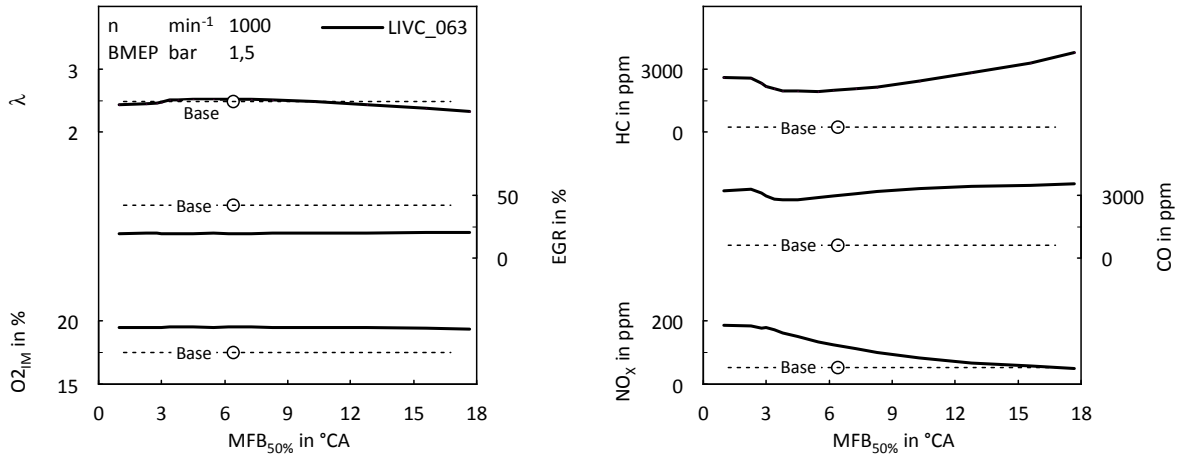

Figure 4.24: Effect of $MFB_{50\%}$ on air excess ratio, EGR, oxygen concentration and pollutant emissions when applying LIVC_063 at 1000 min^{-1} and a BMEP of 1,5 bar

was realized by using an earlier main injection timing for higher rates of EGR. Considering the left chart, it can be seen that a higher rate of EGR (lower NO_x) leads to an increase of BSFC while the exhaust temperature (T_{41}) remains nearly constant. Since not only the $MFB_{50\%}$ but also PMEP (not illustrated) is constant, a probably reason for the BSFC increase is the decrease of the isentropic exponent due to the variation of EGR and air excess ratio.

The left chart in figure 4.26 shows the exhaust mass flow through the aftertreatment system ($\dot{m}_{\mathrm{exh\,41}}$, upstream low pressure EGR branching) and at tail pipe position ($\dot{m}_{\mathrm{exh\,TP}}$, downstream low pressure EGR branching). It can be seen that the tail pipe mass flow, which is relevant for emissions, becomes lower for higher rates of EGR. Due to this, the emissions plotted in the right chart, are considered not as concentrations but as mass flows. Since branching of the low pressure EGR is downstream the EAS, the relevant mass flow for exhaust thermomanagement, which is also representative for mass of cylinder charge, is independent from EGR. Considering the right chart, makes clear that increasing EGR in order to maintain base engine NO_x emissions, means an increase of HC and CO emissions. Since HC and CO emissions result mainly from an incomplete combustion they provide a further explanation – besides decrease of the isentropic exponent – for the increase of fuel consumption observed in figure 4.25. The soot emissions caused by LIVC_063 are clearly lower than this of the base engine.

With findings from the variations considered above (main injection timing and EGR) the adaption of ECU calibration in the operation area relevant for driving cycles (NEDC, FTP 75) was done. The main focus of this task was on combustion stability and engine out emissions. In low load operation area the decrease in volumetric efficiency resulting from LIVC_063 was used for a decrease in charge fuel ratio and hence an increase in exhaust temperature. However, a lower charge fuel ratio means also a reduction of air excess ratio and/or EGR. Thus, a compromise between NO_x and HC as well as CO emissions must be found.

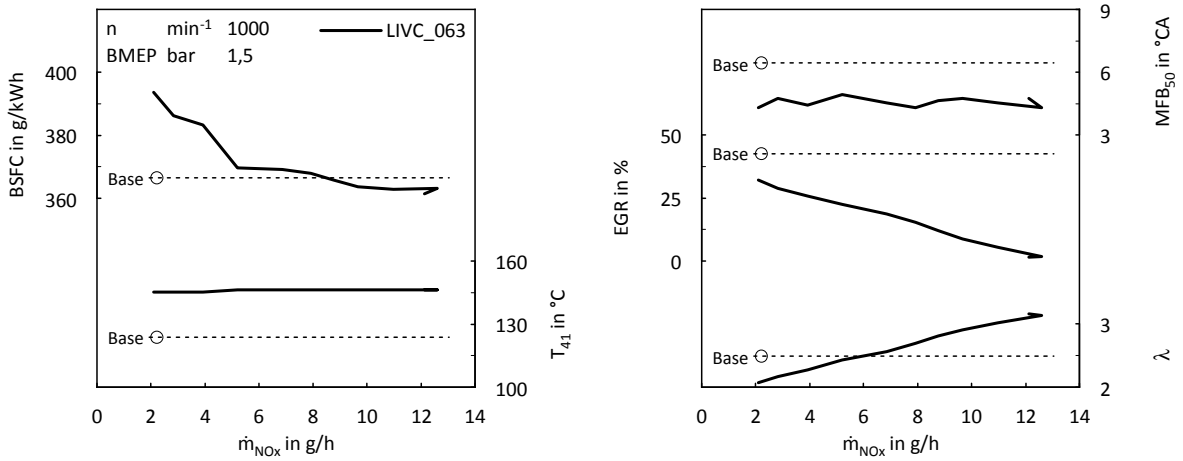

Figure 4.25: Considering BSFC, exhaust temperature, $MFB_{50\%}$, EGR and air excess ratio versus NO_x emissions for an EGR swing with LIVC_063 at 1000 min^{-1} and a BMEP of 1,5 bar

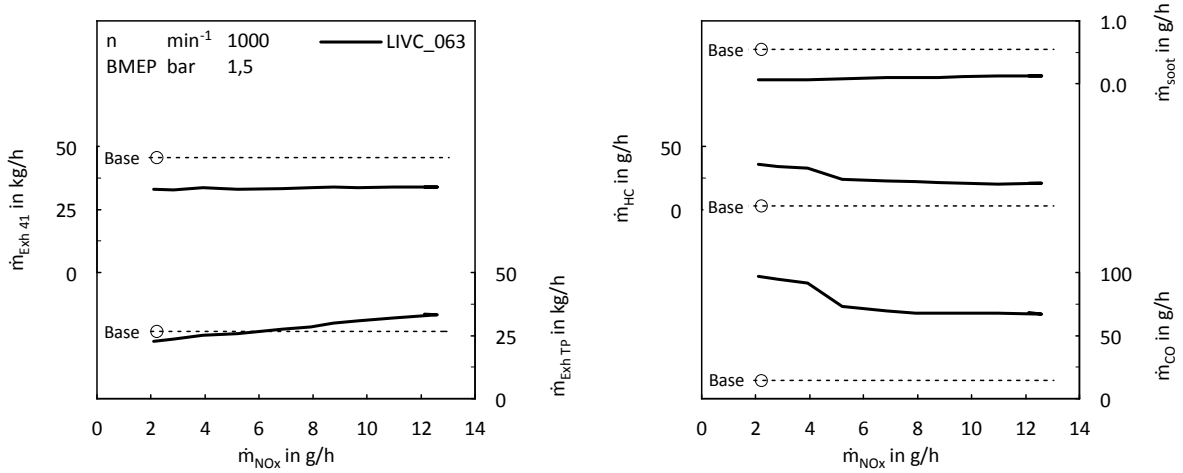

Figure 4.26: Considering pollutant emissions (right) and exhaust gas mass flows (left) versus NO_x emissions for an EGR swing with LIVC_063 at 1000 min^{-1} and a BMEP of 1,5 bar

Figure 4.27 shows a comparison of LIVC_063 with the base engine at 1000 min^{-1} and low engine load. In the left chart an increase of exhaust temperature downstream turbine (T_{41}) of about 20 °C could be observed. The slightly higher BSFC of LIVC_063 is mainly due to the lower air excess ratio and rate of EGR, which means a lower charge fuel ratio. In the right chart it can be seen that the NO_x emissions of LIVC_063 are nearly at the level of the base engine in lowest load area. For higher loads slightly increased NO_x emissions are accepted in order to avoid a further increase of HC emissions, which are already on a higher level compared to the base engine. The reason for lower soot emissions should be discussed by analysing results from cylinder pressure indication.

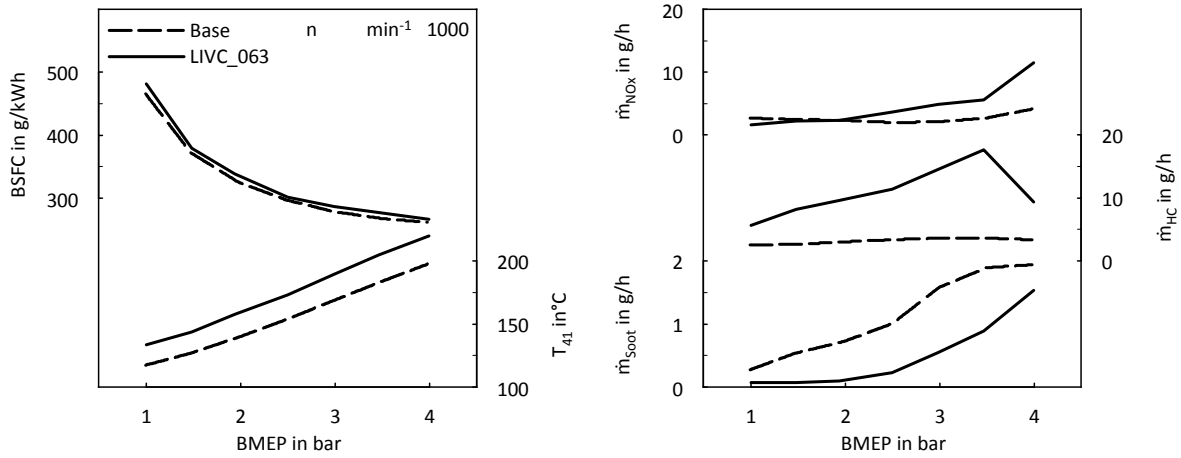

Figure 4.27: Comparison of LIVC_063 and base valve timing concerning fuel consumption, exhaust temperature and pollutant emissions at 1000 min^{-1} and low engine load

Figure 4.28 shows a comparison of LIVC_063 and the base engine concerning cylinder pressure (left chart), injection pattern and net rate of heat release (right chart). The considered operation point is characterized by an engine speed of 1000 min^{-1} and a BMEP of 1,5 bar. Due to the longer ignition delay of LIVC_063 – resulting from lower cylinder pressure and temperature – an advanced injection strategy was applied. However, in contrast to the base engine a clear separation of combustion process in heat release of pilot injection and main injection can not be observed. The retarded combustion of pilot quantity and hence the longer time for homogenization may be the reason for lower soot emissions. As already mentioned the higher degree of homogenization is also the most probably reason for the high level of HC emissions. In context of pilot injections, it is also worth mentioning that the combustion noise identified by cylinder pressure indication is lower for LIVC_063 compared to the base engine.

Although a decrease of NO_x emissions due to LIVC_063 was not the main focus, a brief analysis of the most important effects in this context should be done. As known from fundamentals [35], both availability of oxygen and high temperatures are necessary for NO_x formation. The benefit of LIVC_063 comes from the reduction of effective compression ratio, which means a reduction in cylinder pressure and temperature at the end of the compression

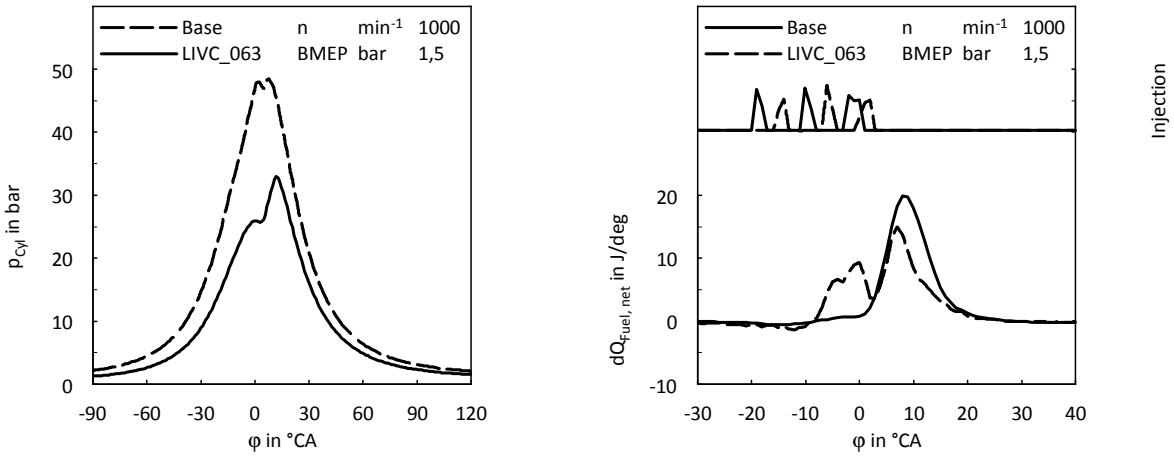

Figure 4.28: Comparison of LIVC_063 and base valve timing concerning cylinder pressure, injection pattern and net rate of heat release at 1000 min^{-1} and a BMEP of 1,5 bar

stroke. Thus, assuming same injection parameters, also the local peak cylinder temperature – relevant for NO_x formation – is lower.

By means of figure 4.29 the NO_x reduction effect of of LIVC_063 should be discussed for low load operation points at 1000 min^{-1}. For this purpose a comparison of LIVC_063 and base valve timing is considered. In addition to the results achieved by application of low pressure EGR (bold curves) also results for engine operation without EGR (thin curves) can be seen. The left chart provides information concerning air excess ratio (λ) and O_2 concentration of the aspirated cylinder charge. Of course, O_2 concentration is identical for the base engine and LIVC_063 when EGR is shut off. Hence the lower NO_x concentration of LIVC_063, which could be seen in the right chart, is only due to the lower peak cylinder temperature. The difference in NO_x mass flows plotted above is slightly higher compared to the difference of concentrations, what is because of the lower exhaust mass flow resulting from LIVC_063 (lower volumetric efficiency). However, considering base engine results achieved with EGR makes clear that a far more significant NO_x reduction is necessary. Of course, declining the O_2 concentration by means of EGR may be done also in case of LIVC_063. However, due to the higher level of HC emissions mentioned above, this is not possible in the same degree. Hence the minimal level of O_2 concentration achievable with LIVC_063 is higher than this of the base engine. Nevertheless, in combination with the lower peak cylinder temperature nearly the same NO_x emissions could be achieved for low load operation points. However, when it comes to operation areas with higher engine load the lower O_2 concentration reduction potential of LIVC_063 could not be compensated entirely by the lower peak cylinder temperature and the lower exhaust mass flow. For maintaining NO_x emissions of base engine valve timing with LIVC_063 also at higher loads, a further decrease of O_2 concentration is necessary. Doing so without an increase in HC emissions requires a higher boost pressure, which enables a reduction of O_2 concentration without a decrease of air excess ratio. However, a higher boost pressure would compensate the lower volumetric efficiency, which means increasing the charge

fuel ratio. Hence the effect of gaining exhaust temperature and cutting exhaust mass flow will disappear. In other words, applying LIVC_063 as exhaust thermomanagement method works only at low engine loads without a drawback in engine out NO_x emissions.

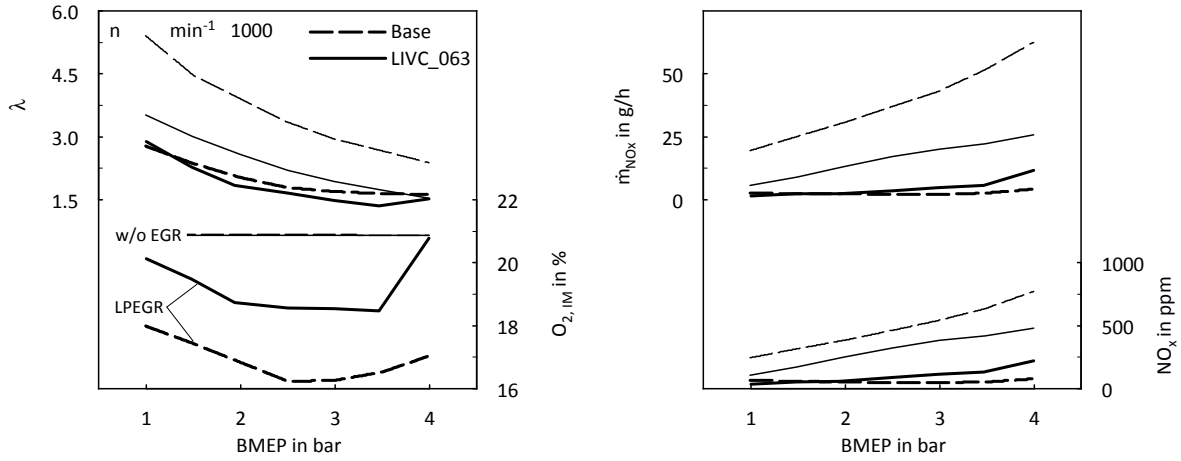

Figure 4.29: Comparison of LIVC_063 and base valve timing concerning air excess ratio, oxygen concentration and NO_x emissions – with and without EGR – at 1000 min^{-1} and low engine load

4.2.2 Transient Operation

As already mentioned, starting the engine featured with LIVC_063 valve timing at cold conditions was not possible by using a conventional starter. Only motoring the cold engine by dynamometer to a speed higher than 1500 min^{-1} provides a cylinder pressure high enough for compression ignition. Hence the application of late intake valve closing is not recommended for engine cold start and the first section of the subsequent warm up process. However, LIVC_063 should be evaluated concerning the potential for maintaining catalyst temperature during low load operation. For this purpose the urban driving cycle (UDC) of the NEDC is considered.

Figure 4.30 shows a comparison of LIVC_063 and base valve timing in this section. Since exhaust temperatures of base engine and LIVC_063 were not exactly at the same level at the start of the test cycle, not the first but the last (4^{th}) city cycle is considered. The left chart shows besides the engine speed characteristic also the cumulated fuel mass for the considered test cycle section. Using LIVC_063 instead of base valve timing means an increase in fuel consumption of about 5 %. However, analysing the exhaust temperatures in the right chart makes clear the benefit of LIVC_063. The temperature downstream turbine (T_{41}) is about 65 °C higher compared to the base engine. Downstream DOC (T_{51}) the difference is even higher. This could be explained by a higher heat release of exothermic reactions in the catalyst, what is mainly due to the higher HC and CO emissions of LIVC_063 (considered subsequently in figure 4.31). A further reason may be a higher conversion rate resulting from the higher exhaust temperature.

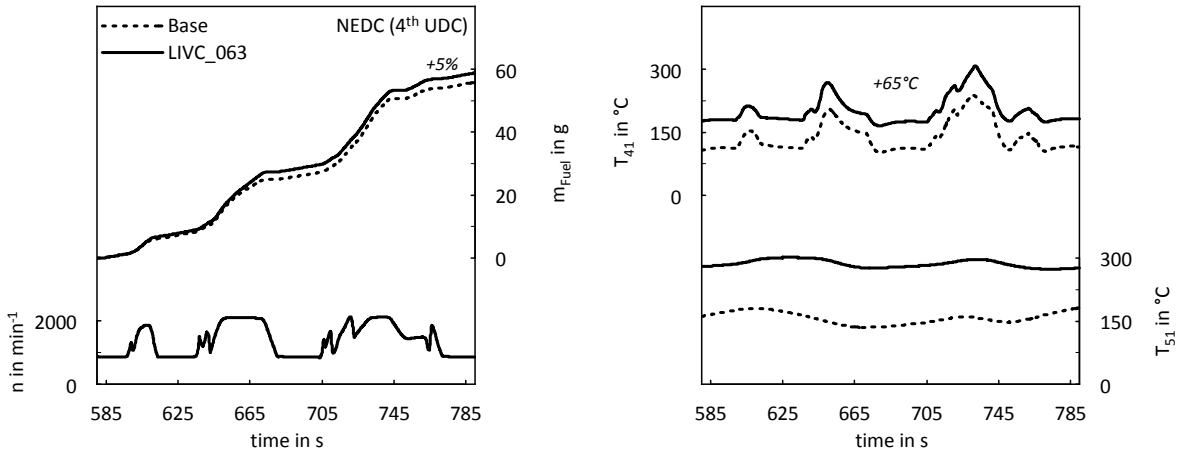

Figure 4.30: Comparison of LIVC_063 and base valve timing concerning fuel consumption and exhaust temperatures during the city cycle of the NEDC

Figure 4.31 shows the effect of applying LIVC_063 instead of the base engine valve timing on engine out emissions. The right chart points out the already mentioned significantly higher HC and CO emissions. The reason for this was already discussed in analysis of steady state results (higher degree of homogenization due to a longer ignition delay). In the left chart the increase of NO_x emissions due to LIVC_063 can be seen. This increase is caused mainly by the higher load sections, which are characterized by a relatively low EGR potential of LIVC_063 (due to the low volumetric efficiency). The lower soot emissions, which were observed also in analysis of steady state measurement data, result – as well as the higher HC and CO emissions – from the higher degree of homogenization.

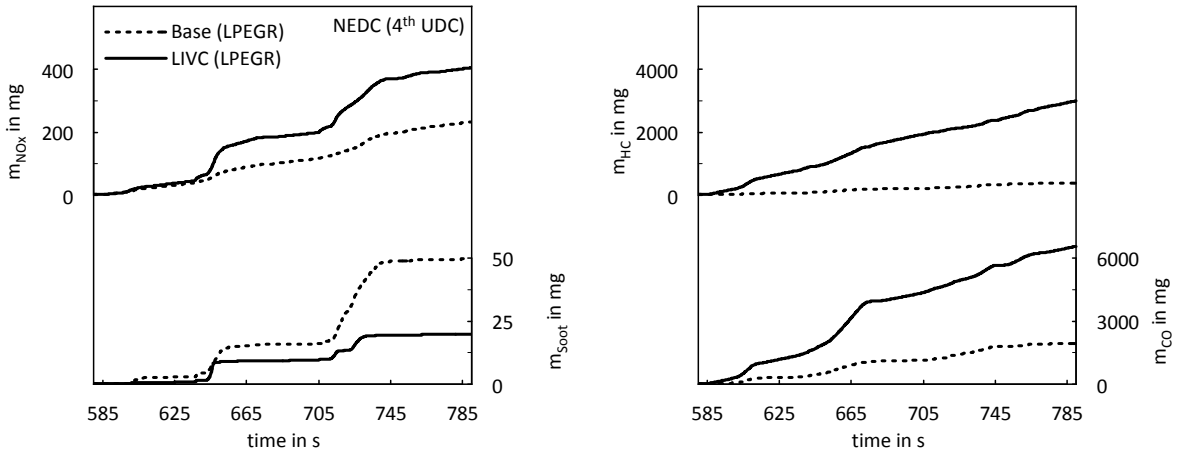

Figure 4.31: Comparison of LIVC_063 and base valve timing concerning pollutant emissions during the city cycle of the NEDC

4.3 Cylinder Deactivation

To investigate the effect of cylinder deactivation on engine test bed, engine A – a 4-cylinder engine – was adapted in order to realize a 2-cylinder operation. For this purpose, on the one hand fuel injection of cylinder 1 and 4 was deactivated by ECU calibration, on the other hand modified camshafts were used. Due to this camshaft modifications actuating of both exhaust and intake valves of cylinder 1 and 4 was disabled. Of course, switching between 2- and 4-cylinder operation was not possible by this realisation of cylinder deactivation.The measuring program was focussed on low engine load and speed operation points. Only warm steady state engine conditions were considered.

Figure 4.32 shows a comparison of 2- and 4-cylinder operation at 1500 min^{-1} and low engine load. The results are plotted versus effective engine torque (τ_{eff}) and not versus BMEP, what is easier for understanding in context of cylinder deactivation. However, to show the effect of shifting active cylinders towards higher engine load, due to operating with only 2 instead of 4 cylinders, the IMEP is used. More exactly it is the averaged IMEP of fired cylinders. The right chart shows the effect of cylinder deactivation on exhaust temperatures. At the position relevant for EAS – downstream turbine (T_{41}) – switching off 2 cylinders leads to a gain in exhaust temperature up to 120 °C (at 30 Nm). Upstream turbine (T_{31}) the temperature gain is even higher. Considering effects on BSFC (left chart) makes obvious that this increase in exhaust temperatures was achieved almost without a penalty in fuel consumption.

Figure 4.33 shows that the air excess ratio (λ) is the limit for 2-cylinder operation mode toward higher engine load. The rate of EGR – plotted below – was adapted in order to reach the same NO_x emissions as in 4-cylinder mode. Hence engine operation without EGR will mean an about 35% higher load potential. The right chart in figure 4.33 points out the cut of exhaust gas mass flow ($\dot{m}_{\mathrm{exh\,41}}$) due to cylinder deactivation. This fact has to be taken into account, if the exhaust temperature gain and the effect on fuel consumption of cylinder

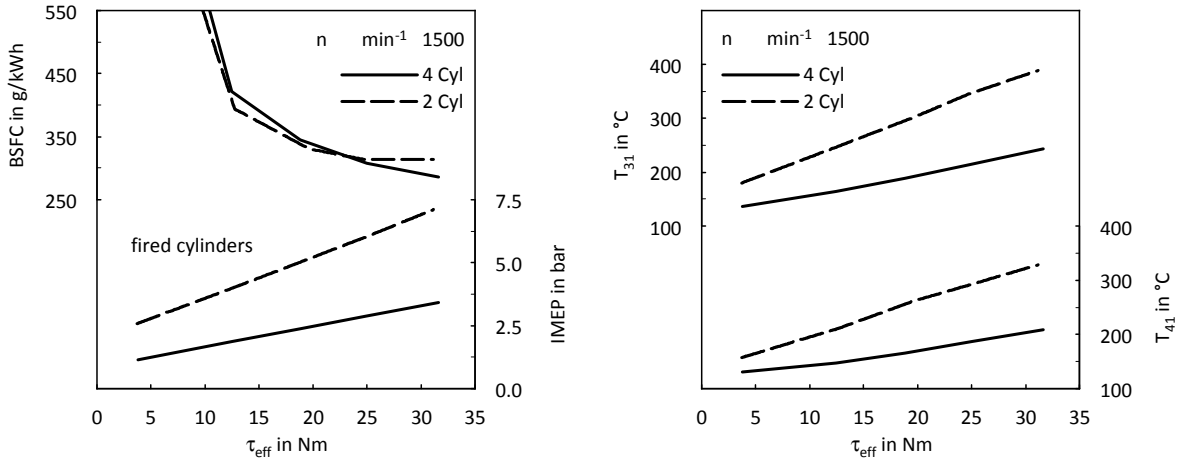

Figure 4.32: Comparison of 2- and 4-cylinder operation concerning fuel consumption, IMEP and exhaust temperatures at 1500 min^{-1} and low engine load

deactivation is compared with these of EEVO, which achieves the exhaust temperature gain without a reduction of mass flow. Considering the compressor pressure ratio (π_{Comp}) plotted in the right chart of figure 4.33, shows that the engine is operated more or less naturally aspirated. As already pointed out by means of simulations (see section 3.4.4) – using the original turbo charger – boosting is almost not possible in 2-cylinder mode at low engine speeds.

Figure 4.34 shows the effect of cylinder deactivation on pollutant emissions. The left chart contains NO_x and soot emissions, while the right chart provides information about HC and CO emissions. As mentioned above, maintaining NO_x emissions was achieved by an adaption of EGR. The slightly higher soot emissions may come from the lower air excess ratio. HC emissions are lower compared to four cylinder operation, which is mainly caused by the higher cylinder temperatures. The same effect explains the cut in CO emissions below an engine torque of about 20 Nm. The significant increase in CO emissions at higher engine load results from the low air excess ratio.

As shown above, the engine load shift resulting from cylinder deactivation leads to a significant increase in IMEP of fired cylinders. However, the downsizing effect is not the only reason for the higher IMEP in 2-cylinder operation. Calculating an inner torque (τ_{i}) based on IMEP and corresponding displacement of relevant (fired) cylinders, delivers higher values for 2-cylinder operation (see figure 4.35). Subtracting the effective torque (τ_{eff}) leads to a calculated friction torque (τ_{f}), which is clearly higher for 2-cylinder operation. Taking into account not only the indicated torque delivered by the fired cylinders but also this of the deactivated cylinders – which is negative – shows that the main difference of 2- and 4-cylinder operation concerning τ_{f} comes not from friction in the narrow sense but from wall heat and blow by losses in deactivated cylinders.

Transient tests in 2-cylinder operation were not done, since the available torque is not sufficient for relevant test cycles (NEDC and FTP 75), see figure 4.36. Even not if EGR is

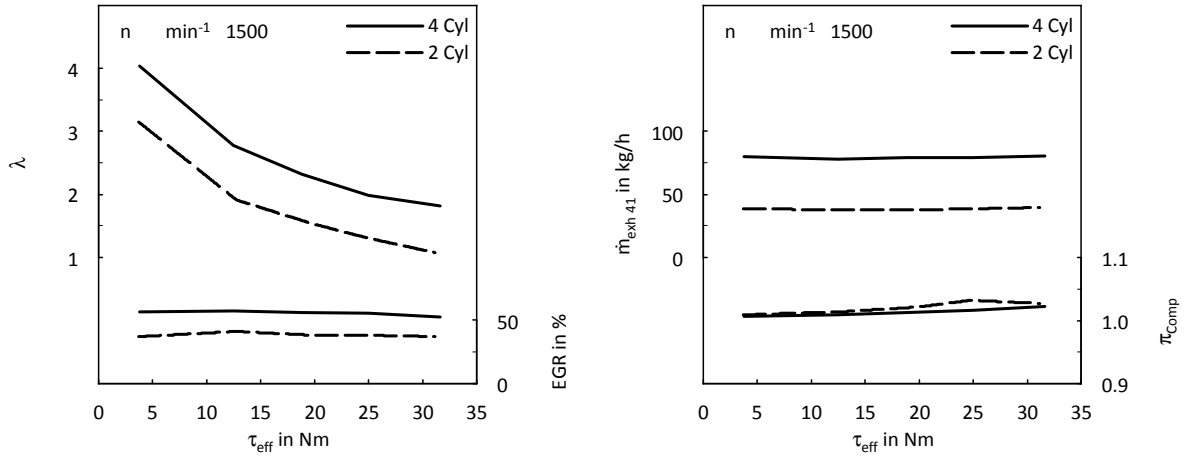

Figure 4.33: Effect of cylinder deactivation on relevant air management parameters at 1500 min^{-1} and low engine load

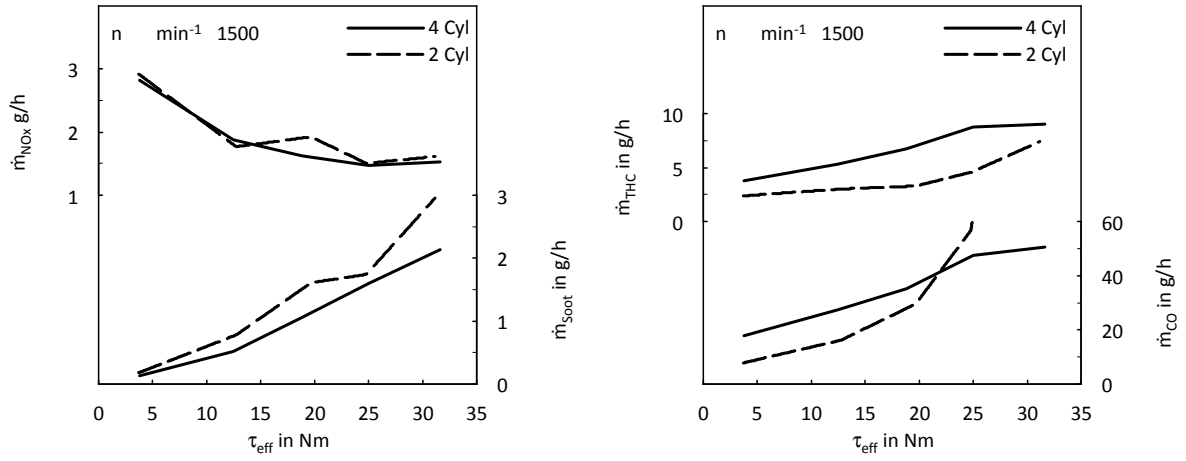

Figure 4.34: Comparison of 2- and 4-cylinder operation concerning pollutant emissions at 1500 min^{-1} and low engine load

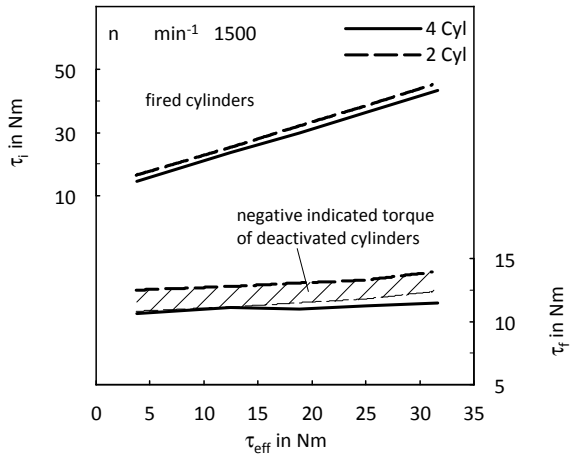

Figure 4.35: Effect of cylinder deactivation on friction, identified by cylinder pressure indication at 1500 min^{-1} and low engine load

deactivated and only the first sections (dashed curves) of driving cylces – of particular interest for exhaust thermomanagement – are considered. The plotted torque speed characteristics are calculated for a medium-sized passenger car, which is a typical area of application for the considered engine. The illustrated load limits refer to an estimation which is based on the steady-state measurement results at 1500 min^{-1} in 2-cylinder operation considered above. Of course assuming a constant load limit versus engine speed is a substantial simplification. Actually the available engine torque tends to be higher at increased speeds, what is mainly because of a higher turbocharger efficiency. However, it does not change the fact that a too low engine torque at 1500 min^{-1} avoids using the 2-cylinder operation mode in the considered test cycles.

In summary this means, cylinder deactivation enables a considerable gain in exhaust temperature nearly without a penalty in fuel consumption. However, for a downsized four cylinder engine with one stage turbo charging the available operation range in two cylinder mode is not sufficient for most relevant sections of driving cycles. Nevertheless, cylinder deactivation could be an interesting option for less downsized engines and the application of powerful engines in light weight vehicles. Moreover, using two stage turbo charging with a high pressure stage, which enables boosting also at mass flow rates relevant for two cylinder operation, makes cylinder deactivation interesting also for a downsized engine.

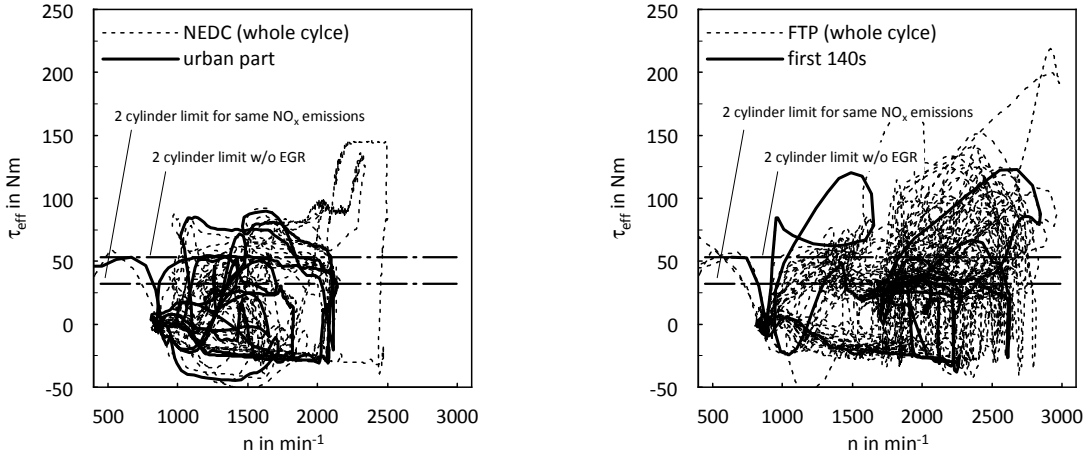

Figure 4.36: Effects of limited load potential resulting from cylinder deactivation on NEDC and FTP 75

4.4 Conventional Exhaust Thermomanagement Strategies

Although the focus of the present work is on exhaust thermomanagement realized by VVT strategies, also exhaust thermomanagement methods using only adaptions of engine calibration were considered. These methods – due to using series engine hardware configuration, hereinafter called conventional strategies – comprise retarded combustion and different EGR strategies. The main objective was the estimation of the potential concerning increase in exhaust temperature and enthalpy flow as well as the effect on fuel consumption and emissions.

4.4.1 Retarded Combustion

The application of a retarded combustion was realized by an adaption of the injection pattern. Both, late main injection timing as well as the utilization of a post injection was considered. Figure 4.37 shows results of a post injection timing (t_{PoI}) variation at different levels of main injection timing (t_{MI}) at 1000 min^{-1} and a BMEP 1 bar. The quantity of post injection (m_{PoI}) was kept constant. In addition also results of base engine calibration and EEVO_080 valve lift are plotted as reference. All illustrated results refer to warm engine conditions. As obvious the increase of exhaust temperature downstream turbine (T_{41}) achieved by EEVO_080 could be reached also by an application of post injection and an adaption of main injection timing. Furthermore the fuel consumption penalty is far lower than this caused by EEVO_080.

However, considering pollutant emissions plotted in figure 4.38 makes obvious the drawback of late main injection timing and post injection. While NO_x and soot emissions are more or less on the same level as the base engine calibration, HC and CO emissions are significantly higher for retarded main injection and particularly post injection timings.

In addition to the illustrated results also different levels of post injection quantity were considered. However, higher quantities are even worse concerning HC and CO emissions. The level of HC and CO emissions observed at warm engine conditions is not acceptable for

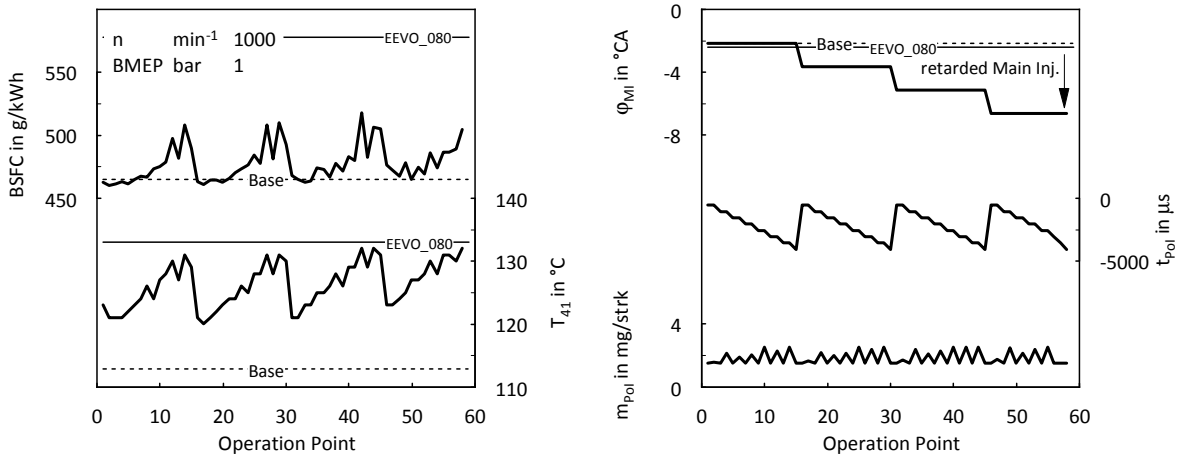

Figure 4.37: Effect of retarded main injection timing and post injection on exhaust temperature and fuel consumption at 1000 min^{-1} and a BMEP of 1 bar

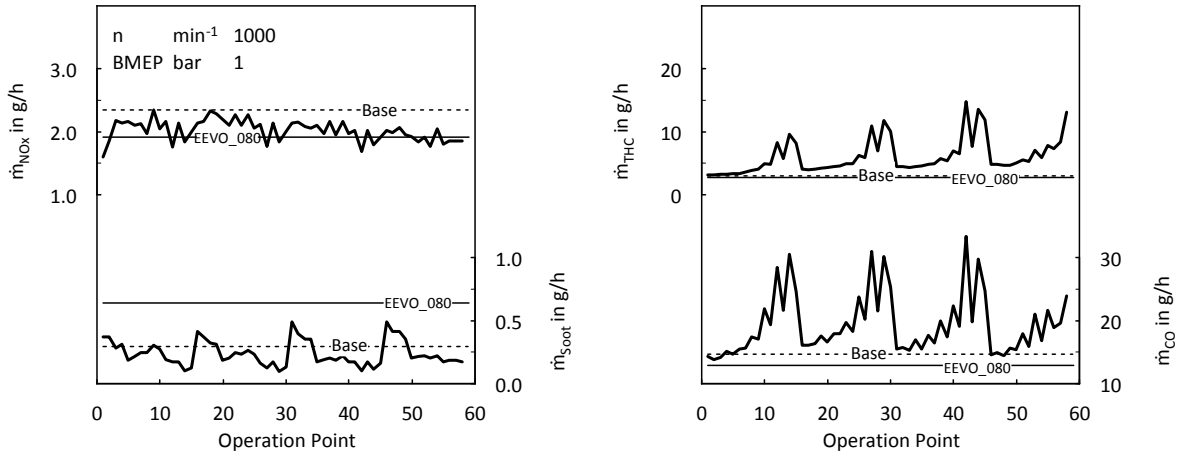

Figure 4.38: Effect of retarded main injection timing and post injection on pollutant emissions at 1000 min^{-1} and a BMEP of 1 bar

tailpipe emissions. Hence the considered retarded combustion strategies are not qualified for DOC heat up methods, which will be applied before catalyst light off. Cold engine conditions – in general – lead to a further increase of HC and CO emissions. As counteraction typical series diesel engine calibration strategies use an advanced main injection timing during cold start and warm up. Hence using a retarded main injection timing (inclusive post injection), would mean doing exactly the opposite of the established method. This is – besides the results achieved at warm engine conditions – another reason why DOC heat up by means of a retarded combustion is not considered more detailed.

Of course, using a retarded combustion after DOC light off, aimed to heat up more downstream located EAS components – e.g. a SCR – is another issue. The heat released in DOC due to conversion of HC and CO emissions could be used as additional source of heat. However, since conversion rate of the methane components contained in HC emissions is very low, a retarded combustion will lead to higher tailpipe HC emissions also after DOC light off. This applies in particular for late post injections, which do not lead to further heat release in cylinder but only in catalyst. Oil dilution by cylinder wall wetting is another problem of late post injections.

4.4.2 High Pressure EGR

Replacement of cooled low pressure EGR by uncooled high pressure EGR seems to be a logical step when it comes to exhaust thermomanagement. As it was shown by means of simulations, switching from low pressure EGR to internal EGR does not mean only a higher temperature of cylinder charge but also a cut in exhaust mass flow across EAS. This applies also for using uncooled high pressure EGR instead of cooled low pressure EGR. Hence in particular effects on exhaust temperature at different positions of the exhaust system should be considered in detail. But also the impact on engine out emissions has to be investigated.

To take into account cold engine conditions, a warm up process at an engine speed of $1000\,\mathrm{min}^{-1}$ and a BMEP of 1,5 bar was considered. Figure 4.39 shows a comparison between applications with low pressure EGR, high pressure EGR and without EGR. Apart from EGR control, ECU calibration (injection, VNT position, ...) is the same for all considered strategies. The left chart points out that relevant differences concerning fuel consumption were not observed. The characteristics below show the air mass flow, which is of course significantly higher for the application without EGR. However, when it comes to exhaust temperature, the total mass of cylinder charge – air mass and mass of recirculated exhaust gas – is a more relevant figure. Considering intake manifold pressure (p_{IM}) and temperature (T_{IM}) – see figure 4.39, right chart – allows an estimation concerning total mass of cylinder charge. Since both air and low pressure EGR mass flow is cooled by CAC, the low pressure EGR application leads to the same intake manifold temperature – $T_{\mathrm{IM}} = 25\,°C$ – as operating the engine without EGR. Also boost pressures of these strategies are nearly identical, what is due to the – compared to high pressure EGR – low effect of low pressure EGR on turbo charging. The uncooled high pressure EGR leads not only to a higher intake manifold temperature (T_{IM}), but also to a lower boost pressure (p_{IM}). The penalty in boost pressure could be explained by a lower turbo charging efficiency resulting from the lower mass flow across turbine and compressor. Taking into account both temperature (T_{IM}) and pressure (p_{IM}), allows the conclusion that the total cylinder mass of the strategies without EGR and low

pressure EGR is nearly identical, while this of the high pressure EGR application is lower. Of course this is based on the assumption of equal volumetric efficiencies.

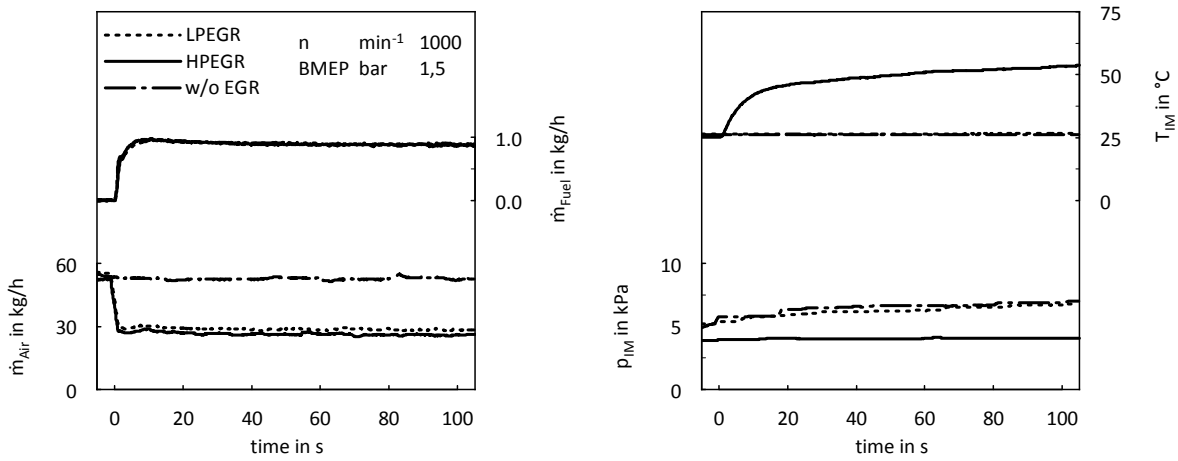

Figure 4.39: Effect of the EGR strategy on fuel consumption and air management parameters during warm up in low load operation

Keeping in mind that the differences in fuel consumption are more or less negligible, a lower cylinder mass and hence a lower charge fuel ratio would mean a higher exhaust temperature. However, considering the left chart in figure 4.40, shows that measured exhaust temperatures for the high pressure EGR application are lower. This applies all the more the more downstream the considered measuring point is located. Assuming that the high pressure EGR application has a higher exhaust temperature in cylinder before EVO, would mean a clearly higher temperature decrease due to wall heat losses in exhaust duct. The most probably reason for lower exhaust temperatures of high pressure EGR application is that the wall heat flow in cylinders, exhaust ports, exhaust manifold and turbine housing is dependent from gas temperature in a more significant way than from mass flow. This would mean, the positive effect of a higher mass flow, namely higher heat capacity, is more relevant than the maybe higher wall heat flow (due to a higher velocity).

Analysing the emission characteristics plotted in the right chart of figure 4.40 makes clear that NO_x emissions of the low pressure EGR application could be achieved also by means of high pressure EGR in this operation point. Despite the higher cylinder charge temperature achieved by using high pressure EGR, the HC emissions are clearly higher than these achieved by low pressure EGR and without EGR. Also soot emissions are slightly higher. A reason for this penalty of high pressure EGR concerning HC and soot emissions may be disadvantages in distribution of EGR to the cylinders, resulting from the more downstream located branching – compared to low pressure EGR. For application without EGR it has to be mentioned that concentrations of HC and soot are clearly lower compared to high pressure EGR and low pressure EGR. However, the higher tail pipe exhaust mass flow leads to comparable or even higher emission mass flows.

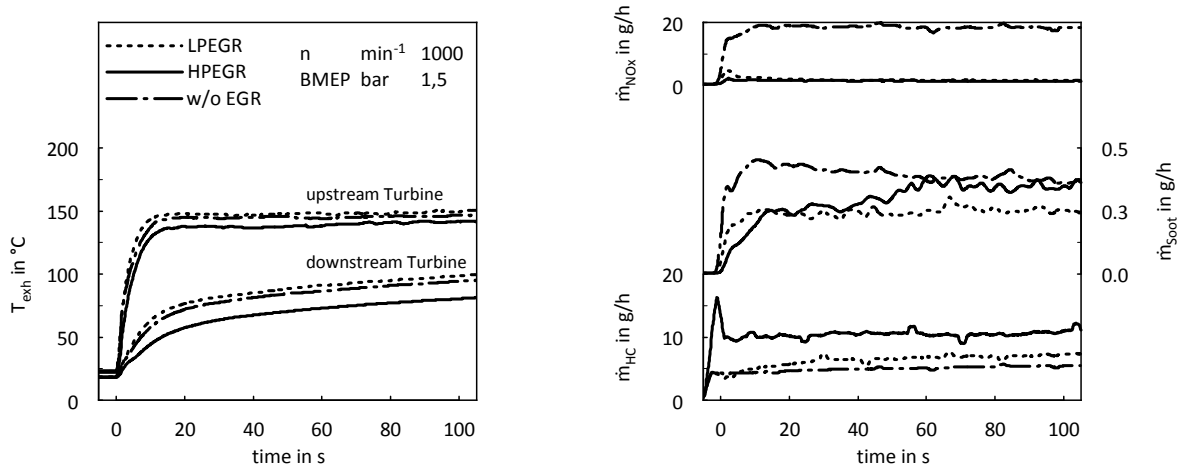

Figure 4.40: Effect of the EGR strategy on exhaust temperatures and emissions during warm up in low load operation

In summary, a benefit of replacing low pressure EGR by high pressure EGR was not observed. Nevertheless, most passenger car diesel engines featured with low pressure EGR have an additional – usually uncooled – high pressure EGR path, which is used mainly during warm up. This has several causes. One benefit of using high pressure EGR instead of low pressure EGR during warm up is avoiding condensation of exhaust gas in the charge air cooler. Exhaust gas recirculated via low pressure EGR path is more or less free of particles. However, also other components resulting from a not ideal combustion are critical concerning cooler fouling [38]. Another reason for using high pressure EGR during warm up may be that the higher temperature of aspirated cylinder charge accelerates the engine heat up process (cylinder wall, coolant, oil, ...), what is in general beneficial in terms of fuel consumption, although it was not observed in the discussed short section of time.

4.5 Validation of Simulation Model

Besides evaluation of effects, which are not or not sufficiently covered by simulation (emissions, transient behaviour, ...) also validation of the simulation model was a motivation for doing experimental investigations on engine test bed.

As shown in section 2.1.2 the results calculated by the base engine model do correlate well with measurement data. However, this means not necessarily a maintenance of correlation after a significant change of valve timing. Hence the measurement results analysed above in detail, should be compared with simulation results. For this purpose the simulation model of the base engine, evaluated in section 2.1.2, was adapted only concerning valve lift curves.

4.5.1 Early Exhaust Valve Opening

The left chart in figure 4.41 shows the valve lift curves of measurement (bold curves). Since actuation of the 2 exhaust valves of each cylinder is synchronous only for base valve timing, the corresponding exhaust valve lift curves – EVL_1 and EVL_2 – are considered separately. As explained in detail in section 4.1, besides reference measurement with original camshafts (Base), two early exhaust valve opening strategies – EEVO_080 and EEVO_105 – were considered on engine test bed. First, the original exhaust camshaft was replaced by a camshaft, which leads to valve lift curves denoted as EEVO_080. This means that the cams which are operating the first exhaust valves of each cylinder cause an 80 °CA earlier opening event. The second cams are identical to the original ones. In the next step the same camshaft was mounted in a position which leads to an additonal advance of 25°CA (EEVO_105). Of course this phasing means a shift of both valve lift curves (EVL_1 and EVL_2). Besides the valve lift curves realized for engine test bed measurement, also intermediate steps (thin curves) were considered in simulation. The right chart in figure 4.41 illustrates what this means for variation of exhaust valve opening ($\Delta\varphi_{\mathrm{EVO},1}$, $\Delta\varphi_{\mathrm{EVO},2}$) and closing events ($\Delta\varphi_{\mathrm{EVC},1}$, $\Delta\varphi_{\mathrm{EVC},2}$). For this purpose the variation of exhaust valve opening of the second exhaust valve ($\Delta\varphi_{\mathrm{EVO},2}$) is plotted versus variation of first exhaust valve opening event ($\Delta\varphi_{\mathrm{EVO},1}$). In addition also the variation of closing events ($\Delta\varphi_{\mathrm{EVC},1,2}$) – equal for both exhaust valves – are illustrated.

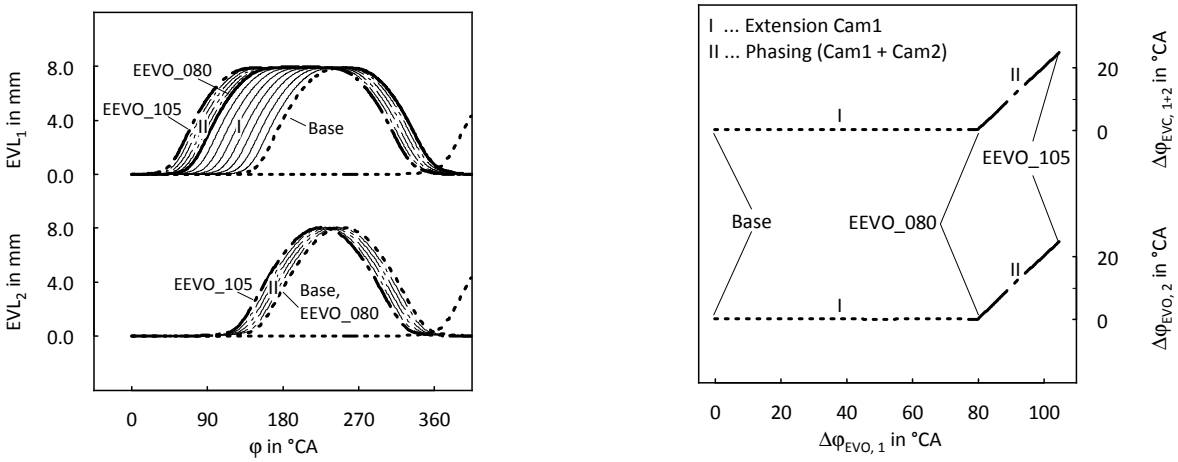

Figure 4.41: Valve lift curves for early exhaust valve opening considered in measurement and simulation

Since correct modelling of exhaust valve opening is a key factor for the present investigations, a verification of this event is inevitable. Figure 4.42 shows the evaluation of the EEVO_080 exhaust valve opening event in an operation point characterized by an engine speed of 1500 min^{-1} and a BMEP of 2 bar. Comparing measured and calculated cylinder pressure curves (left chart) is one way for evaluation. As obvious, the pressure curve of simulation is covered nearly entirely by the measurement curve. Both are characterized by a clearly advanced drop of cylinder pressure compared to operation with base valve lift timing

($\Delta\varphi_{\mathrm{EVO}} = 0$). The right chart in figure 4.42 shows another approach for evaluation of the exhaust valve opening event which is based on the net rate of heat release ($\mathrm{d}Q_{\mathrm{Fuel,\,net}}$) calculated by a thermodynamically analysis of the cylinder pressure curves. As obvious, $\mathrm{d}Q_{\mathrm{Fuel,\,net}}$ has a very flat characteristic after combustion is finished. This is because the heat release resulting from combustion is zero and the wall heat flow is low. The algorithm used for calculation of the net rate of heat release is valid only until EVO, since it does not consider any enthalpy flow. Thus, analysing cylinder pressure beyond EVO by means of this algorithm delivers a drop in $\mathrm{d}Q_{\mathrm{Fuel,\,net}}$ according to the decrease in internal energy which is caused by the enthalpy flow through exhaust valves. Hence this drop could be used as indicator for the exhaust valve opening event. Comparison based on both cylinder pressure curves and net rate of heat releases makes obvious a good correlation of simulation and measurement.

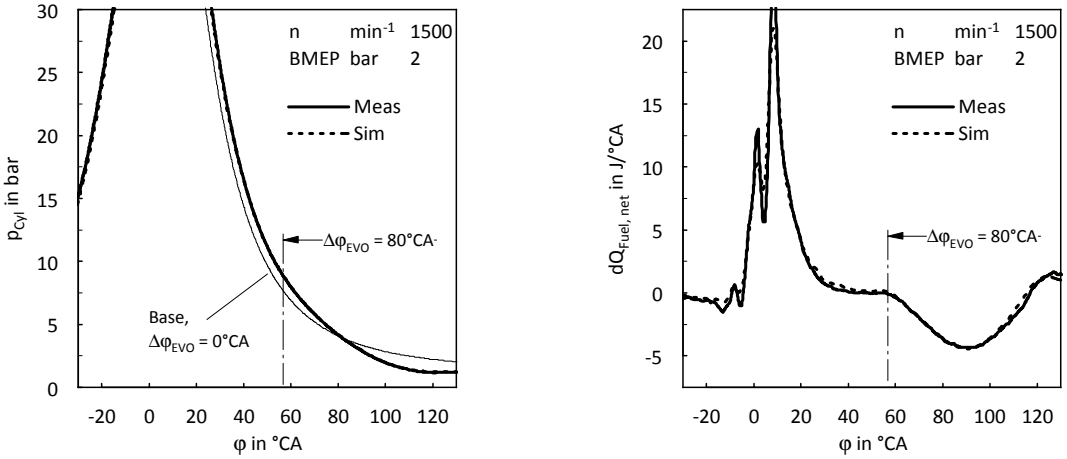

Figure 4.42: Comparison of measurement and simulation concerning effect of EEVO_080 on cylinder pressure and net rate of heat release at 1500 min^{-1} and a BMEP of 2 bar

For evaluation of the EEVO_105 exhaust valve opening event comparison of cylinder pressure curves could be applied in the same way. However, comparison of net rate of heat release is critical, since an overlap of combustion and exhaust valve opening event occurs. In contrast to the EEVO_080 valve lift curve, EEVO_105 does also mean a variation of exhaust valve closing compared to the base valve timing. The advanced closing of exhaust valves leads to an exhaust gas compression which could be identified by an increase of cylinder pressure at the end of the exhaust stroke. Hence comparing measurement and simulation with focus on this event offers a further option for evaluation of valve lift curves. Figure 4.43 shows the cylinder pressure versus volume characteristics of both EEVO_080 and EEVO_105 at 1500 min^{-1} and a BMEP of 2 bar. Considering EEVO_105 (right chart), a good correlation of the mentioned residual gas compression could be identified.

One of the key factors for evaluation of exhaust thermomanagement strategies by means of simulation is the correct calculation of exhaust temperatures and fuel consumption. Hence also the model validation process is focussed on these parameters. When it comes to comparison of calculated exhaust temperatures with measurement, the question arises, whether

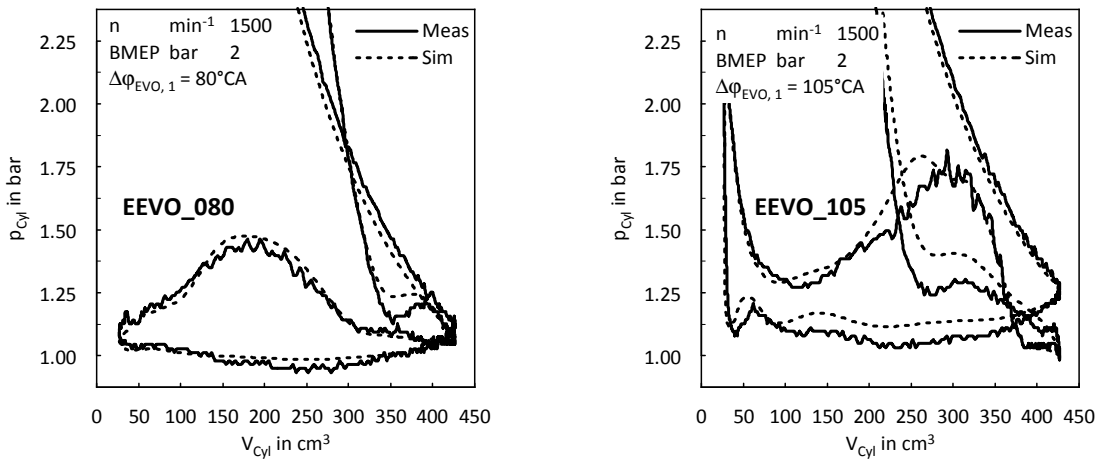

Figure 4.43: Comparison of measurement and simulation concerning effect of EEVO_080 and EEVO_105 on cylinder pressure versus volume characteristics at 1500 min^{-1} and a BMEP of 2 bar

time or mass flow averaged temperatures have to be used. While differences between these temperatures disappear for steady state flow regime, they do not for mass flow characteristics typical for positions near to exhaust valves.

Figure 4.44 shows exhaust temperatures plotted versus variation of exhaust valve opening ($\Delta\varphi_{\mathrm{EVO},1}$). In the left chart the turbine entry (T_{31}) is considered, while the right chart refers to the more upstream position at the entry of the exhaust manifold (T_{EX}). At both positions, the differences between time and mass flow averaged temperatures increases due to advanced exhaust valve opening. Furthermore it can be seen that the differences are higher for the more upstream located sensor (T_{EX}). These dependencies are reasonable, since both parameters – valve timing and distance to exhaust valves – are relevant for mass flow characteristic at the sensor position.

In terms of exhaust enthalpy, the mass flow averaged temperature is relevant. However, the measured thermo couple temperature neither is equal to the mass flow averaged nor to time averaged temperature. Thus, for verification of the simulation model a virtual thermo couple temperature was calculated by taking into account the convective heat flux between gas and sensor. As obvious in figure 4.44, this virtual thermo couple temperature is in between of time and mass flow averaged temperatures. Unless otherwise agreed upon, exhaust temperatures of simulation model considered for evaluation purpose are virtual thermo couple temperatures.

Figure 4.45 shows a comparison of simulation and measurement in an operation point characterized by an engine speed of 1500 min^{-1} and a BMEP of 2 bar. The left chart illustrates the variation of fuel consumption (ΔBSFC) versus exhaust valve opening of exhaust valve 1 ($\Delta\varphi_{\mathrm{EVO},1}$, refer to figure 4.41). To keep in mind that an $\Delta\varphi_{\mathrm{EVO},1}$ variation of more than 80 °CA means an advanced closing of both exhaust valves, also $\Delta\varphi_{\mathrm{EVC},1,2}$ is illustrated. The right chart shows the effect on exhaust temperatures upstream (ΔT_{31}) and downstream (ΔT_{41}) turbine. The calculated characteristic of fuel consumption as well as these of exhaust

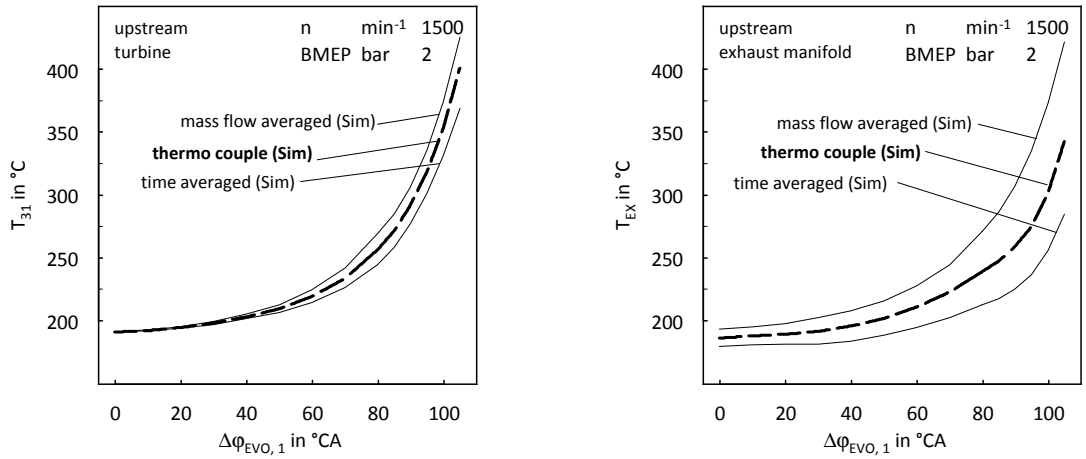

Figure 4.44: Comparison of a virtual thermo couple sensor temperature with mass flow averaged and time averaged temperature concerning effect of early exhaust valve opening at various measuring point positions

the temperatures correlate well with measurement data. Nevertheless, slight differences can be identified. The most relevant sources of error are models for calculation of wall heat flow in cylinders, exhaust ports, exhaust manifold and turbine housing.

This validation process with special focus on fuel consumption and exhaust temperature was done for various operation points. As example for a higher load operation point in figure 4.46 an engine speed of $1750\,\mathrm{min}^{-1}$ and a BMEP of 6 bar is considered. The charts provide the same figures as considered above for evaluation of the lower load operation point. Also the correlation of measurement and simulation is similar.

Of course, also the well known illustration of exhaust enthalpy flow variation ($\Delta\dot{H}_{\mathrm{exh}\,41}$) versus variation of heat losses ($\Delta\dot{Q}_{\mathrm{Loss}}$) could be used for evaluation of simulation results. In figure 4.47 a comparison of measurement and simulation concerning early exhaust valve opening at $1500\,\mathrm{min}^{-1}$ and a BMEP of 2 bar is considered in this way. The slightly lower increase of fuel consumption and exhaust temperature downstream turbine observed in figure 4.45, means a slightly lower variation of exhaust enthalpy flow and heat losses in this evaluation chart. However, correlation of the gradient and hence of thermomanagement efficiency is nearly perfect.

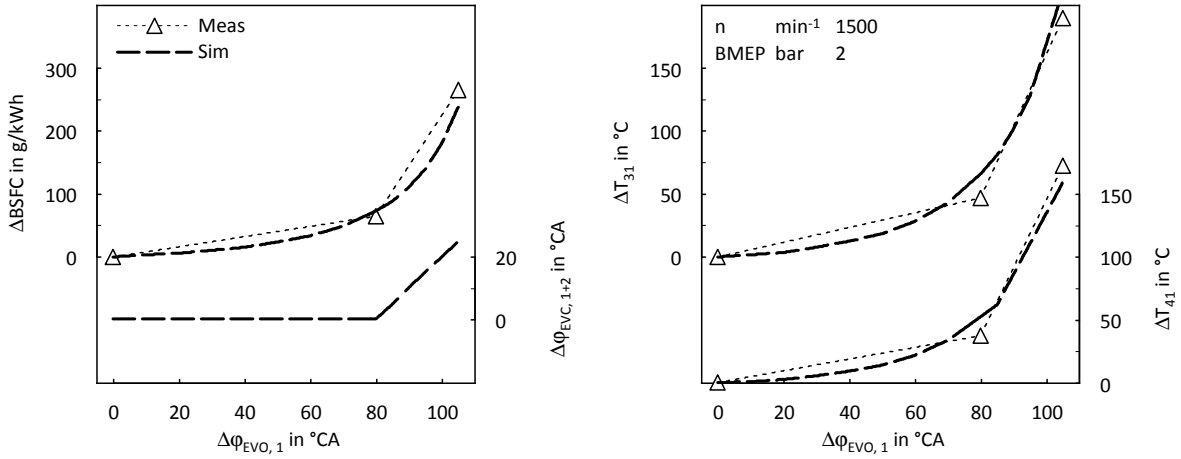

Figure 4.45: Comparison of measurement and simulation concerning effect of early exhaust valve opening on variation of fuel consumption and exhaust temperatures at 1500 min^{-1} and a BMEP of 2 bar

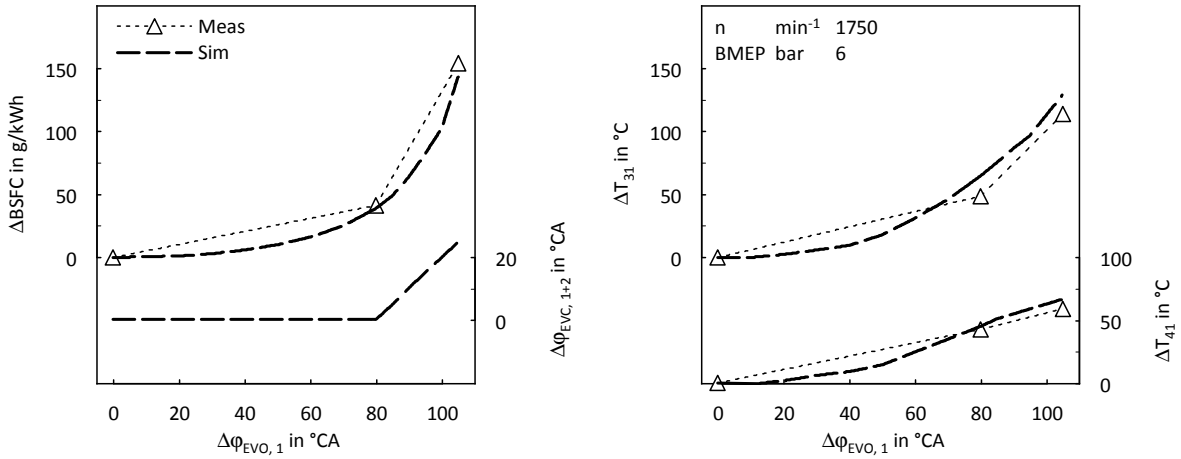

Figure 4.46: Comparison of measurement and simulation concerning effect of early exhaust valve opening on variation of fuel consumption and exhaust temperatures at 1750 min^{-1} and a BMEP of 6 bar

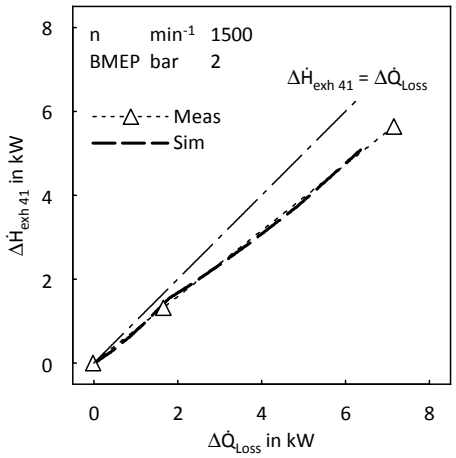

Figure 4.47: Comparison of measurement and simulation concerning variation of exhaust enthalpy flow versus variation of heat losses resulting from early exhaust valve opening at 1500 min^{-1} and a BMEP of 2 bar

4.5.2 Late Intake Valve Closing

As explained by means of simulation in section 3.4.2, the main thermomanagement effect of late intake valve closing (LIVC) results from a decrease in charge fuel ratio achieved mainly by a reduction of aspirated mass flow (air and EGR). Hence also the model validation is focussed on this effect. Similar to the validation process of early exhaust valve opening, not only valve lift curves of camshafts used for engine test bed measurement (Base and LIVC_063) but also intermediate steps were considered, see figure 4.48.

Figure 4.49 shows a comparison between measurement and simulation concerning the most relevant parameters of LIVC. As obvious, the reduction of volumetric efficiency ($\eta_{\mathrm{v,IM}}$) – related to intake manifold conditions – correlates well with measurement. This applies also for the increase of exhaust temperature upstream turbine (T_{31}), what is reasonable, since the cut in volumetric efficiency is the most relevant effect of LIVC concerning increase of T_{31}. However, it must be also mentioned that calculated exhaust temperature downstream turbine (T_{41}) is about 10 °C higher than in measurement. The reason for this is a too low turbine wall heat flow in simulation. When it comes to fuel consumption (BSFC), measurement results show a nearly neutral behaviour of LIVC, while simulation predicts a slight advantage. Analysis of simulation results have shown that the decrease in BSFC comes from a decrease in cylinder wall heat flow. Hence the absence of this effect in measurement is the most probably reason for the differences in fuel consumption. Also the good correlation of PMEP, which restricts differences in fuel consumption to high pressure cycle is an evidence for this.

Figure 4.50 shows a comparison of measurement and simulation concerning cylinder pressure versus volume curves. Besides the characteristics achieved with LIVC_063 (bold curves) also the results referring to the base engine valve timings (thin curves) are plotted. It can be seen that LIVC_063 leads to a flatter increase of cylinder pressure at the beginning of the compression stroke. The lower exhaust back pressure during gas exchange comes from the

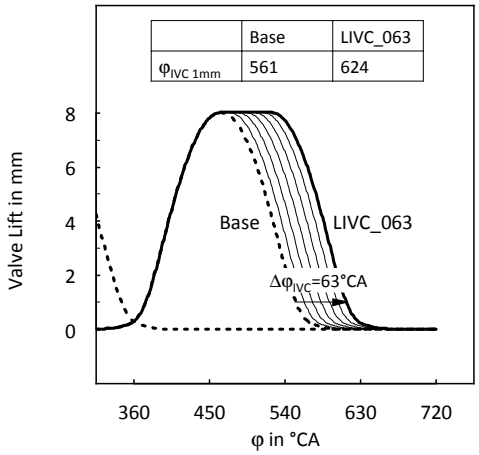

Figure 4.48: Valve lift curves of late intake valve closing considered in measurement and simulation

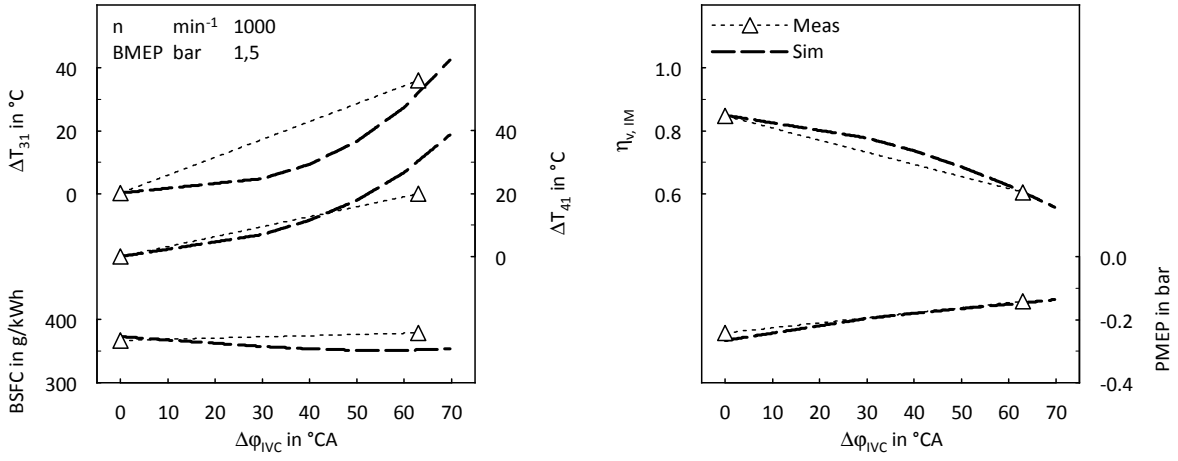

Figure 4.49: Comparison of measurement and simulation concerning effect of late intake valve closing on variation of fuel consumption, exhaust temperatures and gas exchange parameters at 1000 min^{-1} and a BMEP of 1,5 bar

smaller mass which has to be expelled from cylinder. As obvious both effects are covered by the simulation model.

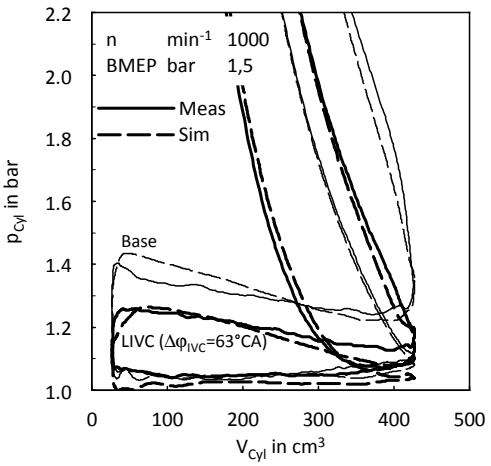

Figure 4.50: Comparison of measurement and simulation concerning effect of late intake valve closing on cylinder pressure versus volume characteristic at 1000 min^{-1} and a BMEP of 1,5 bar

4.5.3 Cylinder Deactivation

As already explained, cylinder deactivation leads to a shift of operation points towards higher load for active cylinders. Since the base model validation was done for a relative wide operation area – compared to the operation range relevant for 2-cylinder mode – a separate validation of cylinder deactivation seems to be not necessary at first sight. Of course, there are differences in gas exchange, comparing 4- and 2-cylinder mode operation with the same IMEP of active cylinders. However, as explained in section 4.3, operating the engine in 2-cylinder mode means – for relevant engine speeds – naturally aspirated operation. Hence gas exchange is of secondary importance in this context. Thus, the actual objective for validation was finding out, if the treatment of deactivated cylinders in simulation model is correct. As already mentioned in discussion of simulation results (section 3.4.4), cylinder wall heat losses occurring in deactivated cylinders due to not adiabatic compression and expansion are taken into account by the simulation model. In this context it has to be kept in mind that the used approach for calculation of cylinder wall heat flow – AVL 2000 model [46], see also section 2.1.1 – is established for a conventional working cycle, however, this means not necessarily an ability for accurate modelling of the wall heat flow in deactivated cylinders. Moreover also differences between measurement and simulation concerning cylinder wall temperature of deactivated cylinders may be a source of error.

Another relevant issue in terms of cylinder deactivation is friction. The simulation model calculates the friction torque from FMEP and overall engine displacement. The FMEP which is an input parameter was derived from measurement by considering not only the active but all cylinders. Doing so leads to an FMEP which does not take into account heat and blow

by losses of deactivated cylinders, what is reasonable, since these effects are covered by the simulation model.

For validation purpose, the part load operation points discussed in section 4.3 were considered. Figure 4.51 shows a comparison of measurement (left chart) and simulation (right chart) concerning the most relevant parameters – fuel consumption and exhaust temperatures. At low engine load, the simulation model predicts a slightly too high fuel consumption for two cylinder operation. However, the differences are small. The effect of cylinder deactivation on exhaust temperatures calculated by the simulation model correlates well with measurement. Slight differences concerning exhaust temperatures downstream turbine at low engine load may occur not only due to an error in modelling turbine but also since the sensor temperature was not completely stable at time of measurement.

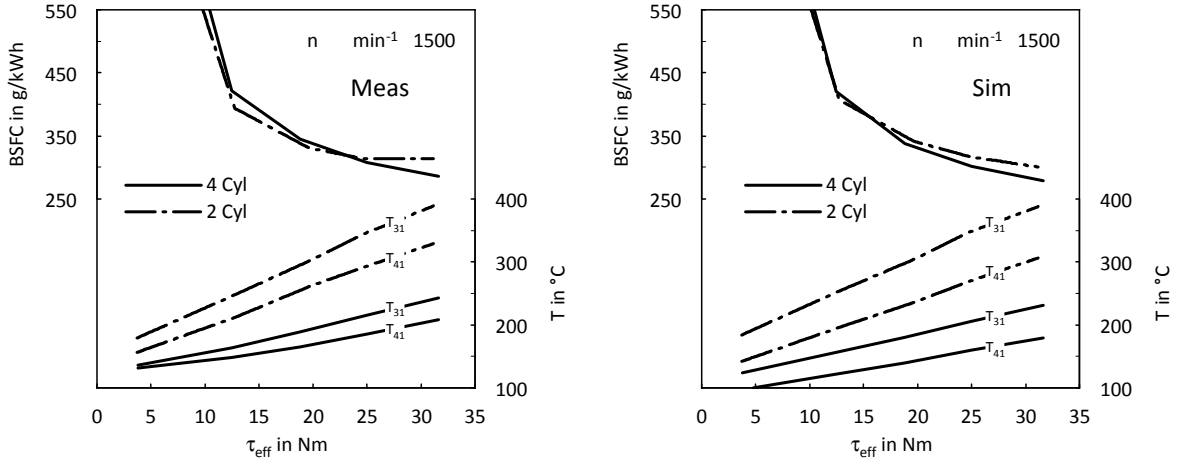

Figure 4.51: Comparison of measurement and simulation concerning effect of cylinder deactivation on variation of fuel consumption and exhaust temperatures at 1500 min^{-1} and low engine load

Figure 4.52 is focused on deactivated cylinders. Comparing the measurement and simulation concerning the average IMEP of the deactivated cylinders, shows a lower – more negative – value of simulation. Thus, the losses occurring in deactivated cylinders due to wall heat flow and blow by are higher in terms of simulation. This deviation may be the reason for the – compared to measurement – slightly worse evaluation of cylinder deactivation by means of simulation (figure 4.51).

The simulation results allow analysing both wall heat flow ($Q_{\mathrm{W,\,Cyl}}$) and blow by enthalpy flow (H_{BB}). As obvious from figure 4.52, the effect of wall heat losses is clearly higher than this of blow by. Hence the reason for the lower IMEP of deactivated cylinders in simulation model comes mainly from wall heat flow. As mentioned above this may be due to a model approach which is not adequate for calculation of the wall heat flow in deactivated cylinders or due to wall temperatures which are different to these of measurement. Nevertheless the effect of the analysed deviations between measurement and simulation in deactivated cylinders on BSFC and exhaust temperatures is small.

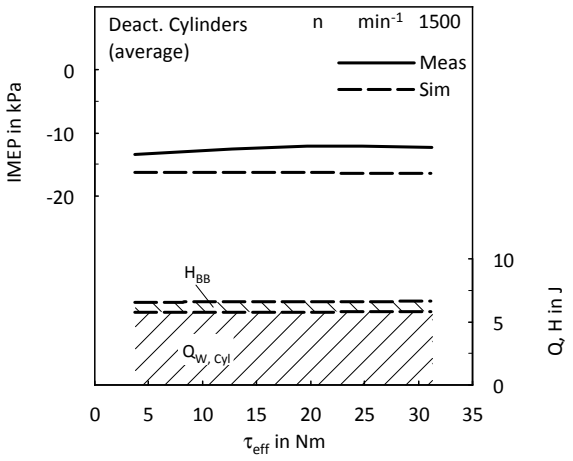

Figure 4.52: Comparison of measurement and simulation concerning the average IMEP of deactivated cylinders. Considering the reason for the negative IMEP in deactivated cylinders – wall heat and blow by losses – by means of simulation at 1500 min^{-1} and low engine load

5 Conclusion

The idea of using valve train variability for increasing the exhaust temperature of a diesel engine is not new. However, in contrast to other publications in this area [8, 9, 15, 22], the present work considers not only effects on exhaust temperature but analyses the benefit of valve train variability for heating up the exhaust aftertreatment. Besides heating up also maintaining the catalyst temperature – avoiding cool down during low load operation after catalyst light off – was considered. In this context it is necessary to find out the influence of exhaust temperature and mass flow on heat up and cool down processes of a catalyst. This was achieved by simulations conducted with a catalyst model based on one-dimensional CFD simulation which takes into account the thermal behaviour of the monolith.

These calculations point out that an increase of exhaust temperature is beneficial for both heat up catalyst and maintaining catalyst temperature, however, the desired mass flow variation is not that clear. For heating up the catalyst a higher mass flow at a given temperature – hence a higher enthalpy flow – is advantageous. However, in terms of maintaining catalyst temperature – characterized by a monolith temperature higher than the exhaust gas temperature – a decline of mass flow should be aimed.

The benefit for the catalyst heat up process resulting from a high exhaust mass flow depends on catalyst type and position. Oxidation catalysts are able to support the heat up process after exceeding the light off temperature. Hence the monolith temperature has to be increased only locally limited (in the most upstream area), what means a lower significance of mass flow than for catalysts which are not featured with a coating for oxidation and hence have to be heated up entirely by the exhaust thermomanagement method. Furthermore the effect of mass flow is the lower the more upstream the catalyst is located. This is due to the fact that a given thermal inertia upstream catalyst means a higher temperature drop for low mass flows.

After pointing out the interaction of exhaust temperature and mass flow with the heat up and cool down process of a catalyst, various alternative valve timings were considered by means of a one-dimensional engine cycle and gas exchange simulation. These calculations have shown that the information, whether only a high exhaust temperature or also a high mass flow is necessary for the considered exhaust thermomanagement task, is extremely relevant in terms of efficiency. While a reduction of mass flow and hence heat capacity of cylinder charge provides the potential for increasing exhaust temperature without an increase of fuel mass, a higher temperature at a constant mass flow – increase of exhaust enthalpy flow – means a penalty in fuel consumption almost in any case. Excepted are only methods, which lead to a decrease of heat losses at least in the same degree as the enthalpy flow increases. However, a VVT method providing this characteristic was not found.

If an increase of exhaust temperature without a decrease of mass flow has to be realized by an adaption of valve timings, only an early exhaust valve opening (EEVO) is adequate. However an EEVO leads not only to a gain in enthalpy flow but also to a significant in-

crease of fuel consumption. The experimental investigations concerning EEVO, which were conducted subsequently on engine test bed, correlate well with the simulation results. In addition to steady operation points, the experimental evaluation of EEVO comprises also transient tests. Considering a cold-start NEDC (New European Driving Cycle), an exhaust valve timing which provides an about 100 °CA advanced exhaust valve opening enables exceeding a temperature level of 200 °C downstream turbine not after 145 (base valve timing) but already after 60 seconds. Assuming that EEVO is applied only until this critical level is achieved, means an increase 2,3 % in overall fuel consumption. Concerning NO_x emissions EEVO is disadvantageous. When it comes to HC emissions, which are of particular interest in terms of exhaust thermomanagement methods applied before catalyst light off, EEVO tends to result in an advantage.

Considering alternative methods – characterized by base valve timing – for increasing exhaust temperature without a reduction of mass flow, an electrical heater (EHeater) located directly upstream catalyst is most promising. Assuming an overall EHeater efficiency of 50 %, what is based on measurement data, the fuel penalty is more or less identical to EEVO. Of course, using a more efficient generator and an electrical system characterized by a higher voltage offers potential for optimization. However, it has to be kept in mind that the idealised case – EHeater efficiency of 100 % – means the energy delivered to the exhaust gas is identical to the increase of indicated work. The caused increase of fuel energy is clearly higher, what is due to the indicated efficiency of the combustion engine which is significantly lower than 100 %. Further alternatives – e.g. a retarded combustion or a reduction of geometrical compression ratio (ε) – are not adequate for application directly after engine cold start. Hence, applying an exhaust thermomanagement method providing an increase of exhaust temperature without a decrease in mass flow will lead to a drawback in fuel consumption – whether EEVO or an EHeater is used.

If a reduction of mass flow is acceptable the situation is quite different. A late intake valve closing (LIVC) as well as cylinder deactivation provide a nearly BSFC-neutral increase of exhaust temperature. This was shown not only by simulation but also by engine test measurements. Also internal EGR by means of a second exhaust event during the intake stroke has the potential for an efficient way of gaining exhaust temperature. Hence these methods are adequate at least for maintaining catalyst temperature at low engine load. When it comes to the application as heat up method, LIVC is not qualified, even if the low mass flow does not matter (e.g. heating up a close coupled DOC, separated from exhaust valves only through a low thermal inertia). This is due to the drawback concerning ignitability (low cylinder pressure and temperature), which avoids an application directly after engine cold start. Cylinder deactivation is not critical in this context. However, using only two instead of 4 cylinders means a limitation of available engine output. This applies all the more for one-stage turbo charging, which does not allow effective boosting in 2-cylinder operation. Hence the engine output in 2-cylinder mode is not sufficient to cope with the relevant test cycles, even not with the first, in case of heat up particularly relevant sections. Of course a supercharging concept which provides relevant boost pressures also in 2-cylinder mode may overcome this problem. Also in case of a 6-cylinder engine, the output available with deactivated cylinders – 3-cylinder operation – may be sufficient for powering a wide range of vehicles in the relevant test cycles. Internal EGR is less critical than LIVC too, concerning

an application directly after engine cold start. However the achievable increase of exhaust temperature is relatively low.

The consequences of these findings for exhaust aftertreatment are clear. Assuming a typical EAS layout comprising a close coupled DOC and DPF as well as a SCR system in the underfloor, for achievement of lowest NO_x emissions, a rapid heat up of the SCR catalyst is necessary. Taking into account position and type of the SCR catalyst requires an exhaust thermomanagement method providing not only a high temperature but also a high enthalpy flow. In other words gaining exhaust temperature in a way that results in a significant reduction of mass flow is not acceptable. Hence a penalty in fuel consumption due to exhaust thermomanagement is nearly inevitable. A reduction of heat up demand could be achieved by different ways. Of course the most obvious way is a more upstream position of the SCR system, what could be achieved e.g. by means of a DPF with SCR coating (SDPF) [4, 17, 5]. If this is not an option – maybe due to packaging – also using a LNT instead of a DOC allows a later light off or even the elimination of the SCR catalyst [13]. Both ways mean for exhaust thermomanagement heating up a more upstream component. Thus, the BSFC-intensive method (e.g. EEVO) has to be applied only for a short time or could be even replaced by a more efficient method (e.g. cylinder deactivation). If the low mass flow, which is more or less implicated by an efficient exhaust thermomanagement method, is acceptable, will finally depend on several parameters (actual thermal inertia upstream catalyst, target emission level and hence maximum time to light off, actual coating of the catalyst, ...)

For further experimental investigations in the area of exhaust thermomanagement, it is recommended to adapt the rapid cool down procedure – used for cool down the engine before cold-start tests – in a way which ensures a dry catalyst at the start of the test cycle. Thus, a delayed catalyst light off due to evaporation of condensed water in the monolith will be avoided. Moreover using an exhaust gas analysis downstream catalyst – in addition to this one uptstream catalyst – is recommended. This enables the identification of the catalyst light off based on conversion of HC and CO emissions. Furthermore, additional temperature sensors located at various positions inside the catalyst (in longitudinal direction) would be able to deliver valuable information concerning the length of catalyst section, which has to be heated up until the light off is achieved.

Of course also the applied simulation methodology has potential for further enhancements. Modelling the engine by means of a so-called real-time approach [28] enables calculation of transient engine cycles within an acceptable calculation time. Due to this it would be not necessary anymore to separate between catalyst simulation and egine cycle simulation. However, it has to be taken into account that a model able to perform transient test cycles must include several engine control functionalities for controlling of e.g boost pressure, EGR or combustion heat release. Moreover the simulation of cold-start tests requires modelling the thermal inertia of several engine components and the coolant. In other words the complexity of the simulation model will clearly increase, which will lead to a singificantly increased time spent on model creation and matching. This clearly higher effort may be reasonable only if the model will be applied not only for evaluation of exhaust thermomanagement methods but also for further issues. Combining the engine model with a vehicle model for evaluation of various hybridisation strategies is one example of this.

List of Figures

Bibliography

[1] Absmeier C., Fischer A., Klering M., Riedl W., Sailer W. and Städter J.: "BMW V8 Motoren - Lösungen für mehr Umweltverträglichkeit und Kundennutzen"; in: *MTZ - Motortechnische Zeitschrift* 59 (12 1998), pp. 786–796

[2] Ando S. and Chujo K.: "The new NISSAN V8 gasoline engine with VVEL AND DIG; Der neue Nissan V8-Benzinmotor mit variabler Ventiltechnik (VVEL) und Direkteinspritzung"; in: *Internationales Wiener Motorensymposium, 31*; 2010, pp. 23–40

[3] Beer M., Held W., Kerkau M. and Rehr A.: "Der neue Motor des Porsche 911 Turbo"; in: *MTZ - Motortechnische Zeitschrift* 61 (11 2000), pp. 730–743

[4] Beichtbuchner A., Bürgler L., Wancura H., Weissbäck M., Pramhas J. and Schutting E.: "HSDI diesel on the way to SULEV - concept evaluation"; in: *Aachen Colloquium Automobile and Engine Technology, 21*; 2012, pp. 1203–1223

[5] Beichtbuchner A., Wancura H., Weissbäck M. and Hadl K.: "Konzepte zur Diesel-Abgasnachbehandlung für die Richtlinie LEV 3"; in: *MTZ - Motortechnische Zeitschrift* 74 (7 2013), pp. 574–579

[6] Blumenröder K., Buschmann G., Kahrstedt J., Sommer A. and Maiwald O.: "Variable Ventiltriebe in Pkw-Dieselmotoren - Potenziale, Grenzen und Realisierungschancen; Variable valve trains for passenger car diesel engines - potentials, limits and ways of realisation"; in: *Internationales Wiener Motorensymposium, 27*; 2005, pp. 280–301

[7] Böckenhoff E. and Herrmann H. O.: "Der Ladungswechsel bei der neuen Generation von Daimler Trucks Nutzfahrzeugmotoren"; in: *MTZ-Konferenz Ladungswechsel im Verbrennungsmotor, 5*; Stuttgart, 2012

[8] Brauer M., Diezemann M., Pohlke R., Rohr J., Severin C. and Werler A.: "Variabler Ventiltrieb - aktives Abgastemperaturmanagement am Dieselmotor"; in: *MTZ-Konferenz Ladungswechsel im Verbrennungsmotor, 5*; Stuttgart, 2012

[9] Diezemann M., Pohlke R., Brauer M. and Severin C.: "Anhebung der Abgastemperatur am Dieselmotor durch variablen Ventiltrieb"; in: *MTZ - Motortechnische Zeitschrift* 74 (4 2013), pp. 308–315

[10] Flierl R., Schmitt S., Kleinert G., Esch H.-J. and Dismon H.: "Univalve - Ein vollvariables mechanisches Ventiltriebsystem für zukünftige Verbrennungsmotoren"; in: *MTZ - Motortechnische Zeitschrift* 72 (5 2011), pp. 380–385

[11] Grigo M., Wurms R., Budack R., Helbig J., Langa Z. and Trost W.: "Der neue 2,0-l-TFSI-Motor mit Audi valvelift system"; in: *ATZextra* 13 (2 2008), pp. 30–35

[12] Grob A., Brinkmann C. and Königstedt J.: "Der neue 4,0-L-V8-TFSI-Motor von Audi Teil 2: Thermodynamik Und Applikation"; in: *MTZ - Motortechnische Zeitschrift* 74 (3 2013), pp. 232–238

[13] Hadl K., Schutting E., Eichlseder H., Beichtbuchner A., Bürgler L. and Danninger A.: "Diesel-Abgasnachbehandlungskonzepte zur Erfüllung künftiger Gesetzgebungen basierend auf dem NOx-Speicherkatalysator"; in: *Internationales Wiener Motorensymposium, 35*; 2014

[14] Honardar S.: "Potenziale von Ladungswechsel-Variabilitaeten im Hinblick auf Emission, Dynamik und Abgastemperaturverhalten beim Pkw-Dieselmotor"; in: *FVV Frühjahrstagung, Informationstagung Motoren*; Leipzig, 2013, pp. 157–192

[15] Honardar S., Deppenkemper K., Nijs M. and Pischinger S.: "Potenziale von Ladungswechselvariabilitäten beim Pkw-Dieselmotor"; in: *MTZ - Motortechnische Zeitschrift* 75 (9 2014), pp. 64–69

[16] Kiefer W., Plodek B., Ehmann P., Feldwisch-Drentrup R. and Diringer J.: "BMW 750i mit elektrisch beheiztem Katalysator"; in: *MTZ - Motortechnische Zeitschrift* 59 (11 1998), pp. 752–761

[17] Knirsch S., Weiss U., Möhn S. and Pamio G.: "Die neue V6-TDI-Motorengeneration von Audi"; in: *MTZ - Motortechnische Zeitschrift* 75 (10 2014), pp. 48–55

[18] Kopp C.: "Variable Ventilsteuerung für Pkw-Dieselmotoren mit Direkteinspritzung"; Dissertation; Otto-von-Guericke-Universität Magdeburg, 2006

[19] Lörch H., Weiss U., Möhn S. and Haas J.: "Combination of electrically heated catalytic converter and SCR@DPF for challenging V-TDI projects"; in: *Internationales Stuttgarter Symposium Automobil- und Motorentechnik, 14*; 2013, pp. 623–636

[20] Maus W., Brück R., Konieczny R. and Scheeder A.: "Der E-Kat als Thermomanagement-Lösung in modernen Fahrzeuganwendungen"; in: *MTZ - Motortechnische Zeitschrift* 71 (5 2010), pp. 340–346

[21] Merker G. P. and Teichmann R.: *Grundlagen Verbrennungsmotoren; Funktionsweise, Simulation, Messtechnik*; 7. Auflage; Wiesbaden: Springer, 2014

[22] Messner D., Bittermann A. and Michl J.: "Ventiltriebsvariabilität zur effektiveren DeNOxierung bei modernen Dieselbrennverfahren; Valve train variability applied on a modern Diesel combustion system for efficient NOx-aftertreatment"; in: *International Exhaust Gas and Particulate Emissions Forum, 7*; Ludwigsburg, 2012, pp. 145–161

[23] Middendorf H., Theobald J., Lang L. and Hartel K.: "Der 1,4-l-TSI-Ottomotor mit Zylinderabschaltung"; in: *MTZ - Motortechnische Zeitschrift* 73 (3 2012), pp. 186–193

[24] Mürwald M., Kemmler R., Waltner A. and Kreitmann F.: "The new four-cylinder gasoline engines from Mercedes-Benz"; in: *MTZ worldwide* 74 (11 2013), pp. 4–11

[25] N. N.; URL: http://presse.mitsubishi-motors.de/concept_cars/motorshow_paris_2010/pdf/2010PMS_LancerOutlander4N1Diesel.pdf

[26] N. N.: *BOOST Manual; User Guide*; AVL LIST GmbH, 2011

[27] N. N.: *BOOST Manual; Theory*; AVL LIST GmbH, 2011

[28] N. N.: *BOOST Manual; Real-Time (RT) Users Guide*; AVL LIST GmbH, 2011

[29] Neußer H.-J., Kahrstedt J., Jelden H., Dorenkamp R. and Düsterdiek T.: "Die EU6-Motoren des Modularen Dieselbaukastens von Volkswagen - innovative motornahe Abgasreinigung für weitere NOx- und CO2-Minderung"; in: *Internationales Wiener Motorensymposium, 34*; 2013, pp. 137–161

[30] Pischinger R., Klell M. and Sams T.: *Thermodynamik der Verbrennungskraftmaschine*; 2. Auflage; Wien [u.a.]: Springer, 2002

[31] Pramhas J., Schutting E. and Bürgler L.: "Ladungswechselseitige Thermomanagementmaßnahmen für Pkw-Dieselmotoren unter zukünftigen Randbedingungen"; in: *MTZ-Konferenz Ladungswechsel im Verbrennungsmotor, 6* (2013), pp. 1–24

[32] Pramhas J., Schutting E., Eichlseder H., Bürgler L. and Danninger A.: "Ladungswechselseitige Thermomanagementmaßnahmen am Dieselmotor; Air management methods for diesel engine thermomanagement"; in: *Tagung Der Arbeitsprozess des Verbrennungsmotors, 14*; Graz, 2013, pp. 301–316

[33] Rembor H.-J. and Bischler T.: "Abgasnachbehandlung mit Online-Brenner"; in: *ATZ-offhighway* 3 (2 2010), pp. 52–61

[34] Roda F.: "Variable Steuerzeiten - ein Mittel zur Optimierung aufgeladener Viertakt-Dieselmotoren"; in: *MTZ - Motortechnische Zeitschrift* 49 (7-8 1988), pp. 303–308

[35] Sams T.: "Schadstoffbildung und Emissionsminimierung bei Kfz, Teil I"; Skriptum; TU Graz, 2007

[36] Schaffer K., Luef R. and Eichlseder H.: "Ventiltriebsvariabilitäten bei Pkw- Dieselmotoren"; in: *MTZ-Konferenz Ladungswechsel im Verbrennungsmotor, 3*; Stuttgart, 2010, pp. 1–21

[37] Schutting E., Neureiter A., Fuchs C., Schatzberger T., Klell M., Eichlseder H. and Kammerdiener T.: "Miller- und Atkinson-Zyklus am aufgeladenen Dieselmotor"; in: *MTZ - Motortechnische Zeitschrift* 68 (6 2007), pp. 480–485

[38] Six C.: "Bewertung eines Ladungs-Kühlkonzepts fur einen PKW-Dieselmotor mit Niederdruck Abgasrückführung mittels transienter 1D-Ladungswechselsimulation"; Diplomarbeit; 2011

[39] Spurk P. C., Pfeifer M., Setten B., Hohenberg G. and Gietzelt C.: "Untersuchung von motorseitigen Regenerationsmethoden für katalytisch beschichtete Diesel-Partikelfilter für den Einsatz im Nutzfahrzeug"; in: *Internationales Wiener Motorensymposium, 24*; 2003, pp. 337–358

[40] Staub P., Grimm M., Pivec R., Eichlseder H. and Schaffer K.: "Neue Potenziale für den Dieselmotor durch erweiterte Variabilitäten"; in: *Tagung Der Arbeitsprozess des Verbrennungsmotors, 9*; Graz, 2003

[41] Tatur M., Tomazic D., Thornton M. and Lamping M.: "Ein Dieselmotorenkonzept zur Erfüllung der Tier-2-Bin-5-Emissionsgesetzgebung"; in: *MTZ - Motortechnische Zeitschrift* 66 (11 2005), pp. 912–919

[42] Terazawa Y., Nakai E., Kataoka M. and Sakono T.: "Der neue Vierzylinder-Dieselmotor von Mazda"; in: *MTZ - Motortechnische Zeitschrift* 72 (09 2011), pp. 660–666

[43] Tomoda T., Ogawa T., Ohki H., Kogo T., Nakatani K. and Hashimoto E.: "Improvement of Diesel Engine Performance by Variable Valve Train System; Leistungsverbesserung von Dieselmotoren durch variable Ventilsteuerung"; in: *Internationales Wiener Motorensymposium, 30*; 2007, pp. 171–185

[44] Unger H., Schwarz C., Schneider J. and Koch K.-F.: "Die Valvetronic"; in: *MTZ - Motortechnische Zeitschrift* 69 (7-8 2008), pp. 598–605

[45] Weißbäck M., Csató J., Glensvig M., Sams T. and Herzog P.: "Alternative Brennverfahren - Ein Ansatz für den zukünftigen Pkw-Dieselmotor"; in: *MTZ - Motortechnische Zeitschrift* 64 (9 2003), pp. 718–727

[46] Wimmer A., Pivec R. and Sams T.: "Heat Transfer to the Combustion Chamber and Port Walls of IC Engines - Measurement and Prediction"; in: *SAE World Congress*; Detroit, USA, 2000

[47] Zapf H.: "Beitrag zur Untersuchung des Wärmeüberganges während des Ladungswechsels im Viertakt-Dieselmotor."; in: *MTZ - Motortechnische Zeitschrift* 30 (12 1976), pp. 461–465

[48] Zuschrott M.: "Betriebsstrategien am direkteinspritzenden Dieselmotor bei variablem Ventiltrieb und Drall"; Diplomarbeit; 2005